

MODELING OF HOURLY STREAM TEMPERATURES WITHIN TWO FORESTED
CATCHMENTS

by

Cindie Hébert

Submitted in partial fulfilment of the requirements
for the degree of Doctor of Philosophy

at

Dalhousie University
Halifax, Nova Scotia
February 2013

© Copyright by Cindie Hébert, 2013

DALHOUSIE UNIVERSITY

DEPARTMENT OF CIVIL AND RESOURCE ENGINEERING

The undersigned hereby certify that they have read and recommend to the Faculty of Graduate Studies for acceptance a thesis entitled “MODELING OF HOURLY STREAM TEMPERATURES WITHIN TWO FORESTED CATCHMENTS” by Cindie Hébert in partial fulfilment of the requirements for the degree of Doctor of Philosophy.

Dated: February 22, 2013

External Examiner: _____

Research Supervisor: _____

Examining Committee: _____

Departmental Representative: _____

DALHOUSIE UNIVERSITY

DATE: February 22, 2013

AUTHOR: Cindie Hébert

TITLE: MODELING OF HOURLY STREAM TEMPERATURES WITHIN TWO FORESTED CATCHMENTS

DEPARTMENT OR SCHOOL: Department of Civil and Resource Engineering

DEGREE: PhD CONVOCATION: MAY YEAR: 2013

Permission is herewith granted to Dalhousie University to circulate and to have copied for non-commercial purposes, at its discretion, the above title upon the request of individuals or institutions. I understand that my thesis will be electronically available to the public.

The author reserves other publication rights, and neither the thesis nor extensive extracts from it may be printed or otherwise reproduced without the author's written permission.

The author attests that permission has been obtained for the use of any copyrighted material appearing in the thesis (other than the brief excerpts requiring only proper acknowledgement in scholarly writing), and that all such use is clearly acknowledged.

Signature of Author

DEDICATION

I dedicate this thesis to my children, Sandrine, Alice and Alexandre.

TABLE OF CONTENTS

LIST OF TABLES	viii
LIST OF FIGURES	x
ABSTRACT	xiii
LIST OF ABBREVIATIONS AND SYMBOLS USED	xiv
ACKNOWLEDGEMENTS	xviii
CHAPTER 1: INTRODUCTION	1
1.1 GOAL AND OBJECTIVES	1
1.1.1 DETERMINISTIC MODEL	3
1.1.2 EQUILIBRIUM TEMPERATURE MODEL	3
1.1.3 ARTIFICIAL NEURAL NETWORK MODEL	4
1.2 THESIS OVERVIEW	5
CHAPTER 2: LITERATURE REVIEW	7
2.1 THERMAL REGIME OF RIVERS	7
2.2 AQUATIC ECOSYSTEMS	11
2.3 HUMAN IMPACTS	15
2.3.1 FOREST HARVESTING	15
2.3.2 CLIMATE CHANGE	22
2.3.3 STREAMFLOW	25
2.4 WATER TEMPERATURE MODELS	27
2.4.1 DETERMINISTIC MODELS	27
2.4.1.1 SOLAR RADIATION	29
2.4.1.2 LONGWAVE RADIATION	31

2.4.1.3 EVAPORATION	31
2.4.1.4 CONVECTION.....	34
2.4.1.5 ADVECTION	35
2.4.1.6 CONDUCTION	36
2.4.2 TEMPERATURE EQUILIBRIUM CONCEPT	38
2.4.3 ARTIFICIAL NEURAL NETWORKS	41
2.4.4 STOCHASTIC AND OTHER STATISTICAL TYPES OF MODELS	47
CHAPTER 3: METHODOLOGY AND STUDY AREA	50
3.1 STUDY AREA	50
3.2 DETERMINISTIC MODEL	53
3.2.1 NET SHORTWAVE RADIATION (H_s)	56
3.2.2 NET LONGWAVE RADIATION (H_l)	57
3.2.3 EVAPORATIVE HEAT FLUX (H_e).....	58
3.2.4 CONVECTIVE HEAT FLUX (H_c)	59
3.2.5 PRECIPITATION HEAT FLUX (H_p).....	60
3.2.6 STREAMBED HEAT FLUXES (H_{bed})	60
3.2.6.1 STREAMBED HEAT FLUX BY CONDUCTION (H_b)	63
3.2.6.2 STREAMBED HEAT FLUX BY GROUNDWATER ADVECTION (H_g)	63
3.3 EQUILIBRIUM TEMPERATURE MODEL	64
3.4 ARTIFICIAL NEURAL NETWORK MODEL.....	67
3.5 DATA COLLECTION	72
3.6 MODELING PERFORMANCE CRITERIA	73
CHAPTER 4: RESULTS.....	75

4.1 DETERMINISTIC MODEL	75
4.1.1 OVERVIEW OF DATA SERIES	75
4.1.2 DETAILED ANALYSIS OF HEAT FLUXES AND WATER TEMPERATURES.....	79
4.1.2.1 PERIOD 1	83
4.1.2.2 PERIOD 2	88
4.1.2.3 PERIOD 3	92
4.1.2.4 PERIOD 4	95
4.1.2.5 PERIOD 5	99
4.1.2.6 PERIOD 6	103
4.1.3 COMPARISON TOTAL HEAT FLUXES AND WATER TEMPERATURES (OBSERVED VS. PREDICTED).....	106
4.2 EQUILIBRIUM TEMPERATURE MODEL	111
4.3 ARTIFICIAL NEURAL NETWORK MODEL.....	123
CHAPTER 5: DISCUSSION AND ANALYSIS OF RESULTS.....	134
5.1 DETERMINISTIC MODEL	134
5.2 EQUILIBRIUM TEMPERATURE MODEL	141
5.3 ARTIFICIAL NEURAL NETWORK MODEL.....	148
5.4 COMPARISON OF WATER TEMPERATURE MODELS	156
CHAPTER 6: CONCLUSION	159
6.1 CONCLUSION	159
6.2 RECOMMENDATIONS.....	161
REFERENCES	165
APPENDIX A Free Body Diagram	200

LIST OF TABLES

Table 3.1. Selected characteristics of Catamaran Brook and Little Southwest Miramichi.....	51
Table 4.1. Selected periods for the river heat budget analysis at both Catamaran Brook and Little Southwest Miramichi River in 2007.....	75
Table 4.2. Comparison of period averages of specific meteorological parameter at two microclimate sites (Catamaran Brook and Little Southwest Miramichi River) and at the meteorological station (MetSta).	79
Table 4.3. Heat fluxes (gain, loss and net) for both river systems.....	82
Table 4.4. Results of modeling performance between predicted total heat flux, $H_t(P)$, and observed total heat flux, $H_t(O)$, for the deterministic model at Catamaran Brook and Little Southwest Miramichi River.	83
Table 4.5. Performance of deterministic model on the basis of predicted vs. observed water temperatures.....	108
Table 4.6. Results of the equilibrium temperature model for prediction of hourly water temperatures at Catamaran Brook and Little Southwest Miramichi.....	118
Table 4.7. Description of the four selected study periods to examine the performance of the water temperature model under different hydrological conditions.....	120

Table 5.1. The values of the thermal exchange coefficient (K) calibrated for each month (April to October) at both Catamaran Brook (Cat Bk) and Little Southwest Miramichi (LSWM).....	144
Table 5.2. Coefficient of determination (R^2) of the regression analysis between the thermal exchange coefficient (K) and selected meteorological parameters (air temperature ($^{\circ}\text{C}$), water temperature ($^{\circ}\text{C}$), incoming solar radiation (W m^{-2}), water level (m), relative humidity (%), and wind speed (m s^{-1})) at Catamaran Brook (Cat Bk) and Little Southwest Miramichi (LSWM).....	145
Table 5.3. Results of the estimation of the daily mean (T_{mean}) and the daily maximum stream temperature (T_{max}) calculated from the predicted hourly water temperatures (equilibrium temperature model) at Catamaran Brook and Little Southwest Miramichi.....	147
Table 5.4. Results of the estimation of the daily mean (T_{mean}) and the daily maximum stream temperature (T_{max}) calculated from the predicted hourly water temperatures (artificial neural network model) at Catamaran Brook and Little Southwest Miramichi.....	153
Table 5.5. Comparison of advantages, disadvantages and data requirement of the three different types of water temperature models.....	158

LIST OF FIGURES

Figure 3.1 Map showing the location of microclimate sites (Catamaran Brook and Little Southwest Miramichi River) and the location of the remote meteorological station.	52
Figure 3.2 Illustration of a feed-forward neural network architecture.....	68
Figure 4.1 Time series plot of selected parameters (air temperature, water temperature, streamflow and precipitation) and study periods for both Catamaran Brook and Little Southwest Miramichi River. The stepped data on Figure 4.1c represents daily mean discharge.	77
Figure 4.2 Detailed analysis of the different heat fluxes at both Catamaran Brook and Little Southwest Miramichi River during Period 1	85
Figure 4.3 Detailed analysis of the different heat fluxes at both Catamaran Brook and Little Southwest Miramichi River during Period 2.....	90
Figure 4.4 Detailed analysis of the different heat fluxes at both Catamaran Brook and Little Southwest Miramichi River during Period 3.....	93
Figure 4.5 Detailed analysis of the different heat fluxes at both Catamaran Brook and Little Southwest Miramichi River during Period 4.....	96
Figure 4.6 Detailed analysis of the different heat fluxes at both Catamaran Brook and Little Southwest Miramichi River during Period 5.....	101
Figure 4.7 Detailed analysis of the different heat fluxes at both Catamaran Brook and Little Southwest Miramichi River during Period 6.....	105

Figure 4.8 Predicted vs. observed total heat fluxes (gains and losses) for each study period (1 to 6) at Catamaran Brook and Little Southwest Miramichi River using the deterministic model.	107
Figure 4.9 Observed water temperatures ($T_w(O)$) and predicted water temperatures ($T_w(P)$) at Catamaran Brook calculated from the predicted total heat flux by the deterministic model.	109
Figure 4.10 Observed water temperatures ($T_w(O)$) and predicted water temperatures ($T_w(P)$) at Little Southwest Miramichi calculated from the predicted total heat flux by the deterministic model.....	110
Figure 4.11 Observed water temperatures ($T_w(O)$) and predicted water temperatures ($T_w(P)$) obtained from the equilibrium temperature model at Catamaran Brook.	113
Figure 4.12 Observed water temperatures ($T_w(O)$) and predicted water temperatures ($T_w(P)$) obtained from the equilibrium temperature model at Little Southwest Miramichi.	115
Figure 4.13 Observed water temperatures ($T_w(O)$), predicted water temperatures ($T_w(P)$) from the equilibrium temperature model and air temperatures (T_a) for the four detailed time periods at Catamaran Brook and Little Southwest Miramichi.	121
Figure 4.14 Observed water temperatures ($T_w(O)$) and predicted water temperatures ($T_w(P)$) obtained from the ANN model at Catamaran Brook.....	128
Figure 4.15 Observed water temperatures ($T_w(O)$) and predicted water temperatures ($T_w(P)$) obtained from the ANN model at Little Southwest Miramichi.....	130

Figure 4.16 Observed water temperatures ($T_w(O)$), predicted water temperatures ($T_w(P)$) from the ANN model and air temperatures (T_a) for the four detailed time periods at Catamaran Brook and Little Southwest Miramichi.....133

Figure 5.1 Predicted ($T_{mean}(P)$) *versus* observed daily mean water temperatures ($T_{mean}(O)$) and predicted ($T_{max}(P)$) *versus* observed daily maximum water temperatures ($T_{max}(O)$) at Catamaran Brook and Little Southwest Miramichi using the equilibrium temperature model.....151

Figure 5.2 Predicted ($T_{mean}(P)$) *versus* observed daily mean water temperatures ($T_{mean}(O)$) and predicted ($T_{max}(P)$) *versus* observed daily maximum water temperatures ($T_{max}(O)$) at Catamaran Brook and Little Southwest Miramichi using the artificial neural network model.....154

ABSTRACT

Water temperature is a key physical habitat determinant in lotic ecosystems as it influences many physical, chemical and biological properties of rivers. Hence, a good understanding of the thermal regime of rivers is essential for effective management of water and fisheries resources. This study deals with the modeling of hourly stream water temperature using a deterministic model, an equilibrium temperature model and an artificial neural network model. The water temperature models were applied on two thermally different streams, namely, the Little Southwest Miramichi River (LSWM) and Catamaran Brook (Cat Bk) in New Brunswick, Canada.

The deterministic model calculated the different heat fluxes at the water surface and from the streambed, using different hydrometeorological conditions. Results showed that microclimate data are essential in making accurate estimates of the surface heat fluxes. Results also showed that for larger river systems, the surface heat fluxes were generally the dominant component of the heat budget with a correspondingly smaller contribution from the streambed (90%). As watercourses became smaller and as groundwater contribution became more significant, the streambed contribution became important (20%).

The equilibrium temperature model is a simplified version of the deterministic model where the total heat flux at the surface is assumed to be proportional to the difference between the water temperature and the equilibrium temperature. The poor model performance compared to the other models developed in this study suggested that the air and equilibrium temperature did not reflect entirely the total heat flux at an hourly scale. The model's best performance was in autumn, where the low water level permitted a more efficient thermal exchange, whereas the presence of snowmelt conditions in spring resulted in poorer performance.

An artificial neural network (ANN) was also developed to predict hourly river water temperatures using minimal and accessible input data. The results showed that ANN models are effective modeling tools, with similar or better results to comparable modeling studies. The ANN model performed best in summer and autumn and had poorer, but still good, performance in spring, explained by the high water levels.

LIST OF ABBREVIATIONS AND SYMBOLS USED

A	cross sectional area (m^2)
a	empirical constant
a_j	activation function of the j^{th} hidden node
b	empirical constant
b_j	bias weight of j^{th} hidden node
bo_{jk}	bias weight of the k^{th} output node coming from the j^{th} hidden node
Cat Bk	Catamaran Brook
C	cloud cover (clear sky (0), mainly clear (0.25), mostly cloudy (0.75) and total cloud cover (1))
c_m	heat capacity of the rock-fluid matrix ($1130 \text{ J kg}^{-1} \text{ }^\circ\text{C}^{-1}$)
c_s	specific heat of the streambed ($775 \text{ J kg}^{-1} \text{ }^\circ\text{C}^{-1}$)
c_w	specific heat of water ($4.19 \times 10^{-3} \text{ MJ kg}^{-1} \text{ }^\circ\text{C}^{-1}$)
D_x	dispersion coefficients in direction of x-axis ($\text{m}^2 \text{ hour}^{-1}$)
D_y	dispersion coefficients in direction of y-axis ($\text{m}^2 \text{ hour}^{-1}$)
D_z	dispersion coefficients in direction of z-axis ($\text{m}^2 \text{ hour}^{-1}$)
e_a	water vapor pressure in the air (mm Hg)
e_s	saturated vapor pressure at the water temperature (mm Hg)
FC	forest cover factor (%)
H_b	streambed heat flux by conduction (W m^{-2})
H_{bed}	total heat flux per area at the streambed-water interface (W m^{-2})
H_c	convective heat flux (W m^{-2})
H_e	evaporative heat flux (W m^{-2})

H_g	streambed heat flux by advective groundwater flow (W m^{-2})
H_{is}	incoming solar radiation at the water surface (W m^{-2})
H_l	net longwave radiation (W m^{-2})
H_p	precipitation heat flux (W m^{-2})
H_s	net shortwave radiation (W m^{-2})
H_{surf}	total heat flux per area at the surface-water interface (W m^{-2})
H_t	total heat flux (W m^{-2})
I	total number of input nodes
i	input node
iw_{ij}	connection weights between the i^{th} input and j^{th} hidden node
J	total number of hidden nodes
j	hidden node
K_p	proportionality constant of the Bowen ratio (usually as 0.61)
K	thermal energy coefficient ($\text{W m}^{-1} \text{ } ^\circ\text{C}^{-1}$)
k	output node
k_m	thermal conductivity of the solid-fluid matrix ($2.2 \text{ W m}^{-1} \text{ } ^\circ\text{C}^{-1}$)
k_s	thermal conductivity of the solids ($2.79 \text{ W m}^{-1} \text{ } ^\circ\text{C}^{-1}$)
k_w	thermal conductivity of water ($0.590 \text{ W m}^{-1} \text{ } ^\circ\text{C}^{-1}$)
lw_{jk}	connection weight between the j^{th} hidden node and the k^{th} output node
<i>LSWM</i>	Little Southwest Miramichi River
N	number of hourly water temperature observations
n	porosity of the rock-fluid matrix (0.27)
n_j	weighted sums of inputs and bias at hidden node j

P	atmospheric pressure (mm Hg)
p	wetted perimeter of the river (m)
Q_g	groundwater flow ($\text{m}^3 \text{s}^{-1}$)
RH	relative humidity (%)
$RMSE$	root-mean-square error as defined in Equation (3.30)
R^2	coefficient of determination as defined in Equation (3.31)
t	time (hour)
T_a	air temperature ($^{\circ}\text{C}$)
T_e	equilibrium temperature ($^{\circ}\text{C}$)
T_g	groundwater temperature at specified (e.g. at 0.1 m)
T_p	rain temperature ($^{\circ}\text{C}$)
T_w	stream water temperature ($^{\circ}\text{C}$)
$T_w(O)$	observed water temperature ($^{\circ}\text{C}$)
$T_w(P)$	predicted water temperature ($^{\circ}\text{C}$)
T_z	streambed temperature at depth z (e.g. at 0.1 m) ($^{\circ}\text{C}$)
$T(z,t)$	riverbed temperature profile with depth z at time step t ($^{\circ}\text{C}$)
V	wind speed (m s^{-1})
v_g	vertical velocity component (negative for upwelling water) (m hour^{-1})
v_x	mean water velocity in direction of x-axis (m hour^{-1})
v_y	mean water velocity in direction of y-axis (m hour^{-1})
v_z	mean water velocity in direction of z-axis (m hour^{-1})
W	river width (m)
x	distance downstream (m)

x_i	i^{th} input node
y	longitudinal distance (m)
y_k	k^{th} output node
y_w	mean water depth (m)
y_p	precipitation (mm)
z	vertical distance (m)
α	slope of the linear regression between air and equilibrium temperature
β	intercept of the linear regression between air and equilibrium temperature
β_s	slope parameter of the sigmoid function
ε_a	atmospheric emissivity
ρ	density of water (1000 kg m ⁻³)
ρ_m	density of the rock-fluid matrix (2300 kg m ⁻³)
ρ_s	density of the sediments at the streambed (2578 kg m ⁻³)
σ	Stefan-Boltzmann constant (5.67 x 10 ⁻⁸ W m ⁻² K ⁻⁴)

ACKNOWLEDGEMENTS

I wish to thank all those people who made this thesis possible and an unforgettable experience for me.

First of all, I would like to express my sincere gratitude to my advisor Dr. M.G. Satish, for his continuous support of my research, and for his patience, motivation, enthusiasm, and immense knowledge. He also was of valuable assistance in the preparation and completion of the thesis.

A special thanks to Dr. Daniel Caissie from Fisheries and Oceans Canada who acted as a co-supervisor for my thesis. His valuable knowledge, comments and suggestions have been greatly appreciated.

I would like to thank other committee members, Dr. El-Jabi and Dr. Watts, and my external examiner, Dr. Nguyen, for their comments and questions. It has greatly contributed to improve my research and thesis. I would also like to thank Dr. Corinne McDonald, from Dalhousie University, who has helped me to extend my knowledge on ANN.

A sincere thank you to my good friend Julie, for her friendship and sincere opinion. Finally, I am very thankful to my family, Kaven, Sandrine and Alexandre for their love, support and encouragement. Merci!

Thank you!

CHAPTER 1: INTRODUCTION

1.1 GOAL AND OBJECTIVES

Water temperature has both economic and ecological significance when considering issues such as water quality and biotic conditions in rivers (Caissie, 2006). As such, fish habitat suitability is highly dependent on stream water temperatures. The thermal regime of rivers is influenced by many factors such as atmospheric conditions, topography, riparian vegetation, stream discharge and streambed thermal fluxes (Poole and Berman, 2001; Caissie, 2006; Webb *et al.*, 2008). It is therefore important to use adequate water temperature modeling approaches to effectively predict water temperature variability.

Water temperature controls the rate of decomposition of organic matter, dissolved oxygen content, and chemical reactions in general. Stream water temperatures have been studied for many years (Macan, 1958; Raphael, 1962; Brown, 1969). Stream water temperature can also impact recreational activities such as swimming and fishing. Early studies mainly focused on the impact of forest harvesting on water temperature, whereas, recent studies have focused on issues related to fish-habitat. For example, studies have found that stream temperature dynamics can influence the habitat conditions and growth rate of different fish species, aquatic invertebrates and other water dwelling animals (Markarian, 1980; Wichert and Lin, 1996; Beitinger and Bennett, 2000; Cox and Rutherford, 2000a, 2000b). Stream temperatures have also been monitored in order to evaluate the impact of human activities due to urbanization (Kinouchi *et al.*, 2007; Nelson and Palmer, 2007), thermal pollution (Bradley *et al.*, 1998) and land-use activities

(Nagasaka *et al.* 1999). Flow reduction and flow alteration have also been observed to have an impact on the thermal regime of rivers (Morin *et al.* 1994; Sinokrot and Gulliver 2000). Understanding of the thermal regime of rivers in forested ecosystems has played an important role in the development of water temperature models. Valuable information was gained from the study of heat exchange processes in forested ecosystems, such as the contribution by solar radiation and conduction (Sridhar *et al.*, 2004; Moore *et al.*, 2005b). Increased interest has also been noted due to the potential effects of climate change on river thermal regimes (Morrison *et al.*, 2002; Morrill *et al.*, 2005; Tung *et al.*, 2006).

Very few studies have predicted hourly stream temperatures, focusing mostly on daily mean water temperatures (Bélanger *et al.*, 2005; Caissie *et al.*, 2007; Larnier *et al.*, 2010). Hourly water temperatures give a better understanding of how much stream temperature varies during the course of the day and to what extent the variation occurs. It also provides minimum and maximum temperature values useful as boundary conditions for water quality modeling (Flint and Flint, 2008) or to assess the stress and recovery period of aquatic resources during high temperature events (Breau *et al.*, 2007).

The goal of the research described herein is to develop hourly water temperature models and apply them to two thermally different streams in two forested catchments of the Miramichi River in New Brunswick. This region is world renowned for its population of Atlantic salmon and offers long-term monitoring of meteorological and hydrological data. The three models selected were: 1) a deterministic model, 2) an equilibrium

temperature model, and 3) an artificial neural network model. The specific objectives of each stream temperature model are described in the following section.

1.1.1 DETERMINISTIC MODEL

Deterministic models estimate changes in river water temperature from energy fluxes at the water-surface interface and at the streambed-water interface. A number of studies have used heat budget models to predict variability in river water temperatures (Evans *et al.*, 1998; Younus *et al.*, 2000; Caissie *et al.*, 2007; Hannah *et al.*, 2008); however, few included stream microclimate conditions as well as the streambed heat flux to predict water temperatures at the hourly time scales. The objective of using the deterministic model was to examine, in detail, the relative contribution of surface vs. streambed heat fluxes for two watercourses under varied meteorological conditions. This was done at specific times to capture various seasonal and climatic conditions. The specific objectives of deterministic modeling are: 1) To develop a heat budget model for two thermally different rivers (Catamaran Brook and Little Southwest Miramichi River, New Brunswick, Canada) using stream microclimate data, 2) To compare observed vs. predicted total heat fluxes for these two watercourses, and 3) To compare the relative contribution of heat fluxes at both the air-water interface and at the water-streambed interface.

1.1.2 EQUILIBRIUM TEMPERATURE MODEL

Deterministic models can be complex and the data needs extensive if all heat components are considered, and the required meteorological and hydrological data are not easily

obtained and accessible. The equilibrium temperature model was first developed to simplify the determination of the total heat flux (Edinger *et al.*, 1968; Chaudhry *et al.*, 1983; Jeppesen and Iversen 1987). The total heat flux at the surface is assumed to be proportional to the difference between the water temperature and an equilibrium temperature T_e (Caissie *et al.*, 2005). Many studies have used the concept of the equilibrium temperature to estimate stream temperatures (Mohseni and Stefan, 1999; Bogan *et al.*, 2003, 2004; Caissie *et al.*, 2005; Marcé and Armengol 2008; Larnier *et al.* 2010); however, few studies have tested this model at an hourly time scale, due to unavailability of hourly data.

In this study the total heat flux was estimated using a function of water temperature and equilibrium temperature. A linear relationship between the equilibrium temperature and air temperature was also assumed, as in Caissie *et al.* (2005). An objective of this study is therefore to develop an hourly water temperature model using the equilibrium temperature concept and to apply this model to two thermally different streams within the Miramichi River basin system.

1.1.3 ARTIFICIAL NEURAL NETWORK MODEL

Artificial neural networks (ANN) have been widely used in the field of hydrology, since the 1990's. Examples include the modeling of precipitation and runoff, water demand predictions, groundwater modeling, and water quality modeling (Govindaraju, 2000a). ANN have become an interesting modeling tool for many reasons. One of the main reasons is the fact that the ANN algorithm has the capacity to recognize relations between

input and output variables without requiring physical explications. This approach can be very useful in hydrology because many of its processes are non-linear, complex, or mathematically incomplete. Artificial neural networks also work well when the data sets contain noise due to the distributed processing within the network (Govindaraju, 2000a). Once calibrated, ANN models are simple to use. Although ANN have been applied in many hydrological studies in recent decades, very few of these studies have dealt with the modeling of river water temperatures (Risley *et al.*, 2003; Bélanger *et al.*, 2005; Karaçor *et al.*, 2007; Sivri *et al.*, 2007; Chenard and Caissie, 2008), especially in an hourly time step (Risley *et al.*, 2003).

Therefore, the objective of this component of the study is to develop an ANN model to predict hourly river water temperatures using minimal and accessible input data. This model was applied to two thermally different watercourses and its performance was compared to other water temperatures models.

1.2 THESIS OVERVIEW

Chapter 2 is a literature review of the processes governing fluvial thermal regimes, its impacts and its influences. Stream temperature models have been in existence for many years, and have been applied in different scientific disciplines. Water temperature studies on aquatic ecosystems and habitat, and the impact of different anthropogenic impacts (forest harvesting, climate change, and streamflow modifications) are also presented. A review of water temperature models used in this study is also presented. This chapter reviews studies using deterministic models, equilibrium temperature models, artificial

neural network models, stochastic models and other types of water temperature models. The methodology describing the detailed application of the three water temperature models used in this study is presented in Chapter 3. Also presented is information on the study area where the models were applied, data collection, and the model performance criteria. Detailed results of water temperature models are presented in Chapter 4 and are discussed in Chapter 5, as along with a comparison between them. Chapter 6 gives the overall conclusion for each specific model and recommendations for future research on water temperature modeling.

CHAPTER 2: LITERATURE REVIEW

The study of stream water temperatures has been of interest to the scientific community for many years (Macan, 1958; Brown, 1969; Hopkins, 1971; Smith, 1972; Vannote *et al.*, 1980; Ward, 1985). In recent years, new technological developments (such as mini data loggers) have facilitated the measurement and the monitoring of stream temperatures and have permitted the development of new techniques for data analysis and modeling (Moore *et al.*, 2005b; Caissie, 2006). This chapter provides a literature review of studies describing the thermal regime and its associated biological impacts of rivers (mainly aquatic habitat). Anthropogenic impacts on stream temperatures, such as timber harvesting and climate change, are also reviewed. The last section provides a review of the different water temperature models used by previous investigators that were also used in this study (deterministic, equilibrium temperature and artificial neural network models) as well as a limited review of certain other models.

2.1 THERMAL REGIME OF RIVERS

The thermal regime of a river is the range and timing of water temperatures experienced in the stream, for a selected period (annual, seasonal, diurnal). Many factors can influence the thermal regime. These can be classified using various methods. Poole and Berman (2001) separated the factors influencing the thermal regime into two categories: internal and external factors. External factors consider the net energy and water inputs. Internal factors are related to the fluvial processes and river characteristics, for example,

riparian zone features, and surface/subsurface water interactions). Temporal and spatial changes in these factors affect and alter water temperature variability along river reaches.

River water temperatures can also be influenced by such factors as atmospheric conditions, topography, stream discharge, and riverbed thermal fluxes (Caissie, 2006). Atmospheric conditions represent the most influential category. These are principally responsible for the heat exchange process at the water surface. Included in this category are solar radiation, air temperature, humidity, and wind speed, and the type and quantity of precipitation. Topography includes latitude/longitude, riparian vegetation, geology, azimuth of the reach and upland shading. Human activities, like timber harvesting, can affect some topographic factors (riparian vegetation), resulting in an increase in river water temperatures, especially for small streams. Stream discharge factors are primarily related to hydraulic conditions (e.g, surface area and water volume). Some stream discharge factors are extremely important, like the volume of water, whereas others can be neglected, like the slope or waterfalls. Streambed conditions can also influence the thermal regime depending on the heat exchange processes at the riverbed. These factors mainly include the heat conduction at the riverbed and the contribution of groundwater flow. Streambed fluxes have been considered in a few studies (Jobson, 1977; Sinokrot and Stefan, 1993; Hondzo and Stefan, 1994; Kim and Chapra, 1997; Webb and Zhang, 1997; Evans *et al.*, 1998); however, as evident from the available literature, this subject has not been thoroughly studied.

The thermal regime of rivers has been widely studied for many years. For example, Macan (1958) studied the seasonal trends in water temperature as well as the influence of

sunshine and other parameters related to water temperature. This descriptive study concluded that the diurnal variation of water temperature was more significant during periods of a clear sky. The largest diel fluctuations in water temperature are generally observed in summer while the smallest diel fluctuations are generally observed in winter, as reported in a study on the Hinaiu in New Zealand (Hopkins, 1971). On a seasonal basis, water temperature varies from the lowest values in spring to maximum water temperature in mid-summer, followed by a cooling period in autumn prior to winter conditions (Vannote *et al.*, 1980). This phenomenon is important for ecological processes and for the flora and fauna of the river's environment (Vannote *et al.*, 1980). Daily fluctuations can be observed on a local scale or along a reach of a stream. For example, upstream waters are generally colder due to groundwater contributions (Vannote and Sweeney, 1980); water temperature tends to be warmer downstream due to a longer run and exposure to heat sources (Danehy *et al.*, 2005). Diel variations are also dependent on climate and physical characteristics of rivers. For example, the downstream sections of rivers are deeper and diel variations are less significant than sections upstream where the depth of water is small. All of these seasonal or daily variations of stream water temperatures are important for aquatic resources. This concept is explained in greater detail in the 'River Continuum Concept' (Vannote *et al.*, 1980).

An important research work on the thermal regime was conducted by Ward (1985) on many rivers in the southern hemisphere. Ward (1985) also observed that diel fluctuations increased further downstream where water sources are less dominated by groundwater and the stream is more exposed to meteorological conditions. Diel fluctuations decreased further downstream in rivers where water depths increased (Ward, 1985). This study also

concluded that the difference in the thermal regime between the southern and northern hemispheres was mainly related to the size of rivers and not to the thermal process. Another factor making the comparison difficult was the presence of particular arid and semi-arid zones in the southern hemisphere, mainly in Australia.

A study by Smith (1972) tried to categorize, without success, the thermal regime of rivers using latitude and altitude as the dominant factors. Due to the complex nature of the thermal process in rivers (Smith, 1975; Smith and Lavis, 1975), no other studies have tried to categorize the thermal regime according to geographical positions. Some studies have shown relations between different parameters of thermal regime. For instance, Webb and Walling (1986) established a relationship between mean temperature and the watershed elevation. However, it was difficult to state specifically that there was a relationship between the mean temperature and watershed elevation because stream water is usually colder at higher elevations. The latitudinal difference in climatic parameters (e.g. air temperature) may be a major influence on stream thermal regime (Liu *et al.*, 2005). Another study investigated the daily and seasonal water temperature to show a relation between water temperature and other parameters such as the stream order, groundwater contribution and cold-water tributaries (Arscott *et al.*, 2001). The temperature variability of a stream is also highly related to the dynamics and proximity of the water source and pathway contributions, the hydro-climatological conditions, streamflow volume and basin characteristics as reported in Brown *et al.*, (2005) and Cadbury *et al.* (2008).

Using multiple linear regressions, the elevation and azimuth were found to be important variables in explaining the average daily temperature patterns (Brown and Hannah, 2008). Water temperature is influenced by micro-thermal conditions, because thermal conditions can often vary greatly within only a few meters of depth (Clark *et al.*, 1999). The thermal regime can also depend on the type of river (Mosley, 1983).

Kobayashi *et al.* (1999) observed evidence of major contributions of subsurface water to stream water. Notably, stream temperature gradually decreased during summer rainstorms after streamflow peaked. Soil temperature increased with depth during the snowmelt period but decreased with depth during the summer. During storm flow recession, stream temperatures related to extreme events (summer storm or snowmelt) were similar to the soil temperature at 1.8 m below the land surface, suggesting that subsurface water contributions to streamflow are derived from this depth. Water temperatures differences within the region can be explained mainly by latitude, but also by morphological conditions, hydrology, water usage, elevation, slope, timber harvesting (Mohseni *et al.*, 2002). Other studies have shown basin-scale stream temperatures are strongly affected by streamwater sources, as well as basin characteristics like altitude, azimuth and stream length (Brown and Hannah, 2008).

2.2 AQUATIC ECOSYSTEMS

Aquatic life and habitats greatly depend on stream temperatures. Researchers have found that stream water temperatures influence aquatic organisms differently (Markarian, 1980; Wichert and Lin, 1996; Beitingger and Bennett, 2000; Cox and Rutherford, 2000a, 2000b). The growth rates of fish and aquatic species distribution are examples of the influence of

the thermal regime of rivers. It is therefore important to have good knowledge of the biological implications of river water temperatures. A change in thermal regime can seriously affect habitat quality and life conditions of aquatic species (Jonsson and Jonsson, 2010). Many studies have researched the implication of thermal regime on water quality, flora and fauna. Most of the studies on the influence of thermal regime on aquatic habitat were carried out during summer months (Elliot and Hurley, 1997; Johnston, 1997; Ebersole *et al.*, 2001; Robinson and Child, 2001; Swansburg *et al.*, 2002). Most of the significant changes in water temperatures occurred throughout the summer, with only some minor variations in winter (Marsh, 1990).

Coutant (1999) was interested in the thermal effect on aquatic organisms as well as the factors influencing thermal regime of rivers. The thermal regime of a river can affect the growth of fish (Edwards *et al.*, 1979; Elliot and Hurley, 1997), and this influence can differ between different life stages (Huntsman, 1942; Garside, 1969; Robinson and Childs, 2001). Another study looked at the combined effect of high water temperatures and low flows on the growth of Atlantic salmon (Swansburg *et al.*, 2002). The thermal regime can also be used as a prediction model of conditions within aquatic ecosystems. For example, Crisp and Howson (1982) managed to predict the growth of trout using regression analysis for periods of 5 to 7 days.

Fish prefer specific temperatures which influences their distribution throughout a stream (Coutant, 1977; Wichert and Lin, 1996). Aquatic organisms are more sensitive to water temperatures above their thermal maxima than they are to those temperatures below their thermal maxima (Hester and Doyle 2011). During high temperatures, salmonids tend to

congregate in specific areas of streams or in thermal refugia (Ebersole *et al.*, 2001). As such, fish tend to cluster in cooler zones, increasing their population density at those sites. Ebersole *et al.* (2001) observed that 10% to 40% of fish populations were crowded in thermal shelters during high mid-day temperatures. Shading in streams can also provide cold-water patches, which can be potential thermal refuges for cold-water fishes during periods of heat stress (Ebersole *et al.*, 2003). Stream temperature is one of the most important variables in determining microhabitat choice for fishes (Baltz *et al.*, 1987). Torgersen *et al.* (1999) observed that behaviour of salmonids can be modified at high water temperatures as this study also reported clustering of fish in cooler areas. Thermal patches in streams should be recognized for the biological potential to provide habitat for species at the limits of their thermal tolerances (Torgersen *et al.*, 1999). Temperature can also influence the movement of fish (Johnston, 1997; Jensen *et al.*, 1998; Hembre *et al.*, 2001), migration (Hembre *et al.*, 2001; Schindler, 2001) and impact on the swimming performance of fish (Myrick and Cech, 2000).

Diel water temperature variations can also affect the mortality, stress or energy reserve of salmonids (Thomas *et al.*, 1986). In North America, fish species already live at their upper limits when it comes to water temperatures (Sinokrot *et al.*, 1995). Lund *et al.* (2002) have studied the impact of water temperatures on Atlantic salmon parr both in the wild and in the laboratory. This study concluded that if juvenile salmon were exposed to high water temperatures over a long period, they would undergo severe protein damages. Another study on Atlantic salmon noted that high temperatures increased the mortality of large salmon first, followed by small salmon and then parr (Huntsman, 1942). For instance, temperatures between 23°C and 25°C amplified the risk of mortality in trout

(Lee and Rinne 1980); temperatures between 27°C and 28°C increased the mortality in juvenile Atlantic salmon (Garside, 1973).

Aquatic species can be affected not only by the temperature within the water column, but also by the temperature within the riverbed or stream substrate (Meisner *et al.*, 1988; Crisp, 1990; Evans *et al.*, 1995; Acronley, 1999; Cox and Rutherford, 2000b). Since many aquatic species use the riverbed for spawning and laying eggs, their development is directly influenced by stream conditions (Combs and Burrows, 1957; Combs, 1965; Alderdice and Velsen, 1978; Beer and Anderson, 2001). In fact, the hatching of Atlantic salmon eggs is highly influenced by water temperature, as reported in Johnston (1997). Optimal incubation periods are situated around 6°C (Peterson *et al.*, 1977). Other studies showed that streambed temperature influenced the streams by eliminating frost conditions on rivers in winter and reducing high stream temperatures in summer (Webb and Walling, 1993). This study showed that the hatching period could be advanced by more than 50 days depending on temperature conditions.

Riparian vegetation also plays an important role in stream temperature dynamics by providing shade for aquatic fishes (Beschta, 1997). The increase in stream temperatures as a result of canopy removal can cause high stress levels, greater vulnerability to disease, and make aquatic species defenceless against predators. Water temperatures help to regulate the biological activity of aquatic organisms; biological activity has been shown to double for every 10 °C increase in water temperature (Brown and Krygier, 1967). The

rate of food evacuation and feeding activity of fishes are also influenced by water temperatures (Salvatore, 1987).

2.3 HUMAN IMPACTS

2.3.1 FOREST HARVESTING

Knowing the thermal regime of rivers in forested ecosystems is important in water temperature modeling. It provides information on the heat transfer process and the solar radiation contribution. The impact of timber harvesting is a very common study subject found in literature on thermal regime of forested ecosystems. Many studies have shown increases in stream water temperatures following forest harvesting, caused primarily by changes in solar radiation, but also influenced by stream hydrology and morphology (Moore *et al.* 2005b). Brown and Krygier (1970) studied the long-term effects of two clear-cutting operations on the thermal regime of two small streams in Oregon. The annual maximum temperature increased from 14 °C to 30 °C one year after logging began. This was mainly caused by stream exposure to direct solar radiation. An important study over a 30 year period on Salmon Creek (Oregon) observed an increase in daily maximum and minimum water temperatures of 6 °C and 2 °C after timber harvesting (Beschta and Taylor, 1988). Additional impacts of timber harvesting were related to the occurrence of major floods. Another study (1969-1989) on the same stream demonstrated an increase of water temperature of 8 °C (Hostetler, 1991). A more recent study conducted on a clear-cut stream in British Columbia observed a daily maximum temperature increase of up to 5 °C after logging (Moore *et al.*, 2005a).

A study on the Alsea River (Oregon) observed an increase of 7.8 °C on mean annual water temperature due to the impact of cutting down the trees on a river floodplain (Brown and Kryeger, 1967). This same study highlighted the fact that small streams are more vulnerable to small increases in water temperature due to their weak thermal capacity caused by having a small water volume. Another study evaluating the impact of timber harvesting on small streams observed an increase of 6.7 °C in water temperature (Swift and Messer, 1971). Rayne *et al.* (2008) undertook a 3-year study in the Nicola River watershed in British Columbia, to examine the impact of removing riparian vegetation on water temperatures in headwater streams with lentic sources such as wetlands and lakes. The removal of riparian shade was found to increase the maximum water temperatures by 1 °C to 2 °C. Using long-term data, Johnson and Jones (2000) found an increase of 7 °C in the maximum water temperature after the removal of some riparian vegetation. St-Hilaire *et al.* (2000) did not find a significant impact of timber harvesting on water temperatures, but observed an increase during summer storm events.

Timber harvesting can affect streams for many years after logging. Murray *et al.* (2000) estimated a 5 to 15 years period for a stream to find its natural thermal regime after the loss in riparian vegetation. Brown and Krygier (1970) showed a 6 year period was required for the recovery of maximum summer temperatures. Studied streams in Oregon have only returned to pre-harvesting conditions after 15 years according to Johnson and Jones (2000). Macdonald *et al.* (2003) have studied the water temperatures before and after timber harvesting following different cutting scenarios. Five years after the cutting, water temperature stayed within 4 °C to 6 °C higher than normal and diurnal variation was higher regarding the selected treatment.

Partial timber harvesting can also influence the thermal regime of rivers. One study showed an increase of 5 °C in the summer water temperature after a cut of 66% of the vegetation in the buffer zone for a period of more than 7 years (Feller, 1981). Jackson *et al.*, (2001) noted increases for only 2 of 7 clear-cut streams in their study. They supposed that the layer of slash left after logging was deposited along the stream and acted as an insulating blanket.

Studies have shown that the greatest impact on stream water temperature following timber harvesting is usually observed in summer (Gray and Evington, 1969; Brown and Kryeger, 1970; Feller, 1981; Moore *et al.*, 2005b). A study of Rishel *et al.* (1982) has shown an increase in summer mean and maximum water temperatures, as well as a change in their duration. Winter stream temperature changes have not been well documented but appear to be smaller in magnitude (Moore *et al.*, 2005b). For example, Holtby (1988) observed an increase in water temperature due to logging (Carnation Creek) mainly in summer (3.2 °C in August) but also in winter (0.7 °C in December). Streams showed significant changes in stream temperature as early as February and as late as November (Lynch *et al.*, 1984). The effects of riparian vegetation can be observed throughout the year; however, they are most noticeable during spring and reach a maximum in summer (Malcolm *et al.*, 2008). Holtby and Newcombe (1982) observed stream water warming as well as an augmentation in diel variation in Carnation Creek. Another study examining the impact of riparian vegetation on the West Coast showed that changes in water temperatures were mainly observed at high water temperatures (Mitchell, 1999). For instance, no changes were observed for water temperatures lower

than 3 °C. But the augmentation was in the order of 2 °C to 3 °C for water temperatures exceeding 15 °C.

The development of good water temperature models is essential to estimate the impact of timber harvesting on stream water temperatures. Brown (1970) stipulated that river water temperatures are directly proportional to the increase in heat inputs and inversely proportional to streamflow. A model estimating solar radiation using the sun's position, stream location and orientation was developed by Chen *et al.* (1998a). This model was then applied at the Upper Grande Basin (Oregon) to study different scenarios of riparian vegetation restoration (Chen *et al.*, 1998b). Groundwater flow can also play a role in stream cooling after clear-cut logging as reported by Mellina *et al.* (2002). A slight cooling of streams was also observed due to increased mid-summer discharges caused by timber harvesting (Gravelle and Link, 2007). In Georgia, a study examined the impact of forest harvesting on a river with a 12 m wide buffer zone (Hewlett and Fortson, 1982). The study predicted an increase of 3.2 °C in stream temperatures while they actually observed an increase of about 9 °C. Shanley and Peters (1988) demonstrated groundwater contributions to the thermal regime in the Georgia Piedmont watershed. This study showed that groundwater inputs during storm events can affect short-term water temperature behaviour in small catchments.

Some studies looked at the impact of timber harvesting on aquatic resources. A study of timber harvesting on Carnation Creek (BC) confirmed that water temperature changes could affect aquatic resources (Holtby, 1988). Water temperature changes seemed to affect the development of the flora and fauna for many years after logging (Lynch *et al.*,

1984; Holtby, 1988; Hostetler, 1991), especially at low streamflow (Hetric and Brusven, 1998). For example, higher water temperatures in winter can force fishing movement downstream as much as six weeks earlier than usual (Scrivener and Andersen, 1984). This premature movement of fish could result in early arrival at sea resulting in a limitation of food resources. Curry *et al.* (2002) noticed a warming in autumn and spring for 2 years after initial harvesting that could alter many biological processes. Sensitive stage of aquatic biota could be affected by time shifting of summer maxima and increase in early summer stream temperatures (Mitchell, 1999).

Studies have also shown the importance of vegetation in buffer zones near streams for protection against the heating processes (Burton and Likens, 1973; Zwieniecki and Newton, 1999; Leblanc and Brown, 2000; Murray *et al.*, 2000; Dent *et al.*, 2008; Hrachowitz *et al.*, 2001). Some studies have shown, though, that buffer zones did not provide significant protection against the increase of water temperatures (Hewlett and Fortson, 1982; Brosfokske *et al.*, 1997; Curry *et al.*, 2002; Sridhar *et al.*, 2004). The thermal regime of rivers can be affected after clear-cut harvesting with or without a riparian buffer strip. Other vegetation parameters like leaf area index, average tree height, and streamside vegetation buffer width, are more closely correlated with maximum stream temperature (Sridhar *et al.*, 2004). Channel morphology and stream orientation can influence the exposure to solar radiation and therefore the effectiveness of buffer zones in response to clear-cut harvesting (Gomi *et al.*, 2006). In a small stream in western Washington, Brosfokske *et al.* (1997) showed that even with a more conservative buffer zone, the microclimate conditions near some streams were altered. Chen *et al.* (1995) also discussed the effect of clear-cut on microclimate. A temperature rise as much

as 11 °C was observed even though a partial buffer strip of trees and shrubs was left in place to provide shades for the stream (Hewlett and Fortson, 1982).

Theurer *et al.* (1985) have studied the impact of vegetation restoration on the Tucannon River (USA). This vegetation has decreased mean daily and maximum water temperatures to improve the quality and availability of aquatic habitat. Maximizing riparian vegetation along streams can considerably reduce the lethal stream temperatures for aquatic habitat as reported by Chen *et al.* (1998). Since small streams (shallow depth and small discharge) are very sensitive to ambient air temperature and solar radiation, buffer strips or riparian vegetation should be protected along small streams suffering from timber harvesting (Mitchell, 1999). Riparian vegetation can also help regulate water temperatures and decrease the amplitude of the diel temperatures by moderating daytime high temperatures and low temperatures at night (Leblanc and Brown, 2000). Webb and Crisp (2006) examined the outcome of planting coniferous forests on a stream's thermal regime. Mean water temperatures were lowered by approximately 0.5 °C with the largest reduction being observed in summer. Johnson (2004) studied a reach having a width of 150 m under the influence of experimental shading. This study showed that maximum water temperatures declined significantly in the shaded reach, but minimum and mean temperatures were not modified.

Bartholow (1991) investigated the impact of irrigation on water temperature on La Poudre River in Colorado. He concluded that an increase of 13- 23% in riparian vegetation, with an increase in discharge of 3 m³ s⁻¹, could maintain a water temperature within acceptable levels. In some cases, the riparian buffer zones have been shown to decrease the loss of

energy of a stream by acting as a protective cover (Murray *et al.* 2000). The strongest effect of air temperature and relative humidity can generally be measured within 10 m of a stream, although buffer zones of 30 m in width were suggested for three streams in western Oregon (Rykken *et al.*, 2007).

Zwieniecki and Newton (1999) studied the impact of variable buffer zone width on river water temperatures. After timber harvesting, they observed a warming trend along the river to a distance of 150 m from the buffer zone. They concluded that even with timber harvesting, buffer zones were adequate to protect streams against warming, with the exception of a few small streams. Davies and Colley (2000) suggested a forest buffer width of at least 40 m to protect streams in New Zealand. Wilkerson *et al.* (2006) studied 15 streams in western Maine having different treatments of timber harvesting, namely clearcutting with and without a stream buffer, partial cuts, and un-harvested zones. Streams without a buffer zone experienced an increase in weekly mean water temperatures of 1.4 °C to 4.4 °C. They concluded that an 11 m buffer width was required to protect against the effects of clear-cutting.

Beschta (1997) studied the relationship between riparian vegetation, shade and stream temperatures. He found that riparian vegetation could directly and indirectly affect stream temperatures. Riparian vegetation protects the water surface from sunlight and therefore increases solar inputs. Beschta (1997) also found that an un-shaded stream absorbs more than 90% of the solar energy. This study showed that less riparian vegetation can also cause an increase in water temperature as a result of erosion which causes widening of the bed and reduction of the water depth. However, other studies

showed no clear relationship between the forest buffer strip width and the warming of streams (Bourque and Pomeroy, 2001). Buffer zones were not sufficient to protect stream temperatures in the Cascade Mountain Range in western Washington (Dong *et al.*, 1998). Forest buffers provided minimum protection for high stream temperature periods in July, but were more effective in early and late summer. Some temperature models have also included a shading effect to improve their predictability (Tung *et al.*, 2007). Buffer protection against the increase in water temperature is a function of water volume, the stream width, the structure and orientation of vegetation and the area exposed to sun and solar radiation (Larson and Larson, 1996).

2.3.2 CLIMATE CHANGE

Many studies have looked at the impact of climate change on river water temperatures (Meisner, 1990). However, the impact of climate change is difficult to predict due to a lack of long-term water temperature data (Webb, 1996). In eastern Canada, the air temperature is expected to increase by 2 °C to 6 °C in the next 100 years (Parks Canada, 1999). Such an increase will greatly affect stream water temperatures.

Kjellström *et al.* (2007) have studied monthly mean water temperatures from 1901-2000 in three Austrian rivers. Comparison with historical data showed that the predicted changes in extreme temperatures are larger than the natural variability observed during the last century. Extreme temperatures are expected to be greater with climate change. For example, cold temperatures in winter are to decrease and warm summer temperatures are projected to increase. . Studies have shown that long-term trends can be influenced

by catchment characteristics, and contrasts between headwater tributary, outlet and mainstream are observed (Webb and Nobilis, 2007).

Studies conducted on Fraser River (BC) established that climate change could modify the arrival of peak flow and raise summer temperatures (Morrison *et al.* 2002). Summer water temperatures were predicted to increase by 1.9 °C. This study showed that the number of days exceeding 20 °C could also increase. Another study showed that the greater increase in water temperatures would not be in summer, as reported in most studies, but in autumn and winter (Moore *et al.*, 1997). According to different scenarios of climate change, global warming could extirpate some aquatic species or modify their distribution in river systems (Minns *et al.*, 1995; Mohseni *et al.*, 2003). Results by Minns *et al.* (1995) showed a decline in precipitation and in the number of rainy days, as well as an increase in annual maximum temperatures under climate change scenarios. An increase in water temperatures combined with a predicted reduced precipitation could greatly affect the water quality of streams (Nimikou *et al.*, 2000). Morrill *et al.* (2005) are predicting an increase of 2 °C to 3 °C in stream temperatures resulting from an increase of 3 °C to 5 °C in air temperatures. The River Dee in Scotland has experienced an increase in mean daily maximum stream temperatures in winter and spring since the 1960's (Langan *et al.*, 2001). Foreman *et al.* (2001) estimated a warming of 0.022 °C per year (1953-1998) on the Fraser River tributary (BC) due to climatic warming effects.

Increases in summer water temperatures due to climate change could cause the dissolved oxygen in the water to decrease and aggravate the effects of acid precipitation, threatening the growth and life of many aquatic species (Hill and Magnuson, 1990;

Schindler, 2001; Gooseff *et al.*, 2005). Major reductions in stream habitat could result from climate warming for cold and cool water fish species (Eater and Scheller, 1996). Changes in growth rate of fish may be possible, especially in spring and autumn, caused by the increase of water temperature (Hills and Magnuson, 1990). Global warming may also increase groundwater temperatures, affecting the incubation of eggs within the stream substrate (Meisner *et al.*, 1988). Hrachowitz *et al.* (2010) have shown that under a climate change scenario with an increase of 2.5 °C or 4 °C in air temperatures, the thermal habitat of Atlantic salmon and brown trout could potentially be altered.

Cooter and Cooter (1990) predicted that water surface could increase up to 7 °C in the southern United States. Mohseni *et al.* (1999) studied 803 streams from the United States. From these 803 streams, only 39 were found not to be influenced by climatic change. The other 764 streams are projected to increase by 2 °C to 5 °C of their mean annual temperature.

Under an atmospheric CO₂ doubling scenario, Pilgrim *et al.* (1998) estimated an average 4.1 °C increase in stream temperature. Tung *et al.* (2006) predicted an increase of 0.5 °C to 2.9 °C in annual average stream temperatures. When studying forcing parameters, Mohseni and Stefan (1999) showed that water temperatures cannot rise indefinitely due to evaporative cooling at high air temperatures. Upper bound stream temperature represents the highest temperature a stream can physically attain without anthropogenic influences (Mohseni *et al.*, 2003). Climate change effects on stream temperatures will be less than to the changes to air temperature (Bogan *et al.*, 2006), mainly due to evaporative cooling.

Another study stated that under a climate change scenario, all water coming from surface overflows (dams, reservoir and lakes) are going to experience the highest impact (Sinokrot *et al.*, 1995). Riparian vegetation is a proposed solution to minimize the increase of water temperatures due to climate change (Cooter and Cooter, 1990).

2.3.3 STREAMFLOW

Stream temperatures can be as sensitive to streamflow as to meteorological parameters (air temperature, humidity and solar radiation) (Gu and Li, 2002). Decreases in streamflow have been shown to increase water temperatures (Morse, 1972; Dymond, 1982; Hockey *et al.*, 1982; Sinokrot and Gulliver, 2000). This becomes more severe with higher air temperatures. Policies and management options should include streamflow as a critical water quality parameter by increasing flows (decreasing water temperatures) to protect aquatic habitat (Neumann *et al.*, 2006).

Stream flows have a greater impact on stream temperatures over short time scales (e.g. hourly) and for large streams (Webb *et al.*, 2003). A modification in the flow regime can also affect water temperatures in rivers, like a reduction by extraction or diversion of water for hydroelectric projects (Morse, 1972). This situation can increase water temperatures by 1 °C to 2 °C. Extraction of water in a stream can reduce its thermal capacity and results in higher maximum stream temperatures and lower minimum stream temperatures (Dymond, 1982). Sinokrot and Gulliver (2000) confirmed that a reduction in discharge could influence the maximum temperature during low flows in summer and that an increase in discharge could not eliminate, but lower, the risk of occurrence of high temperatures. Hockey *et al.* (1982) studied this type of impact on the Hurunui River

(New Zealand) using a deterministic model. Stream flow was reduced from $62 \text{ m}^3 \text{ s}^{-1}$ to $10 \text{ m}^3 \text{ s}^{-1}$ and water temperatures exceeded $22 \text{ }^\circ\text{C}$ for more than six hours.

The thermal regime of rivers with downstream reservoirs tends to react differently than unregulated rivers. Thermal impacts of regulated rivers include the rise in mean water temperatures, the delay of the annual cycle and the reduction of diel fluctuation (Webb and Walling, 1996). Thermal pollution caused by heat discharges from power plants or wastewater treatment plants can be harmful to aquatic species by increasing the risk of occurrence of high water temperatures (Bradley *et al.*, 1998; Wright *et al.*, 1999). Increasing stream discharge can reduce the amplitude of daily temperature variation, lower the daily maximum water temperature, and reduce the amplitude of water temperatures over a day (Gu, 1998). Daily maximum stream temperatures are more sensitive to flow rate change than daily mean stream temperatures (Gu *et al.*, 1998; Gu and Li, 2002). Thermal regimes downstream of reservoirs are very complex to model as they depend on many factors (Webb and Walling, 1997). The warming trend of water temperatures during open water conditions following the construction of a reservoir on the Lena River watershed could result in earlier snowmelt (Liu *et al.*, 2005).

Water diversion impact in mountain streams was studied by Meier *et al.* (2003). This study showed that water diversion can cause an increase of summer stream temperature ($3.7 \text{ }^\circ\text{C}$) and a decrease of winter stream temperature ($1.8 \text{ }^\circ\text{C}$). High stream temperatures caused by water diversion could increase thermal stress to migrating sockeye salmon (Mitchell *et al.*, 1995). Morin *et al.* (1994) estimated an increase of $1 \text{ }^\circ\text{C}$ to $2 \text{ }^\circ\text{C}$ in stream temperature due to water diversion on the Moisie River.

2.4 WATER TEMPERATURE MODELS

Water temperatures models can be classified into two groups: Deterministic or statistical (Caissie, 2006). The statistical approach predicts water temperatures by relating water temperatures to relevant meteorological parameters (usually air temperature). The deterministic model considers the cause and effect relations between meteorological parameters and the river ecosystem (Raphael, 1962; Morin and Couillard, 1990, Morin *et al.*, 1994). Each approach has strengths and weaknesses; however, when comparing performances, very few differences are generally observed (Marceau *et al.*, 1986).

2.4.1 DETERMINISTIC MODELS

Deterministic models can predict changes in water temperatures when a stream is subject to thermal pollution (Hills and Viskanta, 1976), climate change (Gooseff *et al.*, 2005), land use (Leblanc *et al.*, 1997) or flow reduction (Morin *et al.*, 1994; Mitchell *et al.*, 1995; Meier *et al.*, 2003) among others. Deterministic models are well adapted to thermal effluent problems (mixing effluent) and flexible when dealing with changes in input parameters and different scenarios (Caissie, 2004). They are also very useful for environmental impact studies (Marceau *et al.*, 1986; Morin *et al.*, 1994). The major disadvantage of this type of model is the large number of input parameters required to run the model since most meteorological parameters are not usually available from weather stations. Some of the most commonly used parameters are the net shortwave radiation, net longwave radiation, convection, evaporation/condensation, precipitation, streambed (sediment/geothermal), groundwater and friction (Caissie, 2004). The two most important parameters in deterministic models were found to be air temperature and solar radiation (Sinokrot and Stefan, 1994). For example, Webb and Zhang (2004) calculated

the heat budget of four streams in Devon UK and solar radiation was found to be the main heat source, whereas longwave radiation was the main heat loss.

Brown (1969) used an energy balance model to predict hourly water temperatures on three different streams in Oregon. He established that for un-shaded reaches, net all-wave radiation was the predominant energy source during the day, but that evaporation and convection were not to be neglected, since they accounted for around 10% of the total energy exchange. Conduction of heat was found to be important mainly in bedrock bottom streams. Up to 25% of the energy absorbed was observed to transfer to the bed.

The heat budget of a stream can also be influenced by channel morphology, valley topography, riparian vegetation, stream substrate and river regulation (Webb and Zhang, 1997). Some studies have successfully modeled river water temperatures under ice cover conditions (Hammar and Shen, 1995; Shen *et al.*, 1995). Caissie *et al.*, (2007) have used a deterministic model to predict water temperatures in the Miramichi river system (NB). Solar radiation accounted for most of the energy input. Longwave radiation and evaporation were similar but significant in low relative humidity, high wind speed and warm weather. Convective heat flux was small, but not negligible in the heat budget, since it can influence the variation of water temperatures, i.e., positive or negative heat flux (Caissie *et al.*, 2007). The potential sources of errors identified in this study were attributed to the assumption of the shading factor being constant throughout the year, the influence of snowmelt in spring, and not considering groundwater contribution. Troxler and Thackston (1977) also used a deterministic model and predicted the energy budget for temperature changes downstream of hydroelectric installations.

Leblanc *et al.* (1997) used a deterministic model to observe the effects of land use on water temperature in unregulated urban streams. Sensitivity analyses have shown that shade/transmissivity of riparian vegetation, groundwater discharge, and stream width had the greatest influence on stream temperature (Leblanc *et al.*, 1997; Leblanc and Brown 2000). Gaffield *et al.* (2005) used an energy budget model to predict summer temperatures in small streams (south-western Wisconsin, USA). This study found that the most important factors controlling summer stream temperatures were the inflow of groundwater, shade of riparian vegetation, and channel width. Meteorological data coming from regional meteorological stations or microclimate at the stream level can both be used in deterministic models. However, recent studies have shown that microclimate data seem to better reflect the heat fluxes, especially for smaller streams with important vegetation canopy (Benyahya *et al.*, 2010).

The following sections describe the most common parameters included in deterministic water temperature models namely: Solar radiation, longwave radiation, evaporation, convection, advection and conduction.

2.4.1.1 SOLAR RADIATION

Solar radiation is the radiant energy emitted by the sun. Solar radiation accounts for most of the input energy in most of the studies using a heat budget model (Webb and Zhang, 1997, 1999, 2004; Younus *et al.*, 2000; Johnson, 2004; Webb and Crisp, 2006; Caissie *et al.*, 2007). This component can be measured using sensors (e.g., radiometers or pyranometer devices) or estimated using numerous equations (Allen, 1997; Dingman,

2002). Most studies measure the incoming solar radiation with a pyranometer (Evans *et al.*, 1998; Caissie *et al.*, 2007; Brown and Hannah, 2008; Hannah *et al.*, 2008).

The constantly changing spatial relationship between the sun, the canopy closure of riparian vegetation and the amount of solar energy reaching a stream is very complicated to model (Beschta, 1997). As such, Chen *et al.* (1998a) have developed a model to estimate the solar radiation using the sun position, stream localization and orientation and the riparian shading characteristics. Using a single shade value may introduce errors by ignoring variability within each vegetation category. The angle of sunrays may modify the value of direct and diffuse radiation by controlling the length of the atmospheric path through which it travels and controls the relative surface area on which it intersects (Raphael, 1962). Samani (2000) proposed a method to estimate the solar radiation using only latitude and maximum and minimum air temperature. Yang and Koike (2002) developed a method to estimate surface solar radiation from upper-air humidity. Yang and Koike (2005) presented a model to estimate hourly and daily solar radiation from sunshine duration, air temperature and relative humidity. Dorvlo *et al.*, (2002) developed an artificial neural network model to estimate solar radiation from latitude, longitude, sunshine hours and the month of the year. Other studies, such as Allen (1997), estimated daily and monthly solar radiation for clear sky days using minimum and maximum air temperature measurements. This model was very effective for monthly solar radiation, but not as accurate in smaller time steps. Ringold *et al.* (2003) recommended the use of hemispheric imagery to estimate stream solar exposure, in which data could be collected at multiple sites and averaged over an area.

2.4.1.2 LONGWAVE RADIATION

When it comes to longwave radiation, most studies have included the longwave radiation emitted from the atmosphere and the water, but few have included the radiation coming from the forest canopy (Rutherford *et al.* 2007). The longwave radiation coming from the forest canopy was shown to be important for small and medium size streams (Benyahya *et al.*, 2010). The longwave radiation was also found to be the main source of heat loss in many heat budget models (Webb and Zhang, 2004; Caissie *et al.*, 2007). Most studies have estimated the longwave radiation using the Stefan-Boltzmann Law (Caissie *et al.*, 2007; Benyahya *et al.*, 2010; Singh and Singh, 2001). In winter, the longwave radiation increases and can surpass solar radiation, causing the net radiation to be an energy sink (Hannah *et al.*, 2004; Webb and Zhang, 2004). The long-wave radiation is relatively constant over the day and experiences highest values during clear sky periods in summer (Sridhar *et al.*, 2004).

2.4.1.3 EVAPORATION

When the water vapour pressure in the air is less than the saturated vapor pressure at the water surface, water evaporates into air, thus removing heat from water in two ways: energy required to evaporate (most important) and bodily removal of heat contained in the water removed by evaporation (Raphael, 1962). There are many evaporation equations available, depending on the type of data available, making it very difficult for practitioners to select the appropriate method. Most evaporation equations were developed to estimate the evaporation rate for lakes (Rasmussen *et al.*, 1995; Sing and Xu, 1997a; Rosenberry *et al.*, 2007). Methods of measure or estimation of the evaporation rate can be divided into five groups (Xu and Singh, 2001): 1) water-energy

budget (Bolsenga, 1975; Finch and Gash, 2002; Martinez *et al.*, 2006), 2) mass-transfer method (Morin and Couillard, 1990; Sinokrot and Stefan, 1993), 3) combination of available energy and aerodynamic terms using the Penman equation (Penman, 1948), 4) radiation based methods using the Priestley-Taylor equation (Priestley-Taylor, 1972) and 5) temperature based methods (Thornwaite, 1948). The efficiency and results of the estimation of evaporation is highly dependent on the type of equations used (Benyahya *et al.*, 2010) and can be site specific (Singh and Xu, 1997a).

The Penman method combines the aerodynamic and the radiation process to estimate the evaporation rate (Penman, 1948). The main disadvantage of the Penman method is in the determination of the net radiation and the vapor pressure deficit needed in the equation. Therefore many studies have used modifications of this method to simplify the calculations (Valantzas, 2006). The Penman-Monteith equation has been widely used because of its detailed theoretical base and because it can accommodate small time periods (e.g., hourly, daily) (Samani, 2000). However, the extensive records of climatological data that this method requires are often not available. Most radiation based methods used the net radiation to estimate the evaporation (Xu and Singh, 2000). One of the most commonly used radiation-based methods is the Priestly-Taylor equation (Priestley-Taylor, 1972; Stewart and Rouse, 1976). This method was used by Finch and Gash (2002) where they developed a simple finite difference model to predict the change in heat storage, and where the evaporation rate of a reservoir was estimated. The mass-transfer methods are also widely used in studies dealing with the evaporation rate and heat fluxes (Morin and Couillard, 1990; Sinokrot and Stefan, 1993). This approach has been the most widely used method within the stream temperature modeling literature.

For time steps shorter than daily (e.g., hourly), the net radiation approach does not seem to have a significant relationship with open water evaporation (Grander and Hedstrone, 2011). This study showed that the most significant parameters affecting the hourly evaporation rate were wind speed, difference between water-land temperatures and vapour pressures. The vapor pressure deficit was found to be the meteorological variable with the greatest correlation to pan evaporations at an hourly time scale (Xu and Singh, 1998). Singh and Xu (1997b) also found that vapor pressure gradient and wind speed were the most influential parameters for estimation of daily and monthly evaporations. In this study, the difference in vapor pressure gradient and wind speed was included in the estimation of evaporation rates using the mass-transfer method.

Measuring evaporation rates at small time-steps is a relatively difficult process, needing very high resolution devices. Evaporation models usually use meteorological parameters as inputs, since they are readily accessible and easily measured (Tan *et al.*, 2007). Andersen and Jobson (1982) compared two well-known techniques for estimating annual lake evaporation using climatological meteorological data. The dominant factors influencing evaporation were the solar radiation, air temperature, water temperature and relative humidity (Keskin and Terzi, 2006).

Longwave radiation and evaporation are of similar magnitude within the energy budget during the summer period (Caissie *et al.*, 2007). Evaporation contributes to the cooling of rivers and it is mainly controlled by wind speed and relative humidity (Gaffield *et al.*, 2005). As such, evaporation is a major component for heat loss in rivers, and this heat

loss can sometimes surpass the longwave radiation heat loss (Webb and Zhang, 2004; Caissie *et al.*, 2007)).

Dace (1972) presented a simple method for estimating evaporative heat losses from water bodies with adjustments for atmospheric stability. Some studies have shown that ANN models can estimate evaporation rates more accurately than the radiation based, mass-transfer and temperature-based models, but were more demanding on training data (Tan *et al.*, 2007).

2.4.1.4 CONVECTION

Heat transfer by convection is transferred between the stream surface and the atmosphere whenever a difference between air and water temperature exists. This heat transfer at the stream surface is usually a small component of heat budget models (Beschta, 1997; Caissie *et al.*, 2007; Benyahya *et al.*, 2010). Many studies have used the approach of Bowen (1926) to calculate the convective heat transfer. The process of evaporation of the water surface into the air is similar to that of the conduction of energy at the water/air surface. Due to this similarity, Bowen (1926) represented a ratio between the heat losses by conduction to that by evaporation. Driving forces are the wind speed and the temperature gradient between air and water (Brown, 1969). Convective heat is generally small but not negligible, since it reflects the variation of water temperatures as a function of the difference between air and water temperature (Caissie *et al.*, 2007).

2.4.1.5 ADVECTION

Advective heat flux can be in the form of precipitation (Kim and Chapra, 1997), tributary inflows, or groundwater inflow. Streams with important sources of groundwater are less influenced by air temperature in explaining stream temperature variability (Teague *et al.*, 2007). Advective heat fluxes coming from groundwater, reservoir releases, or wastewater discharge can have an impact on the thermal regime of rivers. This impact can have an influence many kilometers downstream or until the heat exchange with the atmosphere has again taken over the exchange process (Sinokrot and Stefan, 1993). Groundwater was found to have a greater influence at upstream sites within a watershed and under summer low-flow conditions (Webb and Zhang, 1999). Story *et al.* (2003) found that groundwater inflow was responsible for approximately 40% of the decrease in daily mean maximum water temperatures calculated for one afternoon at Baptiste Creek (BC). The lack of agreement between observed and predicted monthly stream temperature is often related to groundwater contributions, as reported in Webb and Zhang (2004). Caissie *et al.* (2007) developed a heat budget model for Catamaran Brook (NB). Groundwater flow was shown to contribute up to 91% of the total streamflow during small storm events (Caissie *et al.*, 1996) and its impact on river water temperature during such events remains unknown.

The role of precipitation in the heat budget of streams is usually ignored since it is typically less than 1% of the total energy input (Brown, 1969; Webb and Zhang, 1997; Evans *et al.*, 1998; Sridhar *et al.*, 2004). These studies showed that the overall precipitation heat flux is small; however, storm events have been shown to have an impact on stream temperature dynamics. For instance, Brown and Hannah (2007) studied

stream temperature dynamics of an alpine river over two summers (2002 and 2003). They showed that over 75% of storm events produced a decrease in water temperatures (up to 10.4 °C). In some cases, increase of water temperatures were also observed; however, changes were less significant (up to 2.3 °C). Precipitation events influence not only stream temperatures but also streambed temperatures. Brown *et al.*, (2006) showed that streambed temperatures decreased within the substrate up to 0.40 m in depth, following an important precipitation event.

2.4.1.6 CONDUCTION

Some studies have neglected the heat exchange at water and riverbed interface, i.e., streambed fluxes (Caissie, 2004; Sridhar *et al.*, 2004), but others have used it in their modeling of river water temperatures (Brown, 1969; Jobson, 1977; Sinokrot and Stefan, 1993; Kim and Chapra, 1997; Webb and and Zhang, 1997). Bed conduction has been shown to be an important parameter in heat budget of water depth of shallow streams (3 m or less) (Jobson, 1977). Conduction can be important for the energy budget of rock-bottom streams, but to a lesser degree for gravel or mud bed streams (Brown, 1969; Sinokrot and Stefan, 1993). The importance of bed conduction increases as the diel variability in stream temperatures increases (Jobson, 1977). Bed heat flux has been shown to be an important energy sink during the spring and summer (Jobson, 1977; Hondzo and Stefan, 1994; Webb and Zhang, 2004), whereas it is mostly an energy source in autumn (Hannah *et al.*, 2004). Streambed heat conduction may have a significant effect on the diel temperatures in small mountain streams, as reported in some studies (Vugts, 1974; Comer and Grenney, 1977; Sinokrot and Stefan, 1993).

Hondzo and Stefan (1994) showed that streambed heat flux was as large as 40 W m^{-2} . This represented an equivalent of a $0.8 \text{ }^{\circ}\text{C}$ temperature change per meter depth of the river in their study. Jobson (1977) presented a temperature model that accounted for bed conduction without requiring temperature measurements within the bed. His procedure required an estimate of the gross thermal properties of the bed, such as the thermal diffusivity and heat-storage capacity. In the study by Webb and Zhang (2004), the bed conduction contribution to the annual total heat flux was 4% in regulated reaches and 7% in moorland reaches. Bed conduction coming from coniferous reaches had a smaller contribution (<1%) to the annual total heat flux.

Daily average stream temperatures are not very sensitive to the streambed thermal conditions; however, it becomes important for short time scales, i.e., for the prediction of hourly stream water temperatures (Sinokrot and Stefan, 1994). Other studies have also concluded that modeling hourly water temperatures needs to include streambed thermal conductivity (Jobson, 1977; Sinokrot and Stefan, 1993). Although bed heat conduction can be small compared to other energy fluxes, it can act as an important energy sink during the daytime to compensate for the heat gains occurring at the water surface (Leach and Moore, 2011).

Intragravel bed temperatures are important for aquatic resources, such as for the development of salmonid eggs (Acronley, 1999). In this study, streambed temperatures were found to be important in the estimation of timing of different stages of brown trout embryo development. The fluctuation of streambed temperatures decreases with depth, to a depth where temperatures are relatively stable. Bed conduction generally acts as a heat

sink in the summer months and a heat source in the winter months (Webb and Zhang, 2004), since streambed temperatures are usually higher than stream water temperatures during the winter and lower in summer (Ringler and Hall, 1975).

2.4.2 TEMPERATURE EQUILIBRIUM CONCEPT

Deterministic models can become very complex if all heat fluxes are considered. The equilibrium temperature model was first developed to simplify the expression of the total heat flux at the water surface (Edinger *et al.*, 1968; Chaudhry *et al.*, 1983; Jeppesen and Iversen, 1987). The equilibrium temperature is the stream temperature at which no heat exchange would be occurring at the stream. With the equilibrium temperature concept, the net flux at the water surface is expressed using fewer meteorological parameters compared with conventional deterministic models. As such, the total heat flux at the water surface is assumed to be proportional to the difference between the water temperature and an equilibrium temperature T_e (Caissie *et al.*, 2005). The resulting equation is a linear function of water and equilibrium temperatures which defines the total heat flux (Edinger *et al.*, 1968). Some studies have used the equilibrium temperature concept to study the thermal regime in rivers (LeBosquet, 1946; Edinger *et al.*, 1968; Dingman, 1972; Novotny and Krenkel, 1973; Caissie, 2004).

Larnier *et al.* (2010) developed an equilibrium temperature model to estimate daily water temperatures on the Garonne River (France) from 1988 to 2005. The model was calibrated for higher water temperatures (i.e., temperatures above 20 °C), to focus on important aquatic conditions, particularly for migrating freshwater fishes. Equilibrium

temperature was calculated from meteorological parameters using the heat budget equations.

Mohseni and Stefan (1999) used the equilibrium temperature concept to examine the relationship between weekly air and stream temperature, especially at high temperatures under climate change. They showed that the relationship between weekly air and stream temperatures resembles an s-shaped variation, although a linear relationship can be assumed at air temperatures between 0 °C and 20 °C. The levelling out of water temperature at air temperatures over 20 °C is mainly due to higher evaporative cooling.

Marcé and Armengol (2008) examined three different water temperature models: deterministic, equilibrium temperature and a hybrid (combination of both). Even though the equilibrium temperature model had a good performance, they highlighted the limitation of the model for air temperature higher than 19 °C, where the linear relationship between the equilibrium and air temperature lessens.

Herb and Stefan (2011) developed a modified temperature equilibrium temperature model and applied it to two cold-water tributaries of the Mississippi River. This model differs from others as it considers groundwater inflow rates and groundwater temperatures to estimate daily average stream temperatures, which is usually not included in most models. Their model also included climate conditions, riparian shading and stream width, which can be useful for studies of cold-water reaches and climate change.

An equilibrium temperature model was applied to two thermally different streams of the Miramichi River (Catamaran Brook and Little Southwest Miramichi) for estimating daily mean stream temperatures (Caissie *et al.*, 2005). In this study, the equilibrium temperature was expressed as a linear function of air temperature, and the thermal exchange coefficient was assumed constant throughout the study period. The model generally performed well; however poorest performances were observed in spring caused presumably due to snowmelt conditions. The best performances were observed during late summer and autumn when water levels are generally at the lowest of the open water period.

Bogan *et al.* (2003) have showed that weekly stream temperature was related to weekly equilibrium temperature for 596 U.S. Geological Survey stream gaging stations in the eastern and central United States (for water temperatures over 0 °C). This study has also showed that shading and sheltering of streams was important in the modeling of stream temperatures. For streams that were more sheltered and shaded, weekly equilibrium temperature was a better estimator of weekly stream temperature. The effect of shading was found to be even stronger than sheltering (Bogan *et al.*, 2004).

Equilibrium temperature models can be used to examine the effect of different meteorological parameters. Gu (1998) studied the relationship between stream discharge and stream temperatures. This study showed that increasing river discharge can help decrease the amplitude of daily variations as well as daily maximum water temperatures until a critical point, where the effect becomes insignificant. Gu *et al.* (1998) found that the variation of daily maximum temperatures was more related to flow than the daily

mean temperatures. Krajewski *et al.* (1982) developed a graphical technique to estimate the equilibrium temperature and the heat exchange coefficient using solar radiation, cloud cover, air temperature, wind speed, relative humidity and atmospheric pressure.

2.4.3 ARTIFICIAL NEURAL NETWORKS

Artificial neural networks (ANN) are data processing techniques used by scientists to extract maximum information from time series. ANN can be used in different problems among scientists such as engineers, biologists or economists: Pattern classification, clustering/categorization, function approximation, predicting/forecasting, optimization, content-addressable memory and control (Jain *et al.* 1996). The development of ANNs began 50 years ago, aiming to understand the human brain and to imitate its functions. In the last decade, this technique has grown in popularity due to the development of more sophisticated algorithms and the availability of powerful tools for data processing.

ANN is a parallel computing system consisting of an extremely large number of simple processors with many interconnections (Jain *et al.*, 1996). It resembles the brain in two ways: Knowledge is acquired by a learning process and information is stored by interneuron connection strengths (Haykin, 1999). The main benefits of using ANN as a computing tool are the large parallel-distributed structure and its ability to learn and generalize (Haykin, 1999). In most hydrological studies, ANN is used for function approximation, which consists of estimating an unknown function with training patterns (input and output data).

The basic elements used in an ANN are called neurons, which are non-linear algebraic functions, parameterized and with bound values (Dreyfus *et al.*, 2002). The signal goes through each neuron associated with a weight (w) and is modified by a transfer function (f). An ANN consists of a finite number of layers where each layer is composed of a number of neurons. The entrance of the ANN is called the input layer, and the results are obtained at the output layer. The inputs and outputs can be represented by many nodes such as x_i and y_k . The intermediary layers are called the hidden layers. At each node, the information is processed and passed on to the following layer with connection strength (weight). There are connection weights between the input and hidden nodes (iw_{ij}) and connection weights between hidden and output nodes (lw_{jk}). The output is a function of a summation and a transformation of different nodes.

A multilayer network is composed of a set of sensory units (input layer), one or more hidden layers of computation nodes and an output layer of computation nodes (Smith, 1993). The input signal propagates through the network in a forward direction, on a layer-by-layer basis. Errors are calculated between predicted and observed values and the network is then modified to minimize the overall errors. This optimization of the network is done using algorithms. The most popular algorithm is the error backpropagation algorithm based on the error-correction learning rule. It is a popular algorithm mainly due to its simple conception, to its effective computation, and to its efficiency (Smith, 1993). Hidden nodes and the high degrees of connectivity allow a backpropagation network to learn very complex tasks (Haykin, 1999).

Many factors can influence the sample size used with an ANN, like the choice of the modeling technique, the target function and the noise in the data. In fact, the sample size increases with the complexity of the function and the noise to maintain accuracy and prevent overfitting. The largest sample available should be used as long as it fits in the memory or storage. Smith (1993) recommends dividing the sample into three subsamples: Training, validation, and testing. The training subsample generally accounts for approximately 2/3 of the original sample size and it is used to calculate the weights. The validation and testing of subsample are commonly grouped together (and consist of 1/3 of the sample) to measure performance of the network.

Since the 1990's, ANNs have been used in the field of hydrology, namely in modeling of precipitation and run-off, water demand predictions, groundwater and water quality (Govindaraju, 2000a). ANNs have become interesting in those fields for many reasons (Govindaraju, 2000a). The main reason is their capacity to recognize the relation between the input and output variables without any physical explanations. It is very useful in hydrology because most of the events are non-linear, very complex and sometimes unknown. ANNs can also adapt to solutions with time to make up for condition changes. They also work well with data having bias, and once calibrated, they are simple to use.

Govindaraju (2000b) mentioned that the first applications of ANN in hydrology were in precipitation and run-off modeling (Minns and Hall, 1996; Tokar and Johnson, 1999; Thirumalaiah and Deo, 2000; Tokar and Marcus, 2000; Castellano-Mendez *et al.*, 2004). ANN models can also forecast streamflow in rivers using streamflow data from previous

days, precipitation and air temperature data (Moradkhani *et al.*, 2004; Nayebi *et al.*, 2006).

Zealand *et al.* (1999) and Jain *et al.* (2001) developed ANN models to forecast short-term water demand. ANN has also shown to be a good predictor of hourly and daily evaporation rates in equatorial regions (Tan *et al.*, 2007), and have been used to optimize the control of municipal water systems (Bhattacharya *et al.*, 2003).

ANNs are extremely useful in processing large amounts of information, like in remote sensing. Islam and Kothari (2000) evaluated ANNs to define, estimate and predict remote sensing process and data in hydrology, especially for precipitation. Keskin and Terzi (2006) suggested the addition of ANN to other existing models to estimate daily pan evaporation from meteorological data. Rehman (2008) achieved an estimation of the global solar radiation using only time of year, air temperature and relative humidity. ANN applications could be useful in the design of reservoirs, development of water budgets for basins and various other hydrological analyses where other models might be inappropriate (Sudheer *et al.* 2002).

Water quality modeling can be enhanced using ANNs. For example, they were used in Illinois to estimate nitrate concentration in Upper Sangamon River (Suen and Eheart, 2003). In another related study, Bowden *et al.*, (2005b) forecasted the salinity in rivers. ANNs were found to have lower forecasting errors than other models. Salinity of the River Murray (Australia) was effectively forecasted 14-days in advance (Maier and Dandy, 1996).

ANNs are widely use in groundwater modeling. For example, Shigidi and Garcia (2003) showed the utility to approximate the explicit relation of the transmissivity and the hydraulic charge described by the groundwater flow equation. Daliakopoulos *et al.* (2005) used a standard feed-forward ANN to simulate the decreasing trend of the groundwater level for the Messara Valley (Greece).

In the literature, only a few studies have applied ANN in stream water temperature modeling. Bélanger *et al.* (2005) effectively predicted daily water temperatures in Catamaran Brook and Little Southwest Miramichi (NB) for over 10 years using only air temperatures, time and streamflow as input parameters. The inputs included were the current air temperature (°C), air temperature of the previous day (°C), air temperature two days earlier (°C), discharge ($\text{m}^3 \text{s}^{-1}$) and a trigonometric function of time (days). The overall root-mean-square error (RMSE) between observed and predicted water temperatures was 1.06 °C.

Chenard and Caissie (2008) also applied ANN models for Catamaran Brook and Little Southwest Miramichi, and modeled daily maximum and mean stream temperatures. Eight models using different input variables were tested. The best ANN model for predicting daily mean stream temperatures included eight different input parameters: minimum, maximum and mean air temperatures of the current day and those of the preceding day, the day of year and the water level. The best model predicting daily maximum temperatures included the same input parameters, except mean daily air temperature. Results were similar to, and better than, other water temperature modeling studies using an ANN model. Overall RMSEs were 0.96 °C and 1.18 °C for daily mean

and maximum stream temperature, respectively. These models were simple to develop and apply, and allowed many input and output parameters.

Karaçor *et al.* (2007) developed a feed-forward artificial neural network to predict the maximum stream temperature of Degirmendere River (Turkey) for the five days ahead. The ANN was used for 10 river stations using daily water temperature measurements from years 1996 to 2004. The developed feed-forward ANN had six inputs, three hidden layers (with 13, 8 and 5 nodes respectively) and two outputs. The six inputs used were: the time of year, the current, previous (day before) and past (8 days before) stream water temperatures, and the highest and lowest stream temperature recorded in the last 8 days. The outputs are the minimum and maximum stream temperatures for the next five days. The ANN model achieved good results, with average absolute prediction of 0.93 °C, using only past stream temperature data.

Risley *et al.* (2003) have used an ANN model to estimate hourly water temperatures. This model included numerous meteorological data (air temperature, dew-point temperature, shortwave solar radiation, air pressure, and precipitation), riparian habitat characteristics (stream bearing, gradients, depth, substrate, wetted widths, and canopy cover), and basin landscape characteristics (topographic and vegetative), acquired from a geographic information system (GIS). This model was applied on 148 sites in western Oregon over the summer of 1999 (June 21 to September 20, 1999). Their results showed RMSEs ranging between 0.05 °C and 0.59 °C.

Sivri *et al.* (2007) predicted monthly stream temperatures with an ANN model on Firtina Creek (Turkey). They selected a 3-layer network with 5 inputs (local water temperature, dissolved oxygen, PH, air temperature and rainfall), 12 hidden nodes and a single output (stream temperature). The training period included monthly data for one year, and was validated over the two following years.

2.4.4 STOCHASTIC AND OTHER STATISTICAL TYPES OF MODELS

Stochastic models estimate water temperatures by using statistical functions with a number of independent variables (e.g., air temperature, water temperatures of previous days, etc.). Stochastic models do not need a large number of input parameters like deterministic models and therefore this reduces the length of development of the model (Marceau *et al.* 1986). However, stochastic models are generally site specific and are not adapted for environmental impact studies. Stochastic models can also require a longer time series of observations for proper calibration.

Many studies have successfully modeled stream temperature from air temperatures (Stefan and Sinokrot, 1993). Ahmadi-Nedushan *et al.* (2006) applied stochastic models to estimate daily mean stream water temperatures of a large unregulated river (Moisie River, QC). This study related mean daily water temperatures to air temperatures and streamflow indices. They showed that including streamflow indices in stochastic models could improve their performance. Caissie *et al.* (1998) showed that it was possible to predict daily water temperatures for small streams using only air to water relationships. Linear regression was sufficiently accurate to predict water temperatures with a mean deviation less than 1 °C from the observed temperature (Mackey and Berrie, 1991).

Neuman *et al.* (2003) used an empirical model to predict daily maximum temperature (summer period) from daily maximum air temperature and average daily flow. Benyahya *et al.* (2007) modeled the average weekly maximum water temperatures for Deschutes River by using two univariate stochastic methods: autoregressive and periodic autoregressive. On the Nivelles River (France), stochastic models were developed using air temperature and streamflow to estimate mean weekly maximum water temperatures (Benyahya *et al.*, 2008).

Monthly and weekly time scales produced the best linear relations between air and stream temperature (Erickson and Stefan, 2000). Stefan and Preud'homme (1993) used simple linear regression between air temperature and water temperatures to estimate mean daily and weekly water temperatures with a standard deviation around 2 °C. Crisp and Howson (1982) predicted 5-day and 7-day mean water temperatures. They found that the relationship between mean air temperature and mean water temperature is approximately linear, except for when mean air temperature was below 0 °C. This study showed that adding rainfall or stream discharge only made a negligible improvement in the relationship. Even meteorological data taken 50 km from the study area would produce accurate results using regression (Johnson, 2003). Mohseni and Stefan (1999) said that linear regression is not always justified because of the nonlinear stream/air relationship.

Caissie *et al.*, (2001) used regression and stochastic models for modeling maximum daily stream temperatures. A Fourier and Sine function was used to model the long-term annual component of the stream temperature and a second order Markov process was used to model the short-term component. Johnson (1971) found strong correlation

between monthly mean water temperatures and monthly mean air temperatures. Pilgrim *et al.* (1998) used an air-water relationship to predict the increase of stream water temperatures under a climate change scenario.

Doglioni *et al.* (2008) used an evolutionary polynomial regression to forecast water temperature for 5 years, using air temperature as input. Data were sampled at hourly intervals and studied at different time scales (6-hour, 12-hour, 24-hour and 36 hour averages). This approach to modeling stream temperatures may prove cheaper and more efficient than the use of deterministic physically-based models, because it only uses air temperature data, which are relatively easy to collect and are often widely available. The study was also able to estimate maximum daily temperatures in streams in Western Oregon with a precision of less than 1 °C. Guillemette *et al.* 2009 used a multivariate geostatistical approach to estimate monthly maximum water temperatures.

CHAPTER 3: METHODOLOGY AND STUDY AREA

This chapter presents the methodology related to each of the three water temperature models, namely: the deterministic model, the equilibrium temperature model and the artificial neural network model. This section also presents the study area (Miramichi River system) and the two study sites (Catamaran Brook and Little Southwest Miramichi). The instruments used to collect the data are also described. The last section presents three different performance criteria used to test the performance of each water temperature model.

3.1 STUDY AREA

The two reaches (Catamaran Brook and Little Southwest Miramichi River) are located on the Miramichi River System (New Brunswick, Canada), which is world renowned for its population of Atlantic salmon, *salmo salar* (Figure 3.1). This system has an annual precipitation ranging from 860 mm to 1365 mm, with a long-term average of 1142 mm (Caissie and El-Jabi, 1995). The mean monthly air temperature varies between -11.8 °C (January) and 18.8 °C (July). The mean annual runoff was estimated by Caissie and El-Jabi (1995) to be 714 mm, ranging from 631 mm to 763 mm. The vegetation consists mainly of second-growth, mature forest species estimated at 65% coniferous and 35% deciduous (Cunjak *et al.*, 1990).

The first reach is located on the Little Southwest Miramichi River (LSWM) at approximately 25 km from the river mouth (Figure 3.1). The drainage basin of the LSMR

is 1190 km² (Johnston, 1997). The LSWM has a width of approximately 80 m, with an average depth of 0.55 m during mean flow conditions. No lateral variation in water temperatures were observed by Caissie *et al.* (2007), being explained by the well-mixed nature of the river. The forest along the LSWM is mainly composed of 70% hardwood, with a presence of 30% softwood (Cunjak *et al.*, 1990). The canopy closure was less than 20%.

The second reach is was located on Catamaran Brook (Cat Bk) approximately 8 km upstream of the mouth. It is the site of a 15-year multidisciplinary hydrobiological research study aimed at quantifying stream ecosystem processes and the impact of timber harvesting (Cunjak *et al.*, 1990). Catamaran Brook has a drainage area of 27 km² at the study site, an average stream width of 9 m and a depth of 0.21 m. Catamaran Brook is well-mixed due to a high level of turbulence, similar to LSWM, but the brook is more sheltered by streamside vegetation and upland slopes. The canopy closure for Catamaran Brook was estimated at 55%-65% with a forest composition of 60% hardwood and 40% softwood (Cunjak *et al.*, 1990). Some characteristics of both streams are listed in Table 3.1.

Table 3.1. Selected characteristics of Catamaran Brook and Little Southwest Miramichi.

Study site	Drainage area	Width	Depth	Canopy closer	Forest Composition	
					Hardwood	Softwood
Little Southwest Miramichi	11490 km ²	80 m	0.55 m	20%	70%	30%
Catamaran Brook	27 km ²	9 m	0.21 m	55-65%	60%	40%

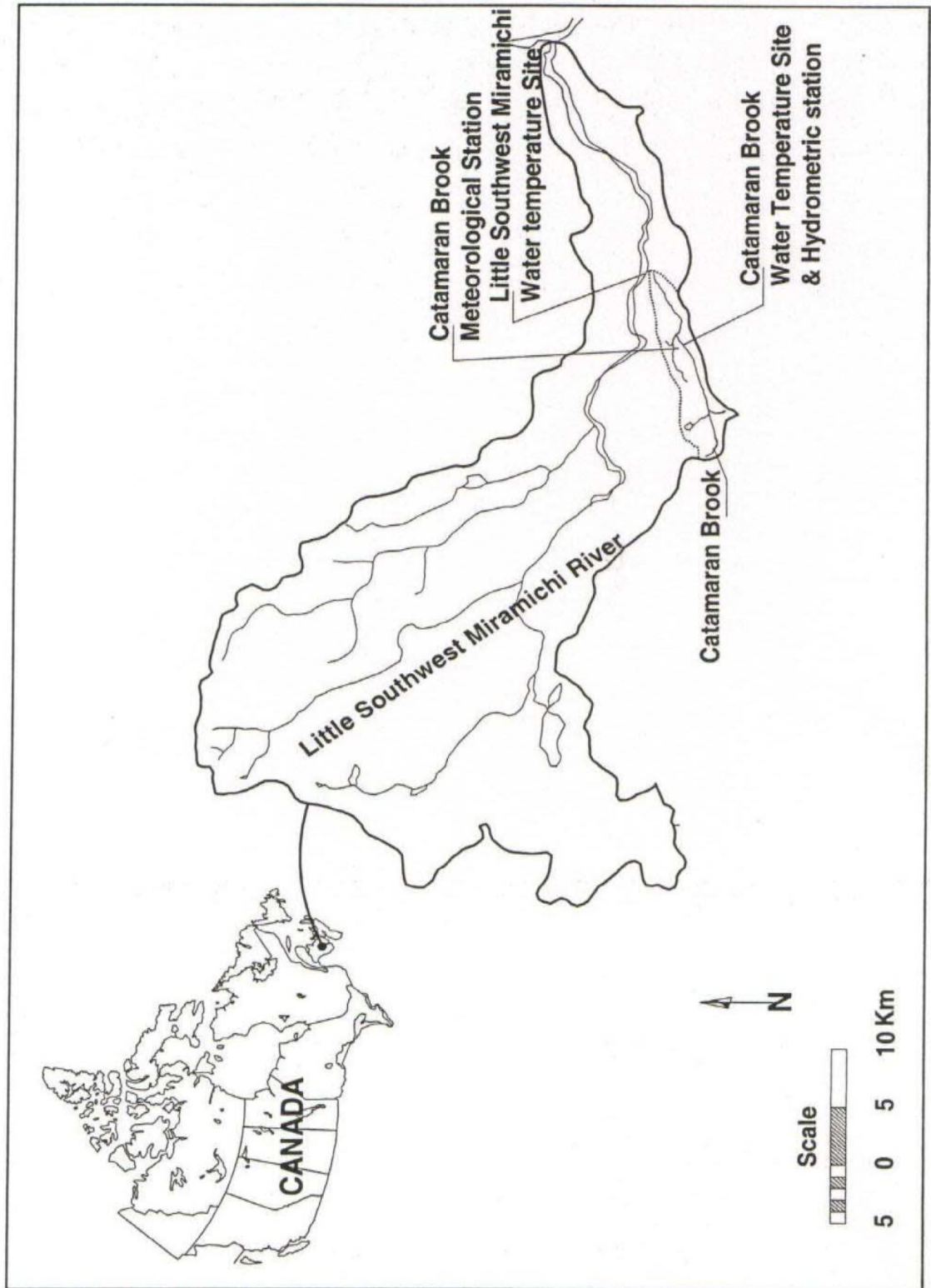


Figure 3.1. Map showing the location of microclimate sites (Catamaran Brook and Little Southwest Miramichi River) and the location of the meteorological station.

3.2 DETERMINISTIC MODEL

The modeling of stream water temperature has been carried out in previous studies using the heat budget approach (Sinokrot and Stefan, 1993; Caissie *et al.*, 2007). This modeling approach uses the general equation for the conservation of thermal energy given by:

$$\begin{aligned} \frac{\partial T_w}{\partial t} + v_x \frac{\partial T_w}{\partial x} + v_y \frac{\partial T_w}{\partial y} + v_z \frac{\partial T_w}{\partial z} - \frac{1}{A} \frac{\partial}{\partial x} \left(AD_x \frac{\partial T_w}{\partial x} \right) - \frac{1}{A} \frac{\partial}{\partial y} \left(AD_y \frac{\partial T_w}{\partial y} \right) - \frac{1}{A} \frac{\partial}{\partial z} \left(AD_z \frac{\partial T_w}{\partial z} \right) = \\ \frac{W}{c_w \rho A} H_{surf} + \frac{p}{c_w \rho A} H_{bed} \end{aligned} \quad (3.1)$$

where, T_w is the water temperature ($^{\circ}\text{C}$), t is the time (hour), x is the distance downstream (m), y and z are the longitudinal and vertical distance (m), A is the cross sectional area (m^2), v_x , v_y , and v_z are mean water velocity in respective directions (m/hour), W is the river width (m), D_x , D_y , and D_z are the dispersion coefficients in the respective directions ($\text{m}^2 \text{ hour}^{-1}$), c_w is the specific heat of water ($4.19 \times 10^3 \text{ MJ kg}^{-1} \text{ }^{\circ}\text{C}^{-1}$), ρ is the water density (1000 kg m^{-3}), p is the wetted perimeter of the river (m), H_{surf} is the total heat flux per area at the surface-water interface (W m^{-2}), and H_{bed} is the total heat flux per area at the streambed-water interface (W m^{-2}).

In water temperature analysis, the average depth conditions are usually assumed (neglecting the z component). In a well-mixed river, water temperature variations along the reach are usually more important than the vertical gradient with depth as well as lateral temperature variability. With these assumptions, the equation (3.1) can be reduced to a one dimensional equation:

$$\frac{\partial T_w}{\partial t} + v_x \frac{\partial T_w}{\partial x} - \frac{1}{A} \frac{\partial}{\partial x} \left(A D_x \frac{\partial T_w}{\partial x} \right) = \frac{W}{c_w \rho A} H_{surf} + \frac{p}{c_w \rho A} H_{bed} \quad (3.2)$$

The dispersion along the river reach (D_x) is most often small compared to the heat transport by velocity (v_x). Downstream changes in water temperatures are usually small compared to the temporal changes. For example, a study conducted in the McKenzie River (Oregon) showed an increase less than 0.09°C/km (Torgersen *et al.*, 2001). The heat flux at both interfaces (water surface and streambed) is important in predicting diel temperature variations, especially in small rivers (Brown, 1969; Jobson, 1977; Sinokrot and Stefan, 1993). In this case, the general 0-D model for vertically well-mixed streams can be simplified as follows:

$$\frac{\delta T_w}{\delta t} = \frac{W}{c_w \rho A} H_{surf} + \frac{p}{c_w \rho A} H_{bed} \quad (3.3a)$$

In most rivers and for heat budget purposes, when they are very wide and shallow, the wetted perimeter (p) may be approximated by the surface river width (W) (Mackey *et al.*, 1998). The wetted perimeter was assumed to be equal to the top water surface width because the two studied streams are effectively very wide and shallow. In fact, the average stream width at Catamaran Brook is 9 m with a depth of 0.21 m. For Little Southwest Miramichi, the average river width is 80 m with a depth of 0.55 m. Therefore, the total heat flux at water surface (H_{surf}) and from the streambed (H_{bed}) can be expressed as the total heat flux (H_t) using the following equation:

$$\frac{\delta T_w}{\delta t} = \frac{W}{c_w \rho A} H_{total} \quad (3.3b)$$

where,

$$H_{total} = H_{surf} + H_{bed} = (H_s + H_l + H_e + H_c + H_p) + (H_b + H_g) \quad (3.4)$$

H_s is the net shortwave radiation (W m^{-2}), H_l is the net longwave radiation (W m^{-2}), H_e is the evaporative heat flux (W m^{-2}), H_c is the convective heat flux (W m^{-2}), H_p is the precipitation heat flux (W m^{-2}), H_b is the streambed heat flux by conduction (W m^{-2}), and H_g is the streambed heat flux by advective groundwater flow (W m^{-2}). Each of the energy fluxes presented in Equation (3.4) are further described below.

A number of studies have used heat budget models to predict variability in river water temperatures (Evans *et al.*, 1998; Younus *et al.*, 2000; Caissie *et al.*, 2007; Hannah *et al.*, 2008); however, few have focused on using stream microclimate conditions as well as the streambed heat fluxes in predicting water surface heat fluxes at the hourly time scales. As such, the present study will focus on these three important issues.

A previous study was conducted within the same region using a deterministic model (Caissie *et al.*, 2007). This study used data from a remote meteorological station (MetSta) to predict stream water temperatures on a daily basis. The present study differs from Caissie *et al.* (2007) in that microclimate meteorological data were used in order to better estimate heat fluxes and potentially improve the model. Also, the modeling was carried out at an hourly time step rather than at a daily time step. Stream microclimate conditions (i.e., data collected 1 to 2 m above the stream) are important to properly estimate water surface heat fluxes because they better represent conditions within the river environment. Otherwise, factors or a parameterization is required to transfer remote station data to the stream environment.

The longwave radiation emitted by the vegetation canopy has been shown to be important for streams with significant overhanging canopy (Benyahya *et al.*, 2010). Most studies have neglected the small amount of energy added by precipitation (Webb and Zhang, 1997; Evans *et al.*, 1998; Hannah *et al.*, 2008). Both of these aspects were considered in this study. Streambed fluxes are also important to the thermal regime of rivers, and are probably very site specific (Caissie *et al.*, 2007). Although it has been studied both directly and indirectly, a complete understanding of its role has yet to be developed. Those who have considered streambed heat fluxes reported that these were most important when seeking to modeling diel variability, e.g., hourly modeling (Sinokrot and Stefan, 1993; Hondzo and Stefan, 1994; Kim and Chapra, 1997; Webb and Zhang, 1997; Evans *et al.*, 1998), and especially for shallow streams (Jobson, 1977).

3.2.1 NET SHORTWAVE RADIATION (H_s)

The incoming solar radiation is both a function of atmospheric conditions (e.g., cloud cover) as well as the riparian vegetation (e.g., canopy closure at the stream level). The net shortwave radiation, also known as the solar radiation, is expressed as the difference between incoming and reflected solar radiation. The reflectivity of the stream is defined as the albedo that expresses the percentage of reflected insolation to incoming insolation. Raphael (1962) showed that the reflectivity (albedo) is generally less than 7% for solar altitudes greater than 30°. And for solar altitude less than 30°, the incoming solar radiation is respectively low and therefore the impact on this parameter is low as well. Most studies showed that the reflected incoming solar radiations were in a range of 3 to 5% (Marcotte and Duong, 1973; Morin and Couillard, 1990; Caissie *et al.*, 2007). Since no measure of the reflected incoming solar radiation was available, a constant value of

3% was used (Sinokrot and Stefan, 1993, Caissie *et al.*, 2007). Therefore, the net shortwave radiation was estimated as follows:

$$H_s = 0.97H_{is} \quad (3.5)$$

where, H_{is} represents the incoming solar radiation at the water surface (W m^{-2}) measured via a pyranometer.

3.2.2 NET LONGWAVE RADIATION (H_l)

The net longwave radiation includes the radiation emitted by the atmosphere, the water surface and the forest canopy. This form of radiation can be calculated using the Stefan-Boltzmann Law. Most water temperature modeling studies have considered the net longwave radiation using both atmospheric and water surface conditions; however, only a few studies have included the longwave radiation emitted by the surrounding vegetation (e.g., Rutherford *et al.*, 1997). This component could become important for a stream with significant overhanging vegetation (Benyahya *et al.*, 2010). When considering the canopy as well as other components of the longwave radiation, the equation given by Singh and Singh (2001) was used here in:

$$H_l = 0.97\sigma \left[(FC + \varepsilon_a(1 - FC))(T_a + 273)^4 - (T_w + 273)^4 \right] \quad (3.6)$$

where, σ is the Stefan-Boltzmann constant ($5.67 \times 10^{-8} \text{ W m}^{-2} \text{ K}^{-4}$), FC is the forest cover factor (%), T_a is the air temperature ($^{\circ}\text{C}$) and ε_a is the atmospheric emissivity. In this equation, the forest temperature is assumed to be equal to that of air temperature with a forest emissivity of 0.97 (Rutherford *et al.*, 1997; Singh and Singh, 2001; Benyahya *et al.*, 2010). The forest cover factor was estimated at 65% for Catamaran Brook and at 20% for

the Little Southwest Miramichi (LSWM) based on field observations. The atmospheric emissivity was calculated using (Morin and Couillard, 1990):

$$\varepsilon_a = (0.74 + 0.0065 \times e_a)(1 + 0.17C^2) \quad (3.7)$$

where e_a is the water vapor pressure in the air (mm Hg) and C is the cloud cover factor (clear sky $C = 0$, mainly clear $C = 0.25$, mostly cloudy $C = 0.75$ and total cloud cover 1).

$$e_a = 4.583 \exp\left[\frac{17.27T_a}{237.3 + T_a}\right] \frac{RH}{100} \quad (3.8)$$

where, RH represents the relative humidity (%).

3.2.3 EVAPORATIVE HEAT FLUX (H_e)

The mass-transfer approach (aerodynamic) is widely used in stream temperature modeling for the estimation of evaporation and the evaporative heat flux (Morin and Couillard, 1990, Sinokrot and Stefan, 1993, Webb and Zhang, 1997, Caissie et al., 2007).

The equation is given by:

$$H_e = (a + bV)(e_s - e_a) \quad (3.9)$$

where, a and b are empirical constants, V is the wind speed at a stated elevation (m s^{-1}) and e_s is the saturated vapor pressure of the air at the water temperature of interest (mm Hg). In Equation (3.9), the evaporative flux represents an energy loss; therefore, H_e becomes negative. The total lake evaporation per month (mm) was available at the nearest station (Miramichi A) and obtained from Canada's National Climate Archive web site (<http://www.climate.weatheroffice.gc.ca/>). Lake Evaporation is calculated using the observed daily values of pan evaporative water loss, the mean temperatures of the water in the pan and of the nearby air, and the total wind run over the pan. The constant a and b

were calibrated so that the evaporation rates so computed were close to meteorological station observations each month for years 1979-1990 (July, August and September). The Miramichi A station data should be somewhat representative of the LSWM evaporation with lower wind speeds; however, Catamaran Brook being more sheltered than LSWM should generally exhibit lower evaporation. The mean monthly evaporation monitored at the Miramichi station was 128.7 mm, 111.2 mm and 76.8 mm for July, August and September for years 1979 to 1990. Evaporation data were not available for the year 2007. At Catamaran Brook, the monthly evaporation calculated was 1.40 mm, 12.1 mm and 9.0 mm for July, August and September of 2007. At LSWM, the monthly evaporation was estimated at 24.3 mm, 37.9 mm and 26.9 mm at July, August and September of 2007. The differences between stream evaporation and lake evaporation can be attributed to the lower wind speed experienced within the stream environment. Substituting coefficients a and b Equation (3.9) becomes:

$$H_e = (6 + 3V)(e_s - e_a) \quad (3.10)$$

3.2.4 CONVECTIVE HEAT FLUX (H_c)

The convective heat flux, also known as sensible heat flux, is the heat exchange that occurs at the air-water surface interface due to the temperature difference between air and water as well as wind speed. The Bowen ratio approach was used, which is given by (Bowen, 1926):

$$\frac{H_c}{H_e} = K_p \frac{(T_w - T_a)}{[e_s - e_a]} \frac{P}{1000} \quad (3.11)$$

where, K_p is a proportionality constant that is usually close to 0.61), and P is the atmospheric pressure (mm Hg). Substituting Equation (3.10) into (3.11), the convective heat flux becomes:

$$H_c = (3.66 + 1.83V) \frac{P}{1000} (T_a - T_w) \quad (3.12)$$

3.2.5 PRECIPITATION HEAT FLUX (H_p)

In most studies dealing with water temperature modeling, the energy from precipitation was assumed to be very small and was therefore neglected (Webb and Zhang, 1997; Evans *et al.*, 1998; Hannah *et al.*, 2008). In this study, precipitation heat fluxes were considered part of the energy heat budget to examine such fluxes in the short-term (e.g., hourly basis), especially during important rain events. Precipitation heat fluxes are a function of the difference in temperature between rainfall and stream water. Assuming the rainfall temperature to be similar to the air temperature, the precipitation heat flux was calculated from the equation provided by Marcotte and Duong (1973):

$$H_p = 1.16y_p(T_p - T_w) \quad (3.13)$$

where, y_p is the precipitation in mm, T_w the stream water temperature (°C) and T_p is the rain temperature (°C) (assumed equal to the air temperature).

3.2.6 STREAMBED HEAT FLUXES (H_{bed})

The heat exchange at the water-riverbed interface has been neglected in most studies using a heat budget model to predict water temperatures (Caissie, 2004; Sridhar *et al.*, 2004). However, others have found this contribution to be important, especially for short time scales (hourly) and shallow streams (Brown, 1969; Jobson, 1977; Sinokrot and

Stefan, 1993; Kim and Chapra 1997; Webb and Zhang, 1997; Jobson, 1977). A water temperature advective-diffusion model (finite difference model) was calibrated for both Catamaran Brook (Cat Bk) and Little Southwest Miramichi River (LSWM) to estimate the riverbed temperature profile ($T(z,t)$). This model was used to predict intragravel temperatures at different depths within the stream substrate using a one dimensional advective-diffusion equation (Caissie and Satish, 2001):

$$k \frac{\partial^2 T_z}{\partial z^2} - v_g c_w \rho_w \frac{\partial T_z}{\partial z} = c_m \rho_m \frac{\partial T_z}{\partial t} \quad (3.14)$$

where, T_z is the streambed temperature at depth z ($^{\circ}\text{C}$), k_m is the thermal conductivity of the solid-fluid matrix ($\text{W m}^{-1} \text{ }^{\circ}\text{C}^{-1}$), v_g is the vertical velocity component (negative for upwelling water) (m hr^{-1}), c_w is the heat capacity of the fluid (e.g. water at $4187 \text{ J kg}^{-1} \text{ }^{\circ}\text{C}^{-1}$), ρ is the density of the fluid (e.g. water at 1000 kg m^{-3}), c_m and ρ_m are the heat capacity ($\text{J kg}^{-1} \text{ }^{\circ}\text{C}^{-1}$) and density (kg m^{-3}) of the rock-fluid matrix, and z is the depth within the substrate (m).

To run the advective-diffusion model, data at both the upper and lower boundaries are required (i.e., at the streambed-water interface and at a specific depth within the substrate). Measured stream water temperatures were used for the upper boundary for both sites whereas measured intragravel temperatures at 3 m were used for the lower boundary based on data from the Cat Bk site. The advective-diffusion model was run and temperatures were estimated at every 0.1 m (for depths 0 m to 1m) and every 0.2 m (for depths 1 m to 3 m). The vertical water velocity component (v_g) was assumed at 0.0020 m hr^{-1} for Cat Bk and 0.0025 m hr^{-1} for LSWM based on previous calibrations and field observations (D. Caissie, unpublished data). Also based on water temperature

observations within a groundwater well at Catamaran Brook, a constant groundwater temperature of 6.5 °C was assumed at a depth of 6 m into the substrate for Cat Bk and LSWM (Caissie and Satish, 2001).

The heat capacity of the saturated porous media in question (c) was estimated using the following equation (Caissie and Satish, 2001):

$$\rho_m c_m = n \rho_w c_w + (1-n) \rho_s c_s \quad (3.15)$$

where, ρ_m is the density of the rock-fluid matrix, ρ_w and c_w are the density of the water and the specific heat capacity of the water (1000 kg m⁻³ and 4187 J kg⁻¹ °C⁻¹), and ρ_s and c_s are the density and specific heat capacity of the streambed. The porosity (n) and the density of the rock-fluid matrix (ρ_m) were estimated from field observations at the Cat Bk and at LSWM ($n = 0.27$ and $\rho_m = 2300$ kg m⁻³). The streambed consisted mainly of granite type rocks with a density (ρ_s) of 2578 kg m⁻³ and a specific heat capacity (c_s) of 775 J kg⁻¹ °C⁻¹. Therefore, the specific heat of the solid-fluid matrix (c_m) was estimated at 1130 J kg⁻¹ °C⁻¹. The thermal conductivity of the saturated sediment k_m was calculated as a function of porosity n (0.27) and thermal conductivity of water k_w (0.590 W m⁻¹ °C⁻¹) and solids k_s (2.79 W m⁻¹ °C⁻¹) with the following equation (Stallman, 1965):

$$k = n k_w + (1-n) k_s \quad (3.16)$$

With the above physical properties and porosity, the thermal conductivity of the saturated sediment (k_m) was calculated at 2.2 W m⁻¹ °C⁻¹ for Cat Bk and LSWM.

3.2.6.1 STREAMBED HEAT FLUX BY CONDUCTION (H_b)

With the above streambed physical properties the heat flux by conduction was estimated using the heat budget method (Hondzo and Stefan, 1994). This approach estimated the rate of variation in riverbed heat storage knowing the temperature over a range of depths and at regular intervals, and by comparing changes in heat storage over time. The streambed heat flux by conduction was calculated using the following equation (Hondzo and Stefan, 1994):

$$H_b = \left(\frac{1}{3600} \right) \rho_m c_m \frac{\partial}{\partial t} \int_0^l T(z, t) dz \quad (3.17)$$

where, $T(z, t)$ is the riverbed temperature profile with depth z at a time step (t) of one hour and other parameters are as described before. The heat transfer was calculated from this equation as temperature changed though time. Energy was transferred from the lotic environment to the streambed and vice versa.

3.2.6.2 STREAMBED HEAT FLUX BY GROUNDWATER ADVECTION (H_g)

The advective heat flux is both a function of the groundwater contribution (vertical velocity component) and the difference between surface water and groundwater temperatures. The advective heat flux was estimated using the formula provided by Sridhar *et al.* (2004):

$$H_g = \rho_w c_w Q_g (T_w - T_g) \quad (3.18)$$

where, Q_g is the groundwater flow ($\text{m}^3 \text{s}^{-1}$) and T_g is the groundwater temperature at a certain depth close to the surface (e.g. at 0.1 m). Given the vertical flow component, the groundwater flow (Q_g) was then estimated for an area of 1 m^2 . The vertical flow velocity (v_g) was negative (for upwelling flow) in the original advection-diffusion heat transport

Equation (3.14); however, upwelling flow becomes a positive discharge in Equation (3.18). To estimate the advective heat flux using (3.18), the groundwater temperature (T_g) at 0.1 m was used from the previously calculated temperature profile of an advective-diffusion model.

In most water temperature studies, meteorological data are usually taken from the nearest meteorological station (e.g., nearest airport), which can be many kilometres away from the stream environment. Also, significant differences can exist between the meteorological data and the stream microclimate (Benyahya *et al.*, 2010). For the deterministic model, data were collected both within the stream environment (microclimate sites) and at a meteorological station (within a cleared area of the forest), for comparison purposes.

3.3 EQUILIBRIUM TEMPERATURE MODEL

Most relevant energy components related to water temperature modeling have been described in previous deterministic studies (Raphael, 1962; Younus *et al.*, 2000; Caissie *et al.*, 2007) as well as in Section 3.2.

Equilibrium temperature models have been proven to be efficient in studies of river water temperatures at daily or weekly time scales (Gu *et al.*, 1998; Mohseni and Stefan, 1999; Bogan *et al.*, 2003; Larnier *et al.*, 2010; Herb and Stefan, 2011). The intention in this study was to develop such a model and assess its performance at an hourly time scales. The equilibrium temperature model was developed to simplify the expression of the total heat flux (Edinger *et al.*, 1968; Morin and Couillard, 1990; Gu *et al.*, 1998; Caissie *et al.*,

2005). The net flux at the water surface is expressed by a simpler equation with fewer meteorological parameters. The exchange of heat flux between the atmosphere and the river is assumed to be proportional to the difference between the water temperature and an equilibrium temperature. The development of this model is provided in Caissie *et al.* (2005). The equilibrium temperature is the water temperature at which the total heat flux at the surface of the river is zero. It is the water temperature that the river is trying to reach under natural steady-state conditions, but can never reach due to changing meteorological conditions. The total heat flux is expressed as a function of water and equilibrium temperatures (Lebosquet, 1946; Edinger *et al.*, 1968, Novotny and Krenkel, 1973). Under such conditions, the total heat flux can be expressed as Newton's Law of Cooling given by the following equation (Morin and Couillard, 1990):

$$H_t = K(T_e - T_w) \quad (3.19)$$

where, T_w represents the water temperature, T_e is the equilibrium temperature ($^{\circ}\text{C}$) and K represents a thermal exchange coefficient ($\text{W m}^{-2} \text{ }^{\circ}\text{C}^{-1}$). After substitution of Equation (3.19) into Equation (3.3b), the changes in water temperature can be expressed by:

$$\frac{\partial T_w}{\partial t} = \frac{W}{c_w \rho_w A} K(T_e - T_w) \quad (3.20)$$

or

$$\frac{\partial T_w}{\partial t} = \frac{K}{c_w \rho_w y_w} (T_e - T_w) \quad (3.21)$$

where, W is the river width (m), A is the area of the cross-section (m^2), W/A is approximated by $1/y_w$, where y_w is the mean water depth (m). Studies have shown a good relationship between air and equilibrium temperature (Mohseni and Stefan, 1999), while

others have shown that T_e can be expressed as a linear function of air temperature (Caissie *et al.*, 2005; Larnier *et al.*, 2010):

$$T_e = \alpha T_a + \beta \quad (3.22)$$

where, α and β are the linear regression coefficient between hourly air and equilibrium temperature. Therefore, Equation (3.21) can be rewritten as follows:

$$\frac{\partial T_w}{\partial t} = \frac{K}{c_w \rho_w y_m} (\alpha T_a + \beta - T_w) \quad (3.23)$$

Some studies have used the equilibrium temperature concept to study the thermal regime in rivers (LeBosquet 1946; Edinger *et al.*, 1968; Novotny and Krenkel 1973) but few have actually modeled water temperatures using this approach (Caissie *et al.*, 2005; Larnier *et al.*, 2010).

The equilibrium model developed for the present study was applied at hourly time steps and for open water conditions, i.e., from April 15 to October 31 for years 1998 to 2007. These years were divided into two groups: Calibration (1998-2002) and validation (2003-2007). The calibration years were used to define the linear relationship between air and equilibrium temperatures, as well as the thermal exchange coefficient (K), using the minimum sum of squared errors (observed vs. predicted). The validation years (2003-2007) were used to test the model, using the parameters previously defined during the calibration period. In order to keep the model simple, the thermal exchange coefficient (K) was considered as a constant for each river as it was the case in previous studies (Caissie *et al.*, 2005; Larnier *et al.*, 2011).

3.4 ARTIFICIAL NEURAL NETWORK MODEL

The third model selected to predict the variability of stream water temperatures was an artificial neural network (ANN). ANNs are widely used in hydrology and the applied earth sciences, particularly in modeling of precipitation and run-off, water demand predictions, groundwater and water quality (Govindaraju, 2000a). Few studies have applied this technique to water temperatures (Bélanger *et al.*, 2003; Sivri *et al.*, 2007; Chenard and Caissie, 2008), and even fewer studies have been carried out using water temperatures (Risley *et al.*, 2003). The study of Risley *et al.* (2003) used such data as meteorological data, riparian habitat characteristics, and watershed physiography. These data are usually not readily available for most streams. The goal of this study was to develop an ANN model using minimal and readily accessible input data. The model of Risley *et al.* (2003) was applied on one short season (June 21 to September 20) and for one only year; whereas, this study applied ANN models to a longer open water season (April 15 to October 31) for 10 consecutive years. This model consisted of a finite number of layers, as presented in Figure 3.2. Each layer is composed of a number of neurons.

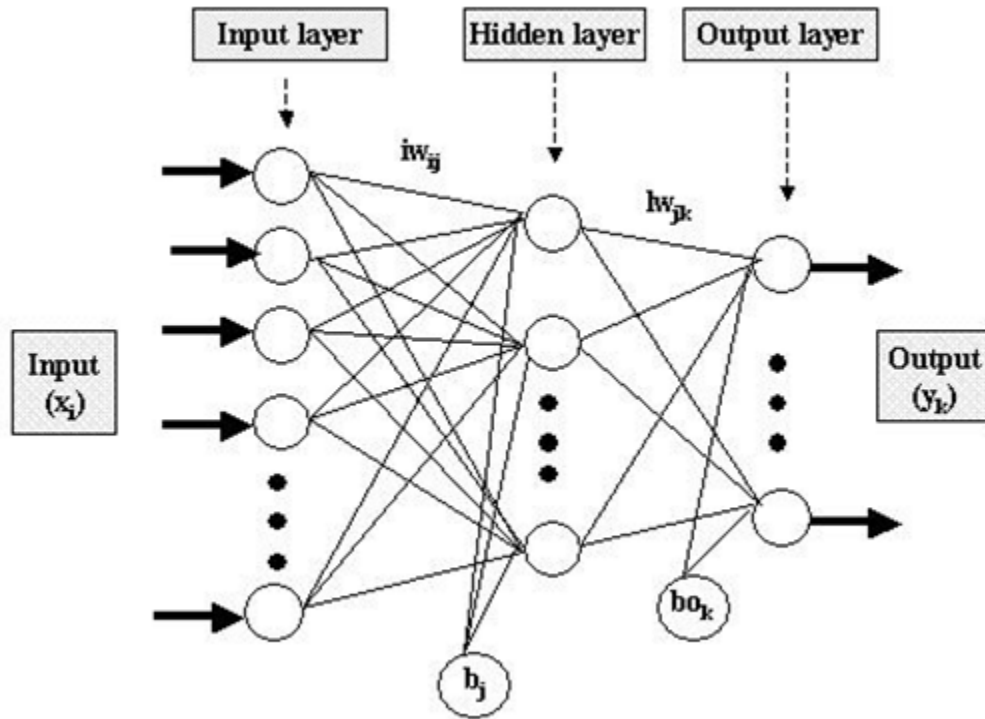


Figure 3.2. Illustration of feed-forward neural network architecture.

First, each input x_i sends its value to all hidden nodes j of the network. Each hidden node calculates the weighted sum of inputs and the bias, using:

$$n_j = b_j + \sum_{i=1}^I iw_{ij}x_i \quad (3.24)$$

where, i is the total number of input nodes, j is the hidden node, iw_{ij} are the connection weights between the i^{th} input and j^{th} hidden node, b_j is the bias weight of each hidden node and x_i is the input node. Each hidden node j computes a function of its sum through an activation function:

$$a_j = f(n_j) \quad (3.25)$$

The activation functions can be sigmoidal, linear, threshold-type, Gaussian or hyperbolic tangent, depending on the type of network and training algorithm employed (Dawson and

Wilby, 2001). The most commonly used activation function found in hydrology is the hyperbolic tangent functions (Govindaraju, 2000a; Shamseldin *et al.*, 2002; Shrestha *et al.*, 2005; Yonaba *et al.*, 2010). The hyperbolic tangent function selected in this study, is given by:

$$f(n_j) = \frac{2}{(1 + e^{(-2n_j)})} - 1 \quad (3.26)$$

where, n_j is the weighted sum of inputs and bias of the hidden node j . This function was selected because it clearly represents the non-linear processes usually found in hydrology, it is an always-increasing function that is continuous and smooth with asymptotic properties, and it has output values between -1 and +1 (Smith, 1993; Jain and Mao, 1996).

In the next step, each hidden node (j) sends its result a_j to all the output nodes (y_k). Each output node value is calculated using:

$$y_k = bo_{jk} + \sum_{j=1}^J a_j lw_{jk} \quad (3.27)$$

where, k is the output node, bo_{jk} is the bias weight of the output node, lw_{jk} is the connection weight for the j^{th} hidden node and the k^{th} output node, and y_k is the output node.

For the application of ANN within the present study, a supervised learning paradigm was used, meaning that the ANN uses pairs of data so as to have a correct answer (output) for every input. The feed-forward backpropagation algorithm was also used. It distributed the error (predicted output – observed output) so as to obtain the lowest or minimal total errors. With this algorithm, the information goes through the network and the network predicts an output. The predicted output is then compared to the observed output (e.g.,

measured water temperature data) and the error is calculated. The error is transmitted in the reverse direction and the weights are readjusted. This iterative process is done many times until the error is less than some desired threshold. The learning process adjusts the weights to minimize the error.

Water temperature data for the ANN was used for the period April 15 (day 105) to October 31 (day 304) and for years 1998 and 2007 at both Cat Bk and LSWM. This period approximately corresponded to the period without ice cover, i.e., open water conditions. Some years had no data for a few days; these days were not included in the ANN model. Data were separated into two samples: training data (1998-2002) and validation data (2003-2007).

Two feed-forward backpropagation ANN models were created using *Matlab Student 7.1.*, to predict water temperatures. The first ANN was developed to predict daily mean water temperatures. The four input parameters of the first ANN were: air temperature ($^{\circ}\text{C}$) of the present and previous day, time of year (day) and mean daily water level (m). For the ANN predicting daily mean water temperature, the air temperature of the previous day was used as input because air and water temperature are strongly correlated at such scales (Kothandaraman, 1971; Cluis, 1972). The simulated daily mean water temperatures from the first ANN were then used as input to the hourly ANN water temperature model. The second ANN was developed to predict hourly water temperature and used six input nodes: air temperature ($^{\circ}\text{C}$) of the present and previous hour, time of day (hour), time of year (day), daily mean water temperature (simulated from the previous ANN model) ($^{\circ}\text{C}$), and mean daily water level (m). The selection of air temperature, as input data, was based on

the availability of such data and its strong correlation to water temperatures (Cluis, 1972; Song and Chien, 1977; Stefan and Preud'Homme, 1993; Mohseni and Stefan, 1999; Bélanger *et al.*, 2005; Chenard and Caissie, 2008). During the training of the second ANN, the observed daily mean water temperatures were used; however during the validation the simulated daily mean water temperatures were used to simulate the hourly temperatures.

The complexity of a function estimated by a neural network increases with the training. During the training, the network will reach a certain number of epochs that will give the best generalization and after this critical point; the ANN model will start overfitting (Maier and Dandy, 2000). The performance is measured during the training and validation phase with a different number of hidden nodes. When the performance during the validation phase starts to decrease for a certain number of hidden nodes, the network should stop the training and use the corresponding hidden nodes. This limiting node procedure for the number of hidden nodes can also be applied to the number of epochs. Smith (1993) suggested limiting the number of hidden nodes within a network and then limiting the training (based on validation sample error) to prevent overfitting. The two ANN models obtained optimal results with five hidden nodes in one hidden layer. The ANN models were adjusted until the difference between predicted and observed water temperatures was minimized.

The ANN model predicting the daily mean water temperatures had four input nodes ($I = 4$), five hidden nodes ($J = 5$) in one hidden layer and only one output node ($K = 1$). The ANN model predicting the hourly water temperatures had six input nodes ($I = 6$), five hidden nodes ($J = 5$) in one hidden layer, and only one output node ($K = 1$).

3.5 DATA COLLECTION

Hourly data were collected at both microclimate sites (i.e., Catamaran Brook and Little Southwest Miramichi River) and at the remote meteorological station (MetSta) from July 4, 2007 (day 185) to October 2 (day 275) for the analysis of the river heat budget (deterministic model). Streambed temperatures and microclimate data were monitored only during the summer of 2007. Data for the equilibrium temperature and ANN models came from the meteorological station (MetSta) only. Water temperature and meteorological data for the equilibrium temperature and ANN models were collected for the period of April 15 (day 105) to October 31 (day 304) and for years 1998 to 2007 at both Cat BK and LSWM. This period approximately corresponded to the period of the year without ice cover, i.e., open water condition. Some years had missing data for a few days and these days were not included in the water temperature models. Data were separated into two samples: training data (1998-2002) and validation data (2003-2007).

Meteorological stations were installed within the stream environment in Catamaran Brook and Little Southwest Miramichi River to monitor microclimate conditions (air temperature, relative humidity, wind speed, solar radiation and water temperature) for the deterministic models. Air temperature, relative humidity, and wind speed were measured 2 m above the water surface using a Vaisala Relative Humidity and Temperature sensor and a RM Young wind monitoring sensor. Water temperature was measured with a 107B Water Temperature Probe (Campbell Scientific Corps.) and direct solar radiation was measured by using a Kipp and Zonen Silicon Pyranometer (at LSWM) and a LI-COR silicon pyranometer (Catamaran Brook). All sensors were scanned every 5 seconds by a CR10 data logger and hourly averages were then calculated.

Precipitation and barometric pressure were obtained from the Catamaran Brook meteorological station, which is located between 1 km (Cat Bk) and 8 km (LSWM) from the stream microclimate sites. This station is located in the middle of a 400 m x 400 m clear-cut area. A tipping bucket rain gauge (TE525) by Texas Electronics Inc. was used to monitor precipitation at approximately 1.2 m above the ground and sheltered by an Alter type wind shield. Barometric pressure was monitored using a setra barometric pressure sensor (Model SBP270) at approximately 2 m above grade. Daily mean discharges were obtained from two Environment Canada's hydrometric stations (01BP001 and 01BP002). Mean water depth was obtained from discharge and a power function relating mean water depth and river discharge as described in Caissie *et al.* (2007). Hourly cloud cover information came from a local weather station (Miramichi station 8 100 989). Streambed temperature sensors were installed in Catamaran Brook during the summer of 2007. The sensors were placed in a single vertical over a range of different depths and up to 3 m within the substrate, to monitor streambed temperatures. The type of water temperature sensor used was the model 107B from Campbell Scientific Canada Corp. They were connected to a CR10 data logger where data were stored.

3.6 MODELING PERFORMANCE CRITERIA

To compare modeling performances for different years and study periods (calibration/validation) three criteria were used: The root-mean-square error (*RMSE*), the coefficient of determination (R^2), and the bias. These criteria were selected because they are often used in modeling studies and results using these performance criteria were available for other water temperature models at Cat Bk and LSWM. The root-mean-

square error (*RMSE*) represents the mean errors associated with the modeling effort. It was calculated using:

$$RMSE = \sqrt{\frac{\sum_{i=1}^N (T_w(O)_i - T_w(P)_i)^2}{N}} \quad (3.28)$$

where, N is the number of hourly water temperature observations, $T_w(O)$ is the observed hourly water temperature and $T_w(P)$ is the predicted hourly water temperature.

The coefficient of determination (R^2) represents the variability in the data that can be explained by the model, found using:

$$R^2 = \left[\frac{N \sum_{i=1}^N T_w(O)_i T_w(P)_i - \left(\sum_{i=1}^N T_w(O)_i \right) \left(\sum_{i=1}^N T_w(P)_i \right)}{\sqrt{\left[N \sum_{i=1}^N T_w(O)_i^2 - \left(\sum_{i=1}^N T_w(O)_i \right)^2 \right] \times \left[N \sum_{i=1}^N T_w(P)_i^2 - \left(\sum_{i=1}^N T_w(P)_i \right)^2 \right]}} \right] \quad (3.29)$$

The overall over or under-estimation exhibited by a given temperature model was of interest. There are various ways to quantify such 'bias'. The measure used in this study was as follows:

$$Bias = \frac{1}{N} \sum_{i=1}^N (T_w(P)_i - T_w(O)_i) \quad (3.30)$$

For the deterministic model, these criteria (*RMSE*, R^2 and *Bias*) were also calculated for total heat flux, where $T_w(P)$ and $T_w(O)$ are respectively replaced by $H_t(P)$ and $H_t(O)$ in the equations above.

CHAPTER 4: RESULTS

4.1 DETERMINISTIC MODEL

4.1.1 OVERVIEW OF DATA SERIES

Hourly data were collected from July 4, 2007 (day 185) to October 2 (day 275) at both microclimate monitoring sites (Catamaran Brook and at Little Southwest Miramichi River), for the analysis of the river heat budget. Six different periods in summer 2007 were selected and each period was selected based on specific water temperature patterns and meteorological characteristics (Figure 4.1). For instance, Period 1 represents a period with the highest air and water temperature during the summer, whereas Period 3 represents low flow conditions (Table 4.1). Period 6 represents autumn conditions and Period 4 was mostly cloudy with a significant amount of precipitation.

Table 4.1. Selected periods for the river heat budget analysis at both Catamaran Brook and Little Southwest Miramichi River in 2007.

Period	Days of year	Dates	Hydrometeorological conditions
1	207-211	July 26-30	Highest water temperatures, high stream flow
2	222-226	August 10-14	Generally clear sky days
3	231-235	August 19-23	Relatively low flow
4	241-245	August 29 - Sept. 2	High precipitation, cloudy days
5	247-251	September 4-8	Great variability in air and water temperatures
6	268-272	September 25-29	Autumn conditions

Figures 4.1a and 4.1b show the hourly air and water temperature time series for the entire study period. Precipitation (hourly) and discharge (mean daily) for both Catamaran Brook (Cat Bk) and Little Southwest Miramichi (LSWM) are presented in Figure 4.1c.

Air temperatures were very similar within the microclimate environment of both streams (Figure 4.1a). The mean air temperature at Cat Bk for the study period was 14.5 °C (−1.3 °C to 31.3 °C). The mean air temperature at LSWM was slightly higher at 15.9 °C (−1.8 °C to 31.4 °C). Although microclimate air temperatures showed similar patterns, water temperatures showed more pronounced difference between the two river systems (Figure 4.1b). The maximum water temperature at Cat Bk occurred on day 206 (July 25) at 22.6 °C with a mean value of 14.4 °C. Water temperatures were higher in LSWM, with a mean temperature of 18.8°C, reaching a maximum of 28.7 °C (day 209; July 28). Discharge was much higher in LSWM (average daily flow of 14.9 m³ s⁻¹) than in the Cat Bk (average daily flow of 0.31 m³ s⁻¹) due to the differences in size of these catchments. Hourly precipitation was measured at the Cat Bk meteorological station (Figure 3.1). The maximum hourly precipitation was recorded on August 8 (11.9 mm; day 220) whereas the maximum daily precipitation, as shown in Figure 4.c, was recorded on July 5 (day 186; 24.9 mm).

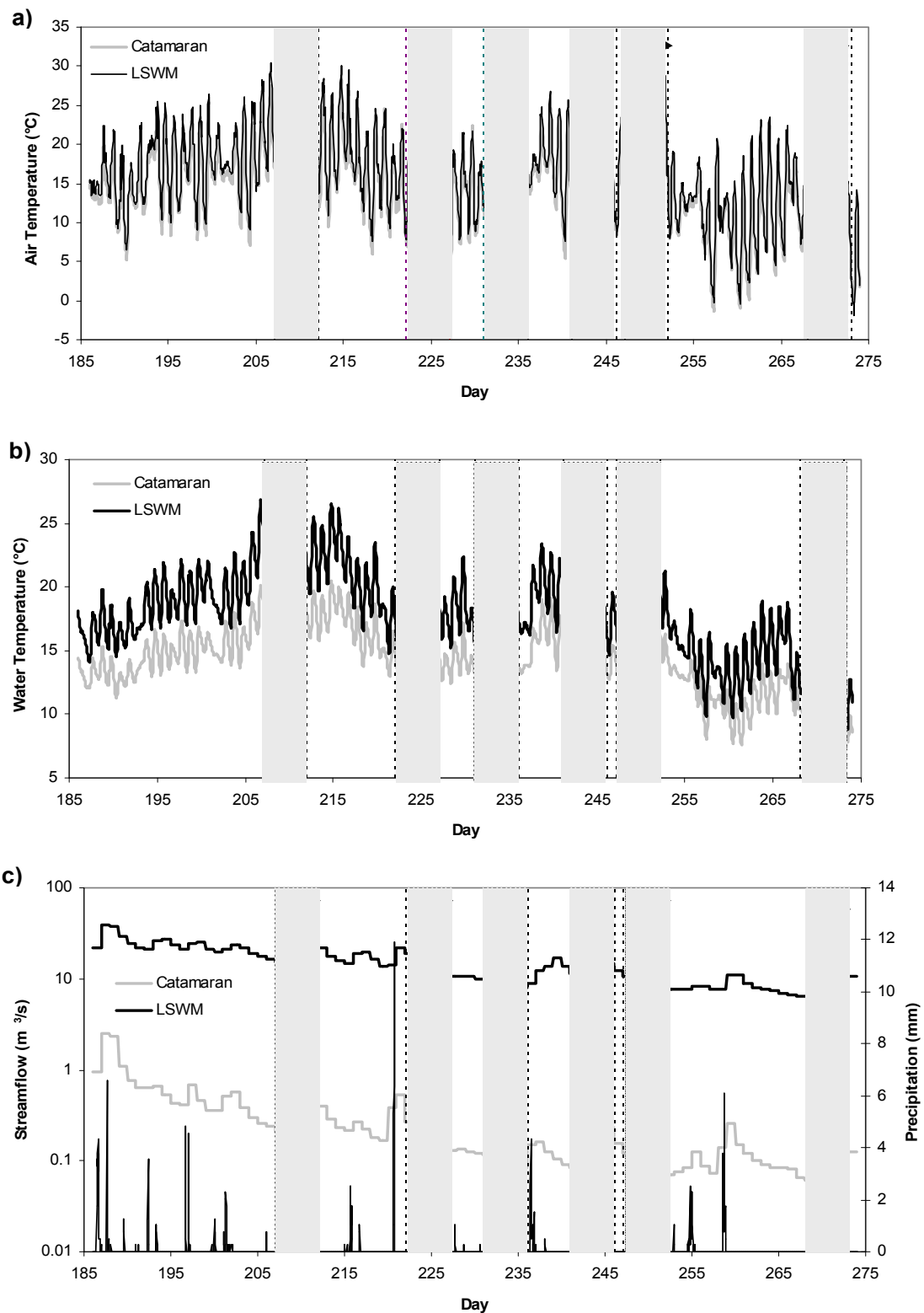


Figure 4.1. Time series plot of selected parameters (air temperature, water temperature, stream flow and precipitation) and study periods for Catamaran Brook and Little Southwest Miramichi River. The stepped data on Figure 4.1c represents daily mean discharge. Shaded bars represent Period 1 to Period 6.

The present study included an examination of the differences between data from a remote meteorological station (MetSta) and those measured within the near-stream environment (microclimate sites). Table 4.2 shows average conditions for each period (Period 1 to 6) for the different microclimate sites as well as those at the meteorological station. The Duncan's multiple range (DMR) test was used to detect statistically significant differences between sites, for each period (SAS 9.1.3). This test evaluates the statistical significance of differences in ranges in sorted samples for pairs of means, using a studentized range statistic. No air temperature ranges were found to be significantly different (all sites, during periods 3, 4, and 5; $p > 0.11$) and no differences were noted between LSWM and the MetSta (all periods). Air temperature at Cat Bk was significantly different than LSWM and MetSta during periods 1 and 2. Mean air temperature at Cat Bk was lower, although less than 2 °C. Relative humidity was significantly different ($p < 0.001$) between sites and for all periods. Most of the difference was attributable to MetSta. The relative humidity at LSWM and Cat Bk was higher than the remote meteorological station (MetSta). As expected, a significant difference ($p < 0.001$) was observed between sites for wind speed for all periods. For example, wind sheltering was strong at the river microclimate sites, with an average wind speed of only 0.06-0.15 m s⁻¹ at Cat Bk and 0.47-0.72 m s⁻¹ at LSWM. The remote MetSta data showed higher wind speeds (1.5-2.3 m s⁻¹). Incoming solar radiation measured was not significantly different ($p > 0.05$) and averaged between 95.5 W m⁻² and 250 W m⁻². However, incoming solar radiation was significantly lower ($p < 0.05$) at Cat Bk, with averages between 28.3 W m⁻² and 100 W m⁻². Although the air temperatures were similar between Cat Bk and LSWM, the water temperature was significantly warmer ($p < 0.001$) at LSWM, 3.5 °C on average. Water temperature varied between

12.2 °C and 19.1 °C at Cat Bk and between 14.8 °C and 23.9 °C at LSWM (Period 1 to 6). Table 4.2 also shows average discharge (for all periods) at Cat Bk and LSWM. As expected, the mean discharge of Cat Bk was significantly different than that of LSWM ($p < 0.001$).

Table 4.2. Comparison of period averages of specific meteorological parameter at two microclimate sites (Catamaran Brook and Little Southwest Miramichi River) and at the meteorological station (MetSta).

Meteorological or hydrologic parameter Site		Period					
		1	2	3	4	5	6
Air Temperature (°C)	Cat Bk ^a	21.3	16.0	11.5	14.4	13.4	12.3
	LSWM ^b	22.7	17.5	12.9	15.6	14.6	13.3
	MetSta ^c	22.8	17.6	12.5	15.4	15.3	13.8
Relative Humidity (%)	Cat Bk	87.1	80.9	78.9	90.5	84.6	93.2
	LSWM	83.2	77.7	75.9	86.4	80.9	90.2
	MetSta	77.5	69.5	71.2	82.0	70.8	83.4
Wind Speed (m s ⁻¹)	Cat Bk	0.09	0.07	0.13	0.06	0.15	0.10
	LSWM	0.61	0.47	0.72	0.49	0.67	0.35
	MetSta	1.7	1.5	1.9	1.5	2.3	1.5
Incoming Solar Radiation (W m ⁻²)	Cat Bk	100	84.2	86.3	44.3	46.7	28.3
	LSWM	224	239	236	158	175	95.5
	MetSta	229	250	236	155	182	99.4
Water Temperature (°C)	Cat Bk	19.1	16.2	12.9	15.0	13.2	12.2
	LSWM	23.9	20.3	16.6	18.4	16.4	14.8
Streamflow (m ³ s ⁻¹)	Cat Bk	0.516	0.180	0.098	0.246	0.092	0.125
	LSWM	21.1	14.3	8.90	13.7	9.10	7.70

a - Catamaran Brook

b - Little Southwest Miramichi

c - Meteorological Station

4.1.2 DETAILED ANALYSIS OF HEAT FLUXES AND WATER TEMPERATURES

A detailed heat flux analysis was carried out for both Cat Bk and LSWM for Period 1 to Period 6 using microclimate data to compare observed and predicted fluxes (Table 4.3). Period 1 consisted of days 207 to 211 (July 26-30, 2007) and included the warmest air

and water temperatures as well as a high discharge event towards the end of the period (Figure 4.1c). The high discharge event was due to 40 mm of rain over a 24-hour period (day 209 and 210). Period 2 consisted of days 222 to 226 (August 10 to 14, 2007), which were days with generally clear skies and no precipitation. Period 3 was a period with relatively low flows and included days 231 to 235 (August 19 to 23, 2007). High precipitation and cloudy days were the main characteristics of Period 4, days 241 to 145 (August 29 to September 2, 2007). Period 5 was selected to examine the heat fluxes during high variability in air and water temperatures from days 247 to 251 (September 4 to 8, 2007). Period 6 was selected for the detailed heat flux analysis representing autumn conditions (e.g. lower water temperatures and heat fluxes), and included days 268 to 272 (September 25 to 29). Important precipitation during Period 6 (total rainfall of 25 mm over 3 days; day 269 to 271) caused an increase in daily stream discharges in both streams (Figure 4.1c).

Heat fluxes related to precipitation were not illustrated on any of the Figures because it was too small (compared to other heat fluxes); however values are provided in Table 4.3. Precipitation fluxes contributed less than 0.2 W m^{-2} at Cat Bk and 0.7 W m^{-2} at LSWM for periods 1, 4 and 6 (Table 4.3).

The total heat flux was calculated using two approaches. The first consisted of calculating the observed total heat flux or $H_t(O)$ whereas the second approach consisted of calculating the predicted total heat flux or $H_t(P)$. The observed total heat flux was calculated based on observed water temperature variability and using Equation (3.3b), based on actual changes in water temperature every hour, (ΔT). The second approach

consisted of calculating each heat flux component (each flux of Equation (3.4)) and adding the components to get the net predicted heat flux. Both of these net heat fluxes were calculated and compared to $H_t(O)$ and $H_t(P)$.

Results of the performance of the deterministic model applied to Cat Bk and to LSWM are shown in Table 4.4. It shows the root-mean-square-error (*RMSE*), the coefficient of determination (R^2) and the bias (*Bias*) calculated using the predicted total heat flux ($H_t(P)$) and observed total heat flux ($H_t(O)$), for the deterministic model.

Table 4.3. Heat fluxes (gain, loss and net) for both river systems.

		Catamaran Brook										
		H_t(O)	H_t(P)	H_{surf}	H_s	H_l	H_c	H_c	H_p	H_{bed}	H_b	H_g
Period 1	Gain	23.8	42.9	41.4	30.0	5.3	2.9	3.0	0.2	1.5	1.5	0.0
	Loss	-27.9	-8.6	-3.7	0.0	-1.6	-1.9	-0.2	-0.1	-4.9	-2.9	-1.9
	Net	-4.1	34.3	37.7	30.0	3.7	1.1	2.8	0.1	-3.4	-1.5	-1.9
Period 2	Gain	19.8	20.9	18.4	16.3	0.9	0.0	1.2	0.0	2.4	2.4	0.0
	Loss	-19.7	-22.9	-16.9	0.0	-8.0	-7.6	-1.3	0.0	-6.0	-4.1	-1.9
	Net	0.2	-2.0	1.6	16.3	-7.1	-7.6	0.0	0.0	-3.6	-1.7	-1.9
Period 3	Gain	15.7	21.2	17.0	15.5	0.5	0.0	1.0	0.0	4.2	3.9	0.3
	Loss	-16.8	-26.1	-21.4	0.0	-9.6	-9.6	-2.2	0.0	-4.7	-3.7	-1.1
	Net	-1.1	-4.9	-4.4	15.5	-9.1	-9.6	-1.2	0.0	-0.5	0.2	-0.7
Period 4	Gain	12.9	12.3	9.9	8.1	0.7	0.3	0.7	0.1	2.5	2.4	0.1
	Loss	-16.4	-16.8	-13.5	0.0	-7.5	-4.7	-1.2	-0.1	-3.3	-2.0	-1.3
	Net	-3.5	-4.4	-3.6	8.1	-6.8	-4.4	-0.5	0.0	-0.8	0.4	-1.2
Period 5	Gain	13.1	17.0	14.1	8.1	2.2	2.4	1.4	0.0	2.9	2.6	0.3
	Loss	-11.5	-18.4	-13.4	0.0	-6.4	-5.8	-1.2	0.0	-5.0	-3.8	-1.2
	Net	1.7	-1.4	0.7	8.1	-4.2	-3.4	0.2	0.0	-2.1	-1.2	-0.9
Period 6	Gain	8.2	11.3	9.5	5.8	1.2	1.6	0.9	0.1	1.8	1.7	0.1
	Loss	-8.9	-13.0	-10.1	0.0	-6.2	-3.0	-0.8	0.0	-2.9	-2.1	-0.8
	Net	-0.7	-1.7	-0.6	5.8	-5.0	-1.5	0.0	0.1	-1.1	-0.4	-0.7
		Little Southwest Miramichi River										
		H_t(O)	H_t(P)	H_{surf}	H_s	H_l	H_c	H_c	H_p	H_{bed}	H_b	H_g
Period 1	Gain	98.2	130.8	126.8	120.9	2.9	0.0	3.0	0.0	3.9	3.9	0.0
	Loss	-115.6	-59.0	-48.4	0.0	-22.7	-21.9	-3.2	-0.7	-10.5	-6.4	-4.2
	Net	-17.4	71.8	78.4	120.9	-19.8	-21.9	-0.2	-0.7	-6.6	-2.4	-4.2
Period 2	Gain	106.9	116.0	110.9	109.1	0.0	0.0	1.8	0.0	5.1	5.1	0.1
	Loss	-101.4	-87.8	-76.3	0.0	-45.4	-25.7	-5.2	0.0	-11.5	-8.0	-3.6
	Net	5.5	28.2	34.6	109.1	-45.4	-25.7	-3.4	0.0	-6.4	-2.9	-3.5
Period 3	Gain	93.5	105.5	96.9	96.3	0.0	0.0	0.7	0.0	8.5	8.0	0.5
	Loss	-90.7	-89.8	-79.7	0.0	-49.2	-24.2	-6.3	0.0	-10.0	-7.6	-2.4
	Net	2.8	15.7	17.2	96.3	-49.2	-24.2	-5.7	0.0	-1.5	0.4	-1.9
Period 4	Gain	66.5	76.5	70.8	70.0	0.02	0.00	0.7	0.1	5.7	5.6	0.2
	Loss	-79.0	-69.6	-63.3	0.0	-39.0	-18.8	-5.2	-0.3	-6.3	-4.1	-2.2
	Net	-12.5	6.9	7.5	70.0	-39.0	-18.8	-4.5	-0.2	-0.6	1.5	-2.0
Period 5	Gain	82.4	93.3	87.0	82.1	1.9	0.4	2.5	0.0	6.4	5.8	0.5
	Loss	-72.4	-63.5	-53.5	0.0	-33.3	-15.6	-4.6	0.0	-10.0	-7.5	-2.5
	Net	10.0	29.8	33.5	82.1	-31.4	-15.2	-2.1	0.0	-3.7	-1.7	-2.0
Period 6	Gain	47.2	53.9	49.0	43.7	2.1	1.6	1.5	0.1	4.9	4.6	0.3
	Loss	-50.6	-57.4	-51.4	0.0	-36.3	-10.8	-4.0	-0.2	-6.0	-4.3	-1.6
	Net	-3.5	-3.4	-2.3	43.7	-34.2	-9.3	-2.5	-0.1	-1.1	0.3	-1.4

Table 4.4. Results of modeling performance between predicted total heat flux, $H_t(P)$, and observed total heat flux, $H_t(O)$, for the deterministic model at Catamaran Brook and Little Southwest Miramichi River.

Period	Catamaran Brook			Little Southwest Miramichi		
	RMSE (W m ⁻²)	R ²	Bias (W m ⁻²)	RMSE (W m ⁻²)	R ²	Bias (W m ⁻²)
Period 1	61.3	0.721	38.4	130.8	0.922	89.2
Period 2	34.1	0.792	-2.2	85.4	0.943	22.2
Period 3	30.3	0.875	-4.8	72.6	0.947	12.9
Period 4	23.2	0.819	-1.1	64.2	0.947	19.5
Period 5	24.8	0.836	-1.6	82.6	0.915	19.9
Period 6	17.7	0.806	-1.0	55.8	0.910	0.1

4.1.2.1 PERIOD 1

Catamaran Brook

Air temperatures at Cat Bk during Period 1 (Figure 4.2a) were high initially (day 207 to 209; peaked at 31.3°C), and decreased thereafter (days 210-211; peaking at 23.2°C). Water temperatures in Cat Bk varied accordingly, between 17.1°C and 22.6°C. Fluxes showed values ranging between -174 W m⁻² and 227 W m⁻². The predicted net heat flux was overestimated during the daytime (day 207 and 208) but good agreement was observed at night on those same days (Figure 4.2a). A significant departure was observed between the two time series, $H_t(P)$ and $H_t(O)$ on day 210, coincidentally with a rainfall event and high discharge. Period 1 had the poorest performance of all periods at Cat Bk, with a *RMSE* of 61.3 W m⁻², a *R*² of 0.721 and a bias of 38.4 W m⁻² (Table 4.4).

When looking at the composition of the total heat flux ($H_t(P)$), it was noticed that the surface heat flux dominated the gains (positive fluxes) during the day and the losses at night (negative fluxes) whereas the streambed heat flux dominated the losses during the

day with small gains at night (Figure 4.2b). Surface heat fluxes exhibited their highest values early in Period 1 in both gains and losses (gains of 200-276 W m⁻² and losses of -50.0 W m⁻²; days 207-209) followed by lower values thereafter. Streambed fluxes were predominately negative throughout the period with values reaching -50.4 W m⁻² during the first 3 days. A slight gain of 17.5 W m⁻² was observed on day 210.

Both the surface and streambed heat fluxes were further analysed by calculating the relative contribution of each component (Figure 4.2c and 4.2d). For example, the net shortwave radiation (H_s) was the major contributor to the surface heat gain during the day, reaching 250 W/m² (Figure 4.2c). During the day, the evaporative heat flux (H_e) was the main component of surface energy loss. At night, the evaporative heat flux became slightly positive, but less than 19.1 W m⁻².

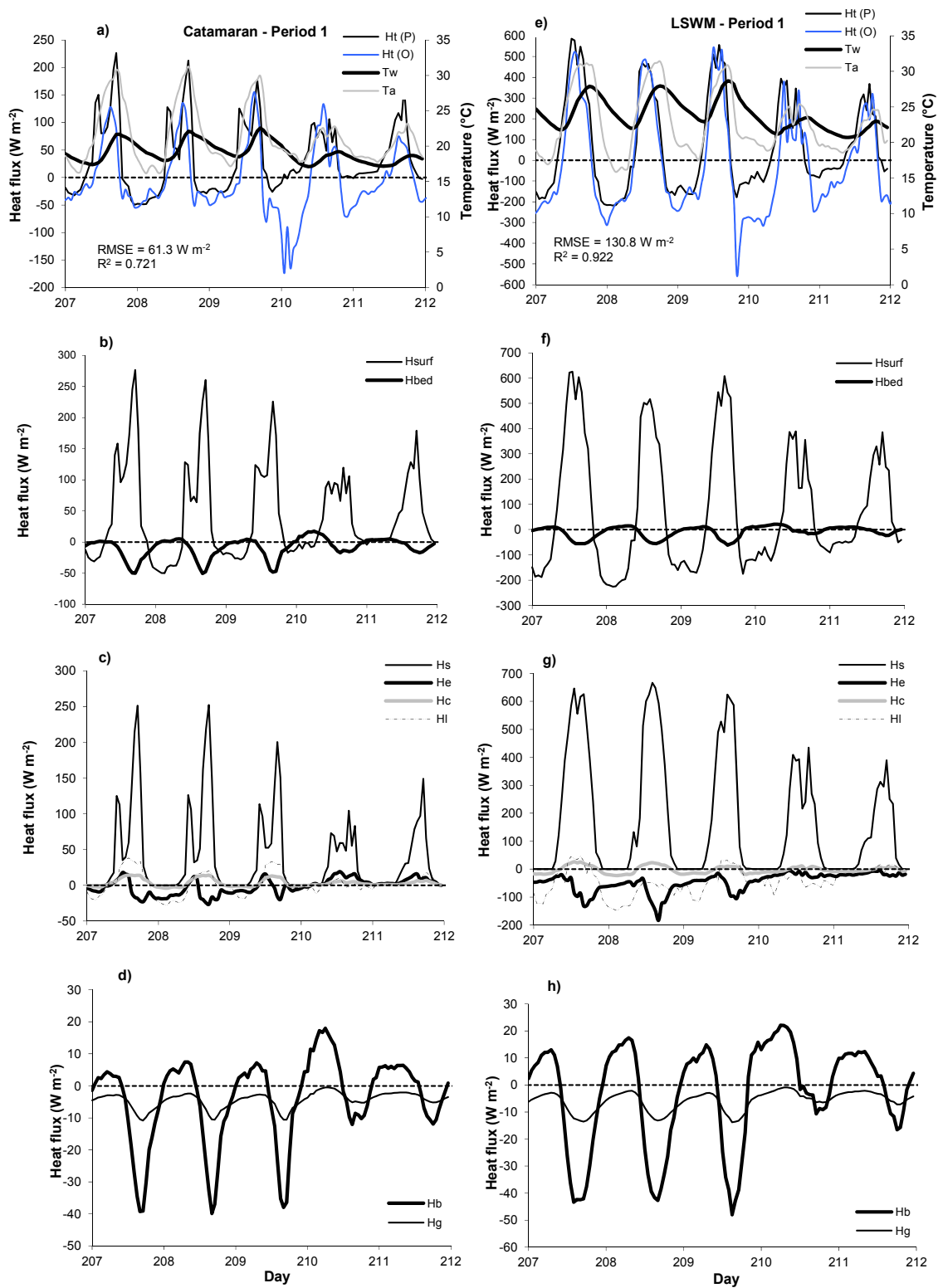


Figure 4.2. Detailed analysis of heat fluxes at Catamaran Brook and Little Southwest Miramichi River for Period 1.

The sensible heat flux (H_c) was lower than most other components, varying between -4.0 W m^{-2} at night and 14.2 W m^{-2} during the day. The net longwave radiation was a major cause of heat gain during the day (after solar radiation) and a major source of heat loss at night. The net longwave radiation generally between -27.7 W m^{-2} at night and 38.4 W m^{-2} during the day. Hourly precipitation heat fluxes (H_p) on day 209 and 210 varied between -5.0 W m^{-2} and 8.7 W m^{-2} for a precipitation event of 40 mm.

Heat flux by conduction was the dominant flux among the streambed fluxes (Figure 4.2d). Streambed conduction provided heat at night, (up to 18.0 W m^{-2} , and was the principal contributor of heat loss during the day, up to -39.9 W m^{-2} . The advective heat flux was significantly smaller than the conductive heat flux and was usually negative throughout the study period (-0.5 W m^{-2} to -10.8 W m^{-2}).

Heat gains and losses, as well as net heat fluxes, are presented in Table 4.3 for all periods. There was a significant difference between the observed and predicted total heat flux during Period 1; predicted total heat gain was calculated at 42.9 W m^{-2} compared to the observed value of 23.8 W m^{-2} . Heat losses showed significant differences as well (predicted -8.6 W m^{-2} and observed -27.9 W m^{-2}). Among the net fluxes of Period 1 the surface fluxes (H_{sur}) were predominately gains (37.7 W m^{-2}) and driven by incoming solar radiation ($H_s = 30.0 \text{ W m}^{-2}$) whereas streambed fluxes (H_{bed}) were predominately losses (-3.4 W m^{-2}). Among the streambed fluxes, both conduction and advective net heat fluxes were losses and of similar magnitude ($H_b = -1.5 \text{ W m}^{-2}$ and $H_g = -1.9 \text{ W m}^{-2}$; Table 4.3).

Little Southwest Miramichi

Air temperatures at LSWM were similar to that of Cat Bk during Period 1 (Figure 4.2a and 4.2e) while water temperature varied between 20.7°C and 28.7°C (Figure 4.2e). Observed ($H_t(O)$) and predicted ($H_t(P)$) total heat fluxes had similar patterns and exhibited significant agreement between the two time series. Total heat flux at LSWM generally varied between -219 W m^{-2} and 587 W m^{-2} ; however there was a significant decline in the observed total flux during the night of day 209, to a low of -552 W m^{-2} (Figure 4.2e). Period 1 also had the poorest performance of all periods at LSWM, with a *RMSE* of 130.8 W m^{-2} , an R^2 of 0.922 and a bias of 89.2 W m^{-2} (Table 4.4).

Surface and streambed heat fluxes were generally in opposite directions (Figure 4.2f) as with Cat Bk. Surface heat fluxes were higher in LSWM than in Cat Bk with peak values reaching 386 W m^{-2} to 625 W m^{-2} . Streambed heat fluxes in LSWM were very similar to those in Cat Bk and ranged from -62 W m^{-2} to 21 W m^{-2} . Among the surface heat fluxes the net shortwave radiation was observed to be the major heat gain, reaching 660 W m^{-2} . Evaporative fluxes and longwave radiation were the most significant heat losses, reaching -183 W m^{-2} (see in Figure 4.2g). Precipitation on day 209 and 210 resulted in a shift toward energy losses (H_p) and ranged between -51.6 W m^{-2} and 5.5 W m^{-2} . The convective energy flux contributed very little to the surface flux (-22.8 W m^{-2} to 26.4 W m^{-2}). The streambed heat flux by advection contributed to the energy loss in LSWM and varied between -13.8 W m^{-2} and -0.9 W m^{-2} (Figure 4.2h). The streambed heat flux by conduction varied between -48.0 W m^{-2} during the day and 22.1 W m^{-2} at night.

Heat fluxes were also determined for LSWM for each period as shown in Table 4.3. Observed and predicted total heat gains were found to be different (observed = 98.2 W m^{-2} and predicted = 130.8 W m^{-2}) with an even greater difference for losses (observed = -115.6 W m^{-2} and predicted = -59.0 W m^{-2}). The surface fluxes (H_{sur}) represented a net gain (78.4 W/m^2) and were driven by incoming solar radiation ($H_s = 120.9 \text{ W m}^{-2}$). Streambed fluxes represented a net loss of -6.6 W m^{-2} , of which, both conduction and advective heat fluxes were losses ($H_b = -2.4 \text{ W m}^{-2}$ and $H_g = -4.2 \text{ W m}^{-2}$) of similar magnitude.

4.1.2.2 PERIOD 2

Catamaran Brook

Cat Bk experienced very few clouds during Period 2 with the exception of the last day (day 226) where a slight increase in cloud cover was observed (Figure 4.3a). Air temperatures during Period 2 varied between 6.8°C and 26.5°C , but day 225 was warmer because the air temperature never dropped below 12.7°C . Water temperatures varied between 12.8°C and 19.4°C . Observed total heat fluxes ($H_t(O)$) values were from -64.9 W m^{-2} to 142 W m^{-2} . Predicted total heat fluxes ($H_t(P)$) values were slightly overestimated during the day, but showed agreement with observed values at night, with both having values varying between -63.0 W m^{-2} and 195 W m^{-2} . The model showed a *RMSE* of 34.1 W m^{-2} , a R^2 of 0.792 and a bias of -2.2 W m^{-2} (Table 4.4).

Surface heat flux (H_{surf}) was the dominant component during Period 2 with values ranging between -71.9 W m^{-2} to 236 W m^{-2} . However, on day 226, which had increased cloud cover, the surface heat flux reached a maximum of 51.1 W m^{-2} (Figure 4.3b). During that

same day the streambed heat flux (H_{bed}) was important as an energy source, reaching a maximum value of 19.1 W m^{-2} . Streambed heat flux was usually negative during the day and slightly positive at the night. Conductive heat flux (H_b) was the dominant of the streambed heat flux, ranging between -35.2 W m^{-2} and 18.1 W m^{-2} (Figure 4.3d). The groundwater contribution (H_g) was less than 8.3 W m^{-2} .

Most of the surface heat flux energy came from the net shortwave radiation (H_s) (Figure 4.3c). Evaporative heat flux (H_e) was mainly negative with very few hours having positive values (less than 3.9 W m^{-2}). Longwave radiation varied between -41.9 W m^{-2} and 23.3 W m^{-2} . With a decrease in air temperature (day 226), the longwave radiation (H_l) and evaporative heat flux (H_e) became mostly negative. The convective heat flux (H_c) was the smallest component of the surface heat flux (less than 12.5 W m^{-2}).

Agreement was observed between the predicted and observed energy gains and losses (see Table 4.3). The observed gain (19.8 W m^{-2}) was close to the predicted gain (20.9 W m^{-2}), while the observed loss rate (-19.7 W m^{-2}) was slightly lower than the predicted loss (-22.9 W m^{-2}). Most of the energy gain was from the result of the net shortwave radiation ($H_s = 16.3 \text{ W m}^{-2}$). The energy loss was a combination of the longwave radiation ($H_l - 8.0 = \text{W m}^{-2}$), evaporative heat flux ($H_e = -7.6 \text{ W m}^{-2}$) and the streambed heat flux ($H_{bed} = -6.0 \text{ W m}^{-2}$).

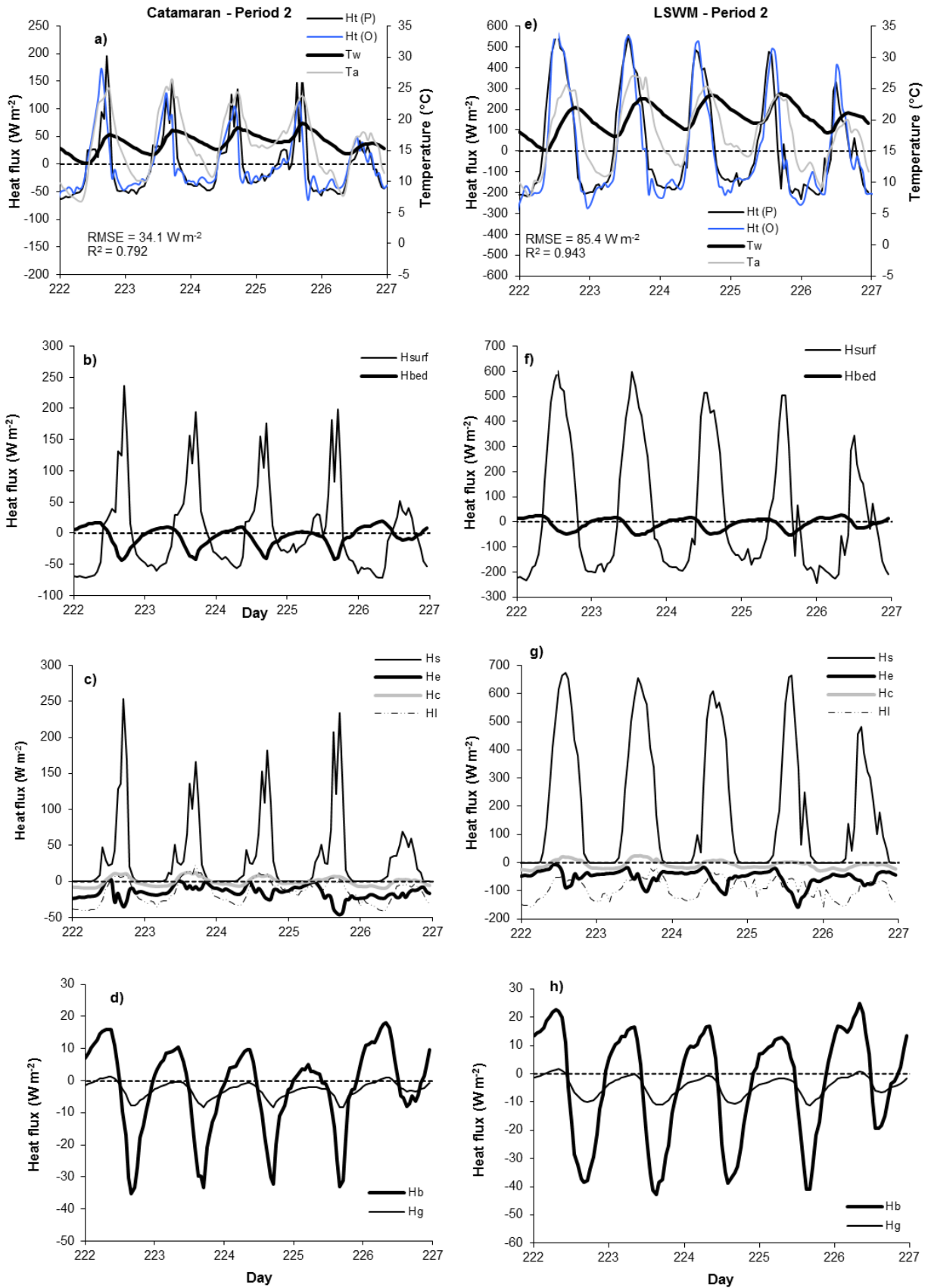


Figure 4.3. Detailed analysis of heat fluxes at Catamaran Brook and Little Southwest Miramichi River for Period 2.

Little Southwest Miramichi

During Period 2, strong agreement was observed between the predicted ($H_i(P)$) and the observed ($H_i(O)$) total heat flux, both varying between -272 W m^{-2} and 565 W m^{-2} (Figure 4.3e), although a slight underestimation was observed during most nights. Air temperature varied between 7.8°C to 27.1°C . Water temperature varied between 15.1°C and 24.2°C . Most energy gains and losses occurred via the surface (-243 W m^{-2} to 601 W m^{-2}). The contribution of the streambed was lower but still important (-53.7 W m^{-2} to 25.7 W m^{-2}) (Figure 4.3f). The model performance gave a *RMSE* of 85.4 W m^{-2} , a R^2 of 0.943 and a bias of 22.2 W m^{-2} for Period 2 (Table 4.4).

Solar radiation (H_s) was the main source of energy with a maximum value reaching 674 W m^{-2} (Figure 4.3e). The longwave radiation ($H_l = -18.5 \text{ W m}^{-2}$ to -157 W m^{-2}) and the evaporative heat flux (-7.4 W m^{-2} to -158 W m^{-2}) only induced energy losses during this period. The smallest component of the surface heat flux was the convective heat flux (H_c) with values within $\pm 29.4 \text{ W m}^{-2}$. The energy from the streambed occurred as conduction ($H_b = -42.8 \text{ W m}^{-2}$ to 24.8 W m^{-2}), with a small contribution from groundwater flow (H_g less than $\pm 11.2 \text{ W m}^{-2}$, Figure 4.3h).

The net surface heat flux (H_{surf}) represented an energy gain (34.6 W m^{-2} ; Table 4.3), whereas the net streambed (H_{bed}) showed an energy loss (-6.4 W m^{-2}). The solar radiation (H_s) was the major component of surface heat flux, with an energy gain of 109 W m^{-2} . The major contributors to the energy losses were longwave radiation ($H_l = -45.4 \text{ W m}^{-2}$) and evaporative heat flux ($H_e = -25.7 \text{ W m}^{-2}$).

4.1.2.3 PERIOD 3

Catamaran Brook

Period 3 was selected as a period because it included days with relatively low flows. Air temperature during Period 3 varied between 2.5°C to 21.6°C, and water temperature varied between 10.5°C and 15.5°C (Figure 4.4a). The predicted total heat flux ($H_t(P)$) was clearly overestimated during this period. Predicted total heat flux ($H_t(P)$) varied from -62.3 W m^{-2} to 205 W m^{-2} , however, the observed total heat flux ($H_t(O)$) only varied between values of -45.8 W m^{-2} and 95.8 W m^{-2} . The *RMSE*, the R^2 and the bias for Period 3 at Cat Bk were 30.3 W m^{-2} , 0.875, and -4.8 W m^{-2} respectively (Table 4.4).

The surface heat flux (H_{surf}) was the major component of the total heat flux, varying between -80.4 W m^{-2} and 246 W m^{-2} (Figure 4.4b). The streambed contribution (H_{bed}) was lower, with energy values ranging between -45.9 W m^{-2} and 22.9 W m^{-2} . Solar radiation (H_s) was the dominant source of energy with heat fluxes reaching up to 253 W m^{-2} (Figure 4.4c). Energy losses were primarily due to longwave radiation ($H_l = -45.5 \text{ W m}^{-2}$ to 18.7 W m^{-2}), and secondarily to the evaporation ($H_e = -33.5 \text{ W m}^{-2}$ to 2.9 W m^{-2}). Convective heat flux (H_c) varied from -12.5 W m^{-2} to 10.4 W m^{-2} . The streambed heat flux (H_{bed}) was mainly composed of the conductive heat flux (H_b), with values ranging from -38.2 W m^{-2} to 20.2 W m^{-2} (Figure 4.4d). The groundwater heat flux (H_g) was less than 7.7 W m^{-2} .

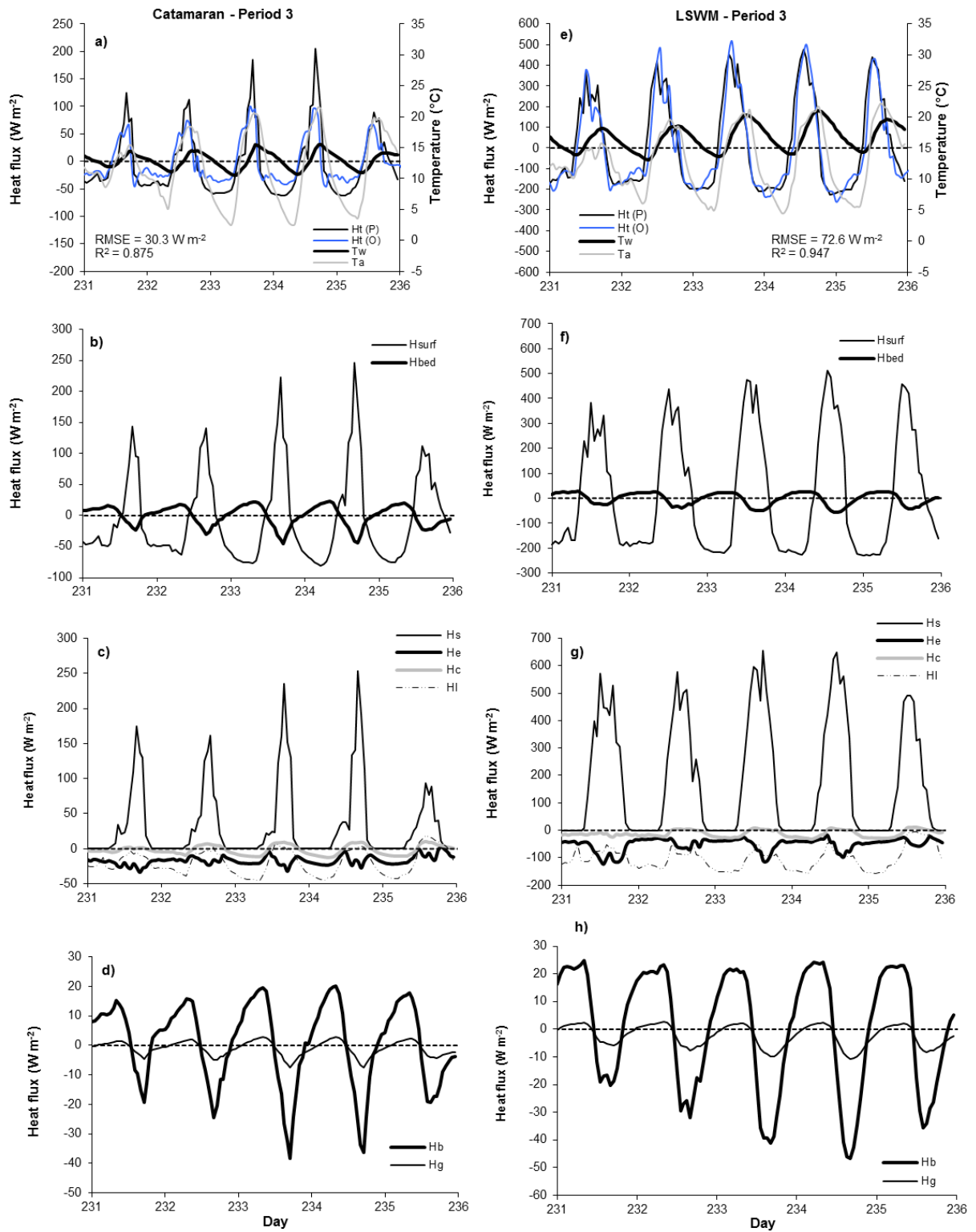


Figure 4.4. Detailed analysis of heat fluxes at Catamaran Brook and Little Southwest Miramichi River, for Period 3.

Predicted total heat flux ($H_t(P)$) resulted in a slight overestimation of the observed total heat flux ($H_t(O)$) ($H_t(P) = 21.2 \text{ W m}^{-2}$; $H_t(O) = 15.7 \text{ W m}^{-2}$), but showed significant agreement for the energy loss ($H_t(P) = -16.8 \text{ W m}^{-2}$; $H_t(O) = -16.4 \text{ W m}^{-2}$) (Table 4.3). Most of the energy gain was due to solar radiation ($H_s = 15.5 \text{ W m}^{-2}$) with a significant contribution coming from the streambed ($H_{bed} = 4.2 \text{ W m}^{-2}$). The energy loss was divided equally between the longwave radiation and evaporative heat flux ($H_l = H_e = -9.6 \text{ W m}^{-2}$). The streambed contribution in terms of energy loss was -4.7 W m^{-2} .

Little Southwest Miramichi

Air temperatures, for Period 3 at LSWM, varied from 4.4°C to 22.2°C (Figure 4.4e). Water temperature showed similar variations throughout the period, with values between 13.1°C and 21.0°C . A better level of prediction than at Cat Bk was observed (Figure 4.4e), comparing predicted ($H_t(P)$) and observed ($H_t(O)$) total heat flux. Total heat fluxes varied between values of -260 W m^{-2} and 500 W m^{-2} . The *RMSE*, the R^2 and the bias were of 72.6 W m^{-2} , 0.947 and 12.9 for Period 3 (Table 4.4).

Surface heat flux (H_{surf}) dominated the total heat flux with values ranging between -230 W m^{-2} and 511 W m^{-2} (Figure 4.4f) whereas the streambed flux (H_{bed}) was smaller (-57.2 W m^{-2} to 27.4 W m^{-2}). Solar radiation (H_s) varied similarly throughout the period (maximum of 655 W m^{-2}) as shown in Figure 4.4g. The longwave radiation (H_l) and the evaporative heat flux (H_e) were the major contributors to the energy losses, with values less than -157 W m^{-2} and -123 W m^{-2} , respectively. The smallest component of the surface flux was the convective heat flux ($H_c = -32.5 \text{ W m}^{-2}$ to 11.5 W m^{-2}). The main contributor to the streambed heat flux (H_{bed}) was the conductive heat flux ($H_b = -46.5$

W m^{-2} to 24.8 W m^{-2}). Groundwater (H_g) contribution was less than 10.7 W m^{-2} (Figure 4.4h).

4.1.2.4 PERIOD 4

Catamaran Brook

During Period 4, days 242 and 243 received over 35 mm of rain, where a significant decrease in air (25.9°C to 3.6°C) and water (18.6°C to 11.5°C) temperature was observed (Figure 4.5a). Only a slight discrepancy was observed between the observed and predicted total heat flux, mostly as an overestimation during the day ($RMSE = 23.2 \text{ W m}^{-2}$, $R^2 = 0.819$ and bias = -1.1 W m^{-2} ; Table 4.4). Predicted total heat flux varied between -64.3 W m^{-2} and 161 W m^{-2} , whereas the observed total heat flux was lower and varied between -71.9 W m^{-2} and 113 W m^{-2} .

As shown in Figure 4.5b, during the rain event, surface heat flux was low ($H_{surf} = -79.2 \text{ W m}^{-2}$ to 186 W m^{-2}), but still higher than the streambed heat flux. Solar radiation (H_s) had very low values ($< 158 \text{ W m}^{-2}$), especially during the storm event ($< 44.9 \text{ W m}^{-2}$). The longwave radiation (H_l) had higher values during the storm event (-13.9 W m^{-2} to 11.4 W m^{-2}) compared to the following days (-45.5 W m^{-2} to -2.2 W m^{-2}). Evaporative heat flux (H_e) followed similar patterns as the longwave radiation, with values between -23.7 W m^{-2} and 8.5 W m^{-2} . Convective heat flux (H_c) was very small throughout the period with variation of energy gains or losses less than 12.6 W m^{-2} . Precipitation heat flux (H_p) was less than 0.1 W m^{-2} for the entire period.

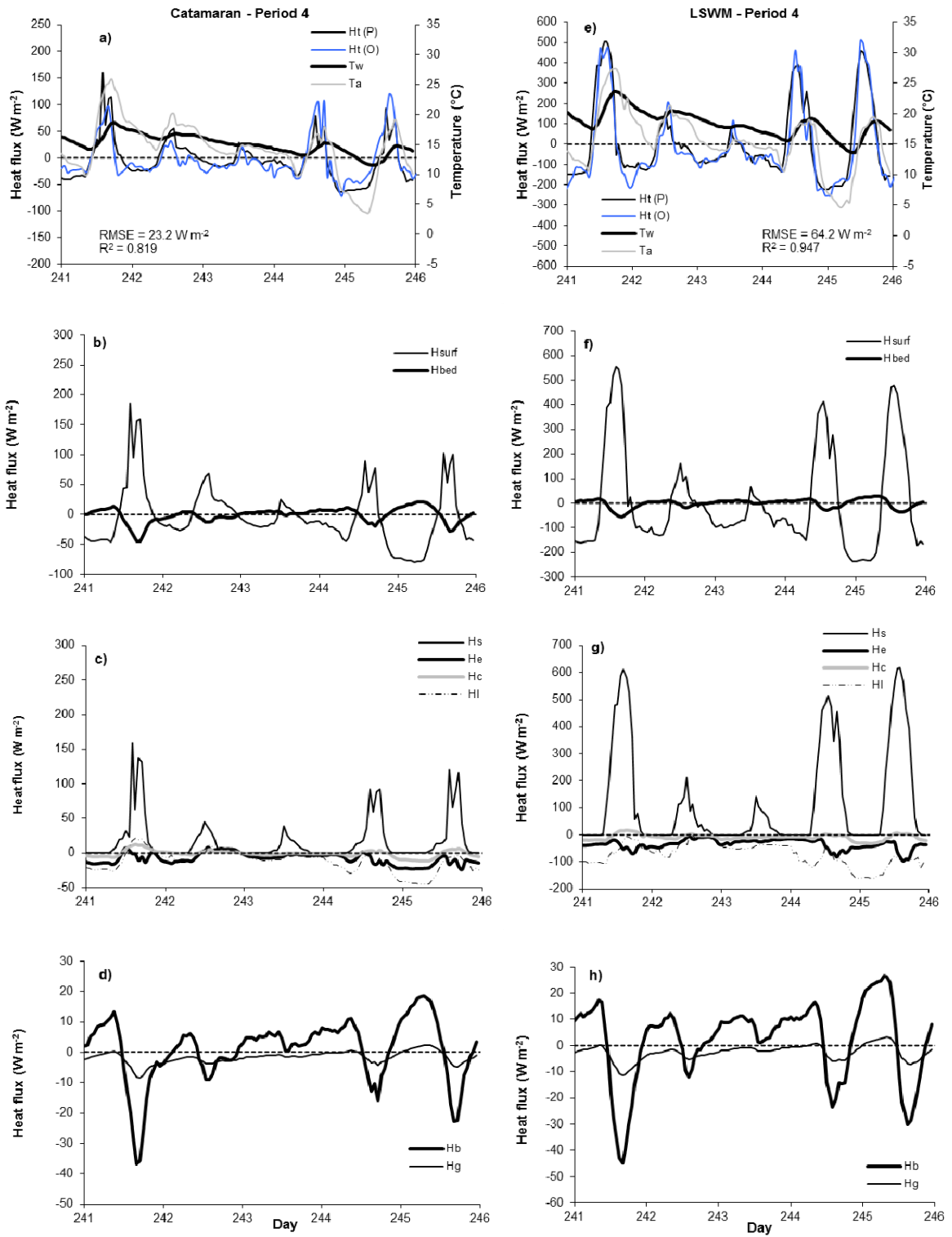


Figure 4.5. Detailed analysis of heat fluxes at Catamaran Brook and Little Southwest Miramichi River for Period 4.

Streambed heat flux (H_{bed}) fluctuated between -44.9 W m^{-2} and 20.8 W m^{-2} , mainly due to conductive heat flux (H_b). Conductive heat flux varied between -36.7 W m^{-2} and 18.5 W m^{-2} , however following the rain event (day 243-244), it remained as an energy gain (0.5 W m^{-2} to 11.1 W m^{-2}). Heat flux by advection (H_g) was very small, less than 8.5 W m^{-2} and mainly an energy loss during most days (Figure 4.5h).

Predicted total heat flux ($H_t(P)$) showed agreement with the observed total heat flux ($H_t(O)$) (Table 4.3). The predicted total energy gain was of 12.3 W m^{-2} ($H_t(O) = 12.9 \text{ W m}^{-2}$) and observed total heat flux was of -16.8 W m^{-2} ($H_t(O) = 12.9 \text{ W m}^{-2}$). Most of the energy gain was from the solar radiation ($H_s = 8.1 \text{ W m}^{-2}$) with an important contribution from the streambed ($H_{bed} = 2.5 \text{ W m}^{-2}$). The energy loss was mainly from the longwave radiation ($H_l = -7.5 \text{ W m}^{-2}$) followed closely by the evaporative heat flux ($H_e = -4.7 \text{ W m}^{-2}$) and the streambed heat flux ($H_{bed} = -3.3 \text{ W m}^{-2}$).

Little Southwest Miramichi

As in Cat Bk, LSWM showed a decrease of air temperature during period 4 (27.3°C to 4.6°C) and water temperature (23.6°C to 13.6°C) caused by a significant precipitation event during day 242 and 243 (35 mm of rain). Total heat flux predictions were close to observed values even if substantial precipitation occurred, showing a *RMSE* of 64.2 W m^{-2} , a R^2 of 0.947 and a bias of 19.5 W m^{-2} (Table 4.4). Predicted ($H_t(P)$) and observed ($H_t(O)$) total heat flux both varied between -252 W m^{-2} and 511 W m^{-2} (Figure 4.5e).

Surface heat flux ($H_{surf} = -238 \text{ W m}^{-2}$ to 556 W m^{-2}) was mostly dominated by solar radiation (H_s) during the day and the longwave (H_l) and evaporative (H_e) heat flux at night (Figure 4.5e and 4.5f). Longwave radiation was mostly negative, with slight energy gains (-161 W m^{-2} to 4.0 W m^{-2}), whereas the evaporative heat flux was observed as only an energy loss (-96.7 W m^{-2} to -4.7 W m^{-2}). Convective heat flux (H_c) varied between -31.1 W m^{-2} and 17.3 W m^{-2} . Precipitation heat flux (H_p) contributed less than 0.3 W m^{-2} to the energy budget.

Conductive heat flux (H_b) varied between -44.7 W m^{-2} and 26.4 W m^{-2} and was the main component of the streambed heat flux (-56.0 W m^{-2} and 29.4 W m^{-2} ; Figure 4.5f). Conductive heat flux in LSWM, similar to Cat Bk, had two days of only heat gains (Figure 4.5h). The groundwater flow (H_g) contributed less than 11.3 W m^{-2} and acted primarily as energy loss.

Predicted total heat flux showed a net energy gain (6.9 W m^{-2}), whereas the observed total heat flux showed a net energy loss (-12.5 W m^{-2}) for Period 4 (Table 4.3). Most energy gain came from the net shortwave radiation ($H_s = 82.1 \text{ W m}^{-2}$). The longwave radiation (H_l) and the evaporative heat flux (H_e) were responsible for most of the energy lost, with values of -39.0 W m^{-2} and -18.8 W m^{-2} respectively. The net contribution of the streambed heat flux (H_{bed}) was very small, at -0.6 W m^{-2} .

4.1.2.5 PERIOD 5

Catamaran Brook

Cat Bk showed a decrease of air and water temperature followed by an important increase during period 5 (Figure 4.6a). Air temperature reached a low minimum on day 249 (-0.7 °C) and increased through day 251 (26.8 °C). Water temperature followed the same pattern as air temperature, but with values between 8.4 °C to 18.6 °C. Predicted total heat flux ($H_t(P) = -68.3 \text{ W m}^{-2}$ to 107 W m^{-2}) generally overestimated the observed total heat flux ($H_t(O) = -35.9 \text{ W m}^{-2}$ to 78.2 W m^{-2}), mostly during the night. The model performance during Period 5 (Table 4.4) showed a *RMSE* of 24.8 W m^{-2} , a R^2 of 0.836 and a bias of -1.6 W m^{-2} .

During the decrease in water temperature, the surface heat flux was very low (minimum of -90.0 W m^{-2} ; Figure 4.6b) and mainly negative due to strong longwave radiation (minimum of -49.0 W m^{-2}) and evaporative heat flux (minimum of -37.5 W m^{-2}). However, during the increase of water temperature, the surface heat flux increased as well (up to 158 W m^{-2}), also caused by the increased longwave radiation (H_l) and evaporative heat flux (H_e), reaching values as high as 40 W m^{-2} . Solar radiation (H_s) varied in a similar manner throughout the period with values reaching a maximum around 90 W m^{-2} (Figure 4.6c).

In contrast to the surface heat flux (H_{surf}), the streambed (H_{bed}) contribution was mainly positive during the decrease in both air temperatures and water temperatures (-50.9 W m^{-2} to 27.6 W m^{-2}), although smaller than the surface heat flux (Figure 4.6b). During the increase in water temperature, the streambed heat flux decreased and became an energy

loss and reached a value of -50.9 W m^{-2} . Most fluctuations of the streambed heat flux was attributed to the conductive heat flux (H_b) with values varying between -42.0 W m^{-2} and 23.4 W m^{-2} (Table 4.6d). The (H_g) by advection followed the same variation as the conductive heat flux, but had smaller values (less than 9.1 W m^{-2}).

Predicted total heat flux showed a net energy loss (-1.4 W m^{-2} ; Table 4.3), whereas the observed total heat flux showed a net energy gain (1.7 W m^{-2}). Most of the energy gain came from the solar radiation ($H_s = 8.1 \text{ W m}^{-2}$), but the contribution of longwave radiation ($H_l = 2.2 \text{ W m}^{-2}$), evaporative heat flux ($H_e = 2.4 \text{ W m}^{-2}$) and streambed heat flux ($H_{bed} = 2.9 \text{ W m}^{-2}$) were present as well. Energy loss was divided among the longwave radiation ($H_l = -6.4 \text{ W m}^{-2}$), the evaporative ($H_e = -5.8 \text{ W m}^{-2}$) and streambed ($H_{bed} = -5.0 \text{ W m}^{-2}$) heat flux.

Little Southwest Miramichi

As in Cat Bk, air the water temperatures in Period 5 (LSWM) showed a decreased in the first few days (days 247 to 249), followed by a rapid increase afterward (Figure 4.6e). Air temperatures decreased as low as $0.7 \text{ }^\circ\text{C}$, and increased to a maximum value of $28.8 \text{ }^\circ\text{C}$. Water temperatures fluctuated between $10.4 \text{ }^\circ\text{C}$ and $23.9 \text{ }^\circ\text{C}$. Predicted total heat flux ($H_t(P) = -199 \text{ W m}^{-2}$ to 600 W m^{-2}) was closely followed by the observed total heat flux ($H_t(O) = -253 \text{ W m}^{-2}$ to 550 W m^{-2}), giving results of an *RMSE* of 82.6 W m^{-2} , a R^2 of 0.915 and a bias of 19.9 W m^{-2} (Table 4.4).

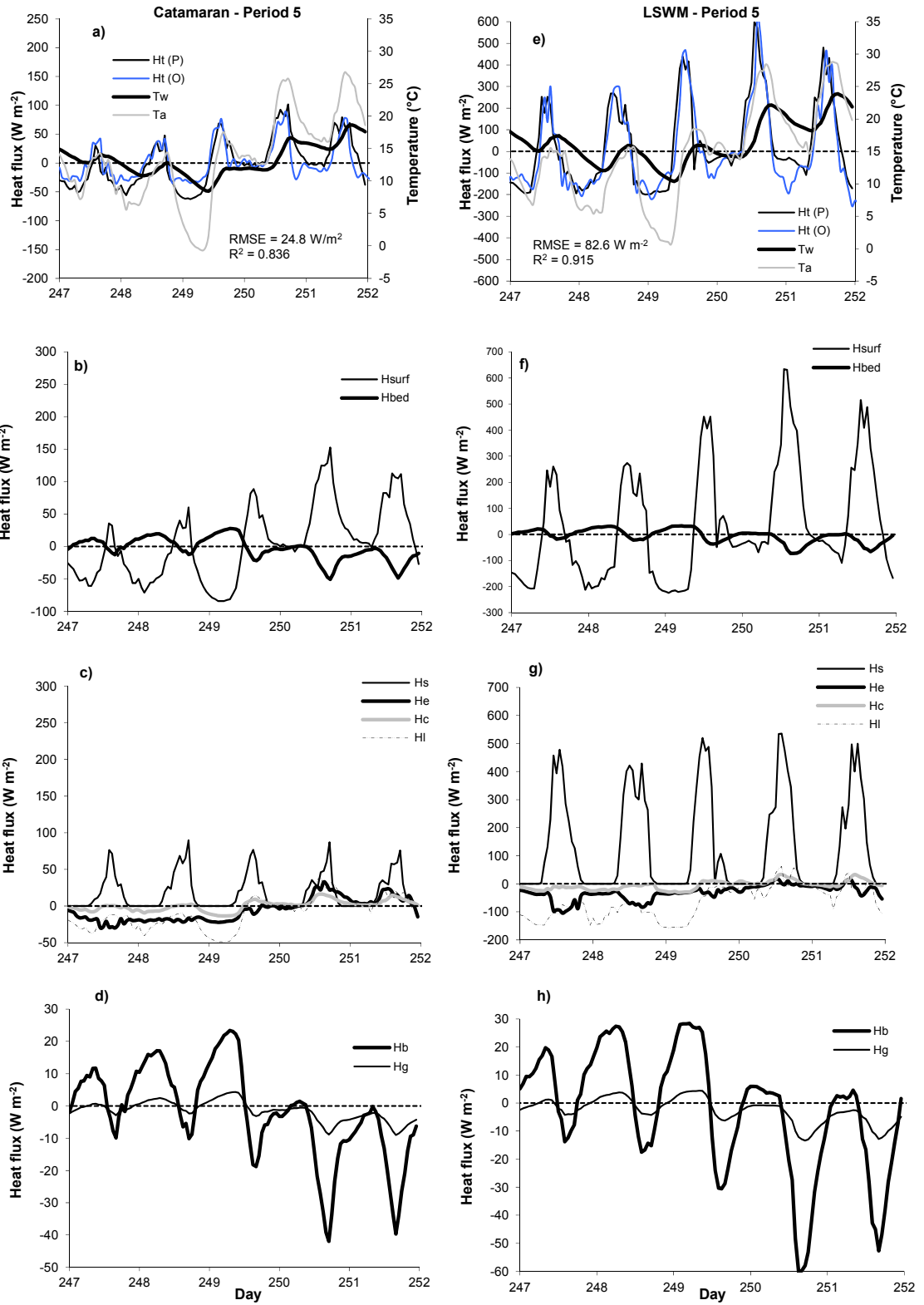


Figure 4.6. Detailed analysis of heat fluxes at Catamaran Brook and Little Southwest Miramichi River for Period 5.

Surface heat flux (H_{surf}) was lower in the first two days (-215 W m^{-2} to 274 W m^{-2}) as shown in Figure 4.6f and increased to higher values afterward (-109 W m^{-2} to 633 W m^{-2}). Streambed heat flux varied between -72.7 W m^{-2} and 32.6 W m^{-2} . Solar radiation (H_s) was the main component of surface heat flux, and remained relatively constant throughout the period, reaching maximums over 420 W m^{-2} . Surface heat flux variations were the result of fluctuations in the longwave radiation (H_l) and evaporative heat flux (H_e) (Figure 4.6g). In the first two days, the longwave radiation ($\leq -69.2 \text{ W m}^{-2}$) and the evaporative heat flux ($\leq -27.3 \text{ W m}^{-2}$) acted only as an energy loss, but increased thereafter with positive values ($H_l = -91.5 \text{ W m}^{-2}$ to 61.3 W m^{-2} ; $H_e = -54.2 \text{ W m}^{-2}$ to 16.0 W m^{-2}). The convective heat flux (H_c) varied between -30.8 W m^{-2} to 33.0 W m^{-2} .

Streambed heat flux (H_{bed}) varied between -72.7 W m^{-2} and 32.6 W m^{-2} throughout Period 5, mainly in the form of conductive heat flux (Figure 4.6d). Conductive heat flux (H_b) was higher during the decrease of air and water temperatures (-17.5 W m^{-2} to 28.4 W m^{-2}), and decreased thereafter to lower values (-60.3 W m^{-2} to 5.9 W m^{-2}) as shown in Table 4.6h. The heat flux by advection (H_g) varied between -13.3 W m^{-2} and 4.4 W m^{-2} .

Predicted heat gains were overestimated (predicted = 93.3 W m^{-2} ; observed = 82.4 W m^{-2} ; Table 4.3), whereas the heat losses were underestimated (predicted = -63.5 W m^{-2} ; observed = -72.4 W m^{-2}). Shortwave radiation ($H_s = 82.1 \text{ W m}^{-2}$) accounted for most of the heat gains (87.0 W m^{-2}). The major component of heat loss was the longwave radiation (H_l) with a heat loss of -33.3 W m^{-2} . The evaporative (H_e) and streambed heat flux (H_{bed}) also contributed significantly to the energy loss, with heat losses of -15.6 W m^{-2} and -10.0 W m^{-2} , respectively.

4.1.2.6 PERIOD 6

Catamaran Brook

In order to contrast conditions during Period 1 (summer conditions), Period 6 was selected because it represented more typical autumn conditions. As such, Period 6 had colder air temperature (4.8 °C to 22.2 °C) and the solar radiation was significantly reduced compared to summer conditions (Table 4.2).

Both observed ($H_t(O)$) and predicted ($H_t(P)$) total heat fluxes showed relatively small variability during most days (-52.6 W m^{-2} and 85.0 W m^{-2}) as indicated in Figure 4.7a. During Period 6, a strong agreement was observed between predicted and observed heat fluxes and the total heat flux was almost neutral at night (no heat losses or gains) for most days. During Period 6, Cat Bk showed the best overall performance of all periods, with *RMSE* of 17.7 W m^{-2} , a R^2 of 0.806 and a bias of -1.0 W m^{-2} (Table 4.4). When looking at the surface vs. streambed heat fluxes, fluxes were observed to be low especially at night (Figure 4.7c and Figure 4.7d). For example, surface heat fluxes (H_{surf}) varied between -65.3 W m^{-2} and 114 W m^{-2} whereas streambed heat fluxes (H_{bed}) varied between -35.6 W m^{-2} and 16.0 W m^{-2} . Peak fluxes from solar radiation (H_s) during this period were less than 53.9 W m^{-2} (Figure 4.7c). Precipitation heat flux (H_p) was between -2.5 W m^{-2} and 14.8 W m^{-2} . The streambed heat flux (H_{bed}) was still dominated by conductive heat flux (-29.5 W m^{-2} to 14.1 W m^{-2}). The advective heat flux (H_g) was small with values ranging between -6.1 W m^{-2} and 1.9 W m^{-2} .

Water temperatures were similar among days of Period 6, varying between 10.0 °C 14.6 °C. Total heat gains and losses were lower during Period 6 and of similar magnitude (Table 4.3). For instance, predicted total heat gain was at 11.3 W m⁻² (observed value = 8.2 W m⁻²) whereas the total heat loss was -13.0 W m⁻² (observed = -8.9 W m⁻²). Although small, surface heat gains (H_{surf}) were dominated by solar radiation gains ($H_s=5.8$ W m⁻²) and heat losses were dominated by the net longwave radiation ($H_l = -6.2$ W m⁻²). The net streambed fluxes (H_{bed}) were -1.1 W m⁻² for this period.

Little Southwest Miramichi

Water temperatures for LSWM during Period 6 were slightly higher than in Cat Bk with values ranging from 11.6 °C to 18.3 °C (Figure 4.7e). In a manner similar to Cat Bk, water temperatures increased in LSWM during the first two days (day 268-269) and then generally decreased until the end of the period.

Observed and predicted total heat fluxes showed agreement during period 6 in LSWM (between -216 W m⁻² and 365 W m⁻²). In fact, Period 6 had the best performance of all the periods at LSWM (RMSE = 55.8 W m⁻²; R² = 0.910; bias = 0.1 W m⁻²) shown in Table 4.4. Surface heat fluxes were similar for most days of Period 6 (-207 W m⁻² to 383 W m⁻²), with the exception of day 270-271 showing lower peak heat gains (< 238 W m⁻²), as shown in Figure 4.7f. Surface heat fluxes (H_{surf}) were generally smaller than during Period 1 at LSWM reflecting more autumn conditions. For instance, peak net shortwave radiation (H_s) was between 217 W m⁻² and 349 W m⁻² with the exception of day 272 where values reached 516 W m⁻² (Figure 4.7g). The net longwave radiation (H_l) was a major source of heat loss in Period 6 with values ranging from -149 W m⁻² to 72.0 W m⁻².

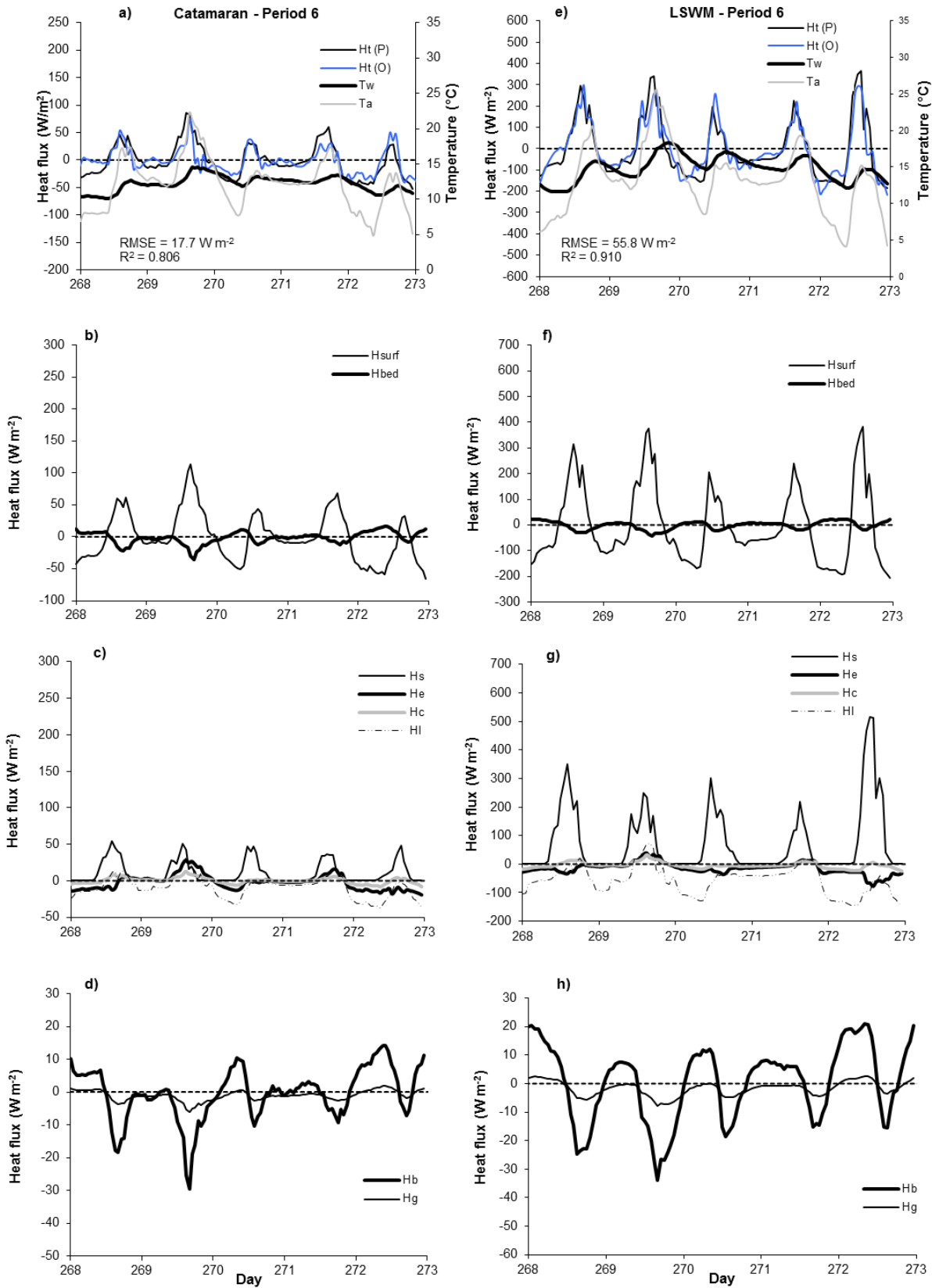


Figure 4.7. Detailed analysis of heat fluxes at Catamaran Brook and Little Southwest Miramichi River for Period 6.

Precipitation heat flux (H_p) varied between -18.2 W m^{-2} and 12.9 W m^{-2} over two days. Similar to Cat Bk, streambed heat fluxes (H_{bed}) were small. Heat flux by conduction (H_b) varied between -33.9 W m^{-2} to 21.0 W m^{-2} (Figure 4.7h). The advective heat flux (H_g) component was also relatively small (-7.7 W m^{-2} to 2.6 W m^{-2}).

Total heat gains and losses, observed and predicted, for LSWM showed agreement during Period 6 (Table 4.3). The predicted heat gain was 53.9 W m^{-2} (observed value = 47.2 W m^{-2}) whereas the predicted heat loss was -57.4 W m^{-2} (observed value = -50.6 W m^{-2}). Among the net fluxes for LSWM, the surface fluxes (H_{surf}) represented a net loss (-2.3 W m^{-2}). The heat gains were mainly from solar radiation (43.8 W m^{-2}) whereas, heat losses were predominately from both the net longwave radiation (-34.4 W m^{-2}) and evaporative fluxes (-9.3 W m^{-2}). The heat gain was dominated by incoming solar radiation ($H_s = 43.8 \text{ W m}^{-2}$). The streambed fluxes (H_{bed}) represented a net loss of -1.1 W m^{-2} for the period and were dominated by the advective heat fluxes ($H_g = -1.4 \text{ W m}^{-2}$).

4.1.3 COMPARISON TOTAL HEAT FLUXES AND WATER TEMPERATURES (OBSERVED VS. PREDICTED)

A comparison of observed vs. predicted total heat gains and losses was carried out for Cat Bk and LSWM for all 6 periods (Figure 4.8). It can be observed from this figure that heat gains and losses show good agreement between observed and predicted values for all periods except Period 1. In fact, during Period 1 heat gains were significantly overestimated, whereas heat losses were underestimated for both Cat Bk and LSWM. For other periods, heat gains were well predicted for Cat Bk and even better predicted for

LSWM. In contrast, heat losses showed less agreement between observed and predicted fluxes.

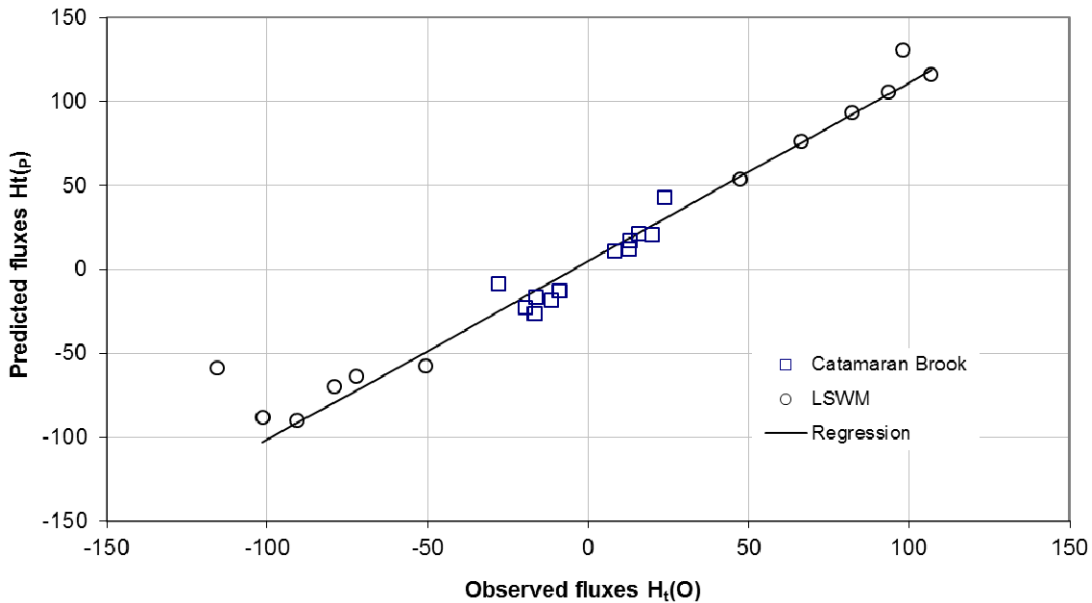


Figure 4.8. Predicted vs. observed total heat fluxes (gains and losses) for each study period (1 to 6) at Catamaran Brook and Little Southwest Miramichi River using the deterministic model.

Figures 4.9 and 4.10 show observed and predicted water temperatures at Cat Bk and LSWM using the deterministic model. The predicted water temperatures were calculated using the predicted total heat flux ($H_t(P)$), in Equation 3.3b. Table 4.5 shows the modeling performance results ($RMSE$, R^2 , bias) between the observed and predicted water temperatures. As with the total heat flux, water temperatures were best predicted in Period 6 and had poorer performance in Period 1, at both LSWM and Cat Bk. Water temperatures at Cat Bk were closely estimated for all periods (Figure 4.9). In Period 1, predicted water temperatures showed a slight overestimation of minimum and maximum water temperatures, although less than 1 °C. The other periods also showed days with a

slight overestimation of the maximum water temperatures. The deterministic model was effective in all periods with *RMSEs* less than 0.33 °C, R^2 higher than 0.970 and biases less than 0.20 °C. Results at LSWM showed equally good performance of the model (Figure 4.10), with *RMSEs* less than 0.23 °C, R^2 higher than 0.992 and biases less than 0.16 °C for all six periods (Table 4.5).

Table 4.5. Performance of deterministic model on the basis of predicted vs. observed water temperatures.

Period	Catamaran Brook			Little Southwest Miramichi		
	RMSE (°C)	R^2	Bias (°C)	RMSE (°C)	R^2	Bias (°C)
Period 1	0.33	0.970	0.20	0.23	0.994	0.16
Period 2	0.25	0.979	-0.01	0.18	0.994	0.04
Period 3	0.29	0.969	-0.05	0.19	0.993	0.03
Period 4	0.18	0.991	0.00	0.14	0.996	0.04
Period 5	0.24	0.994	-0.02	0.21	0.996	0.05
Period 6	0.18	0.983	-0.01	0.15	0.992	0.00

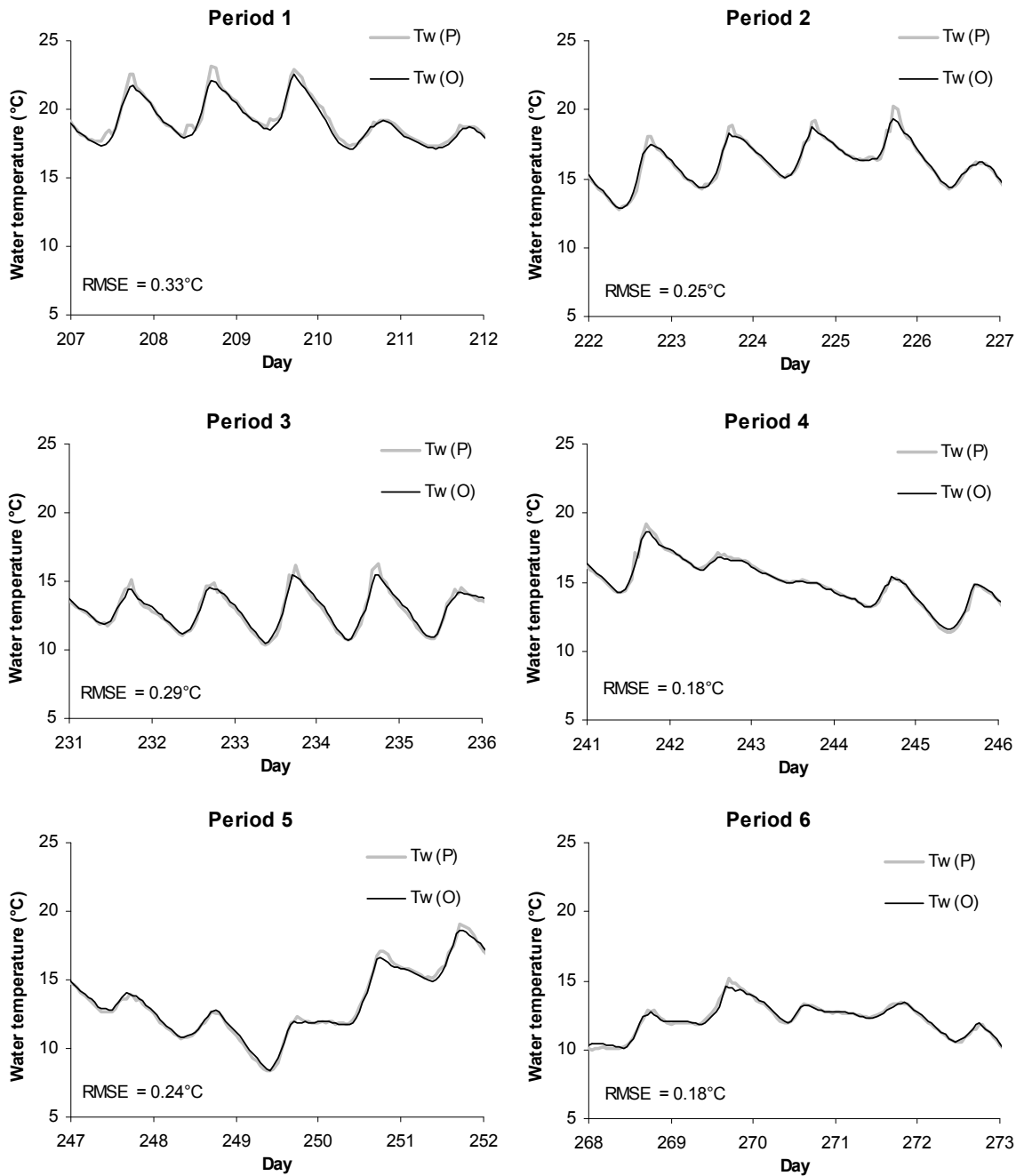


Figure 4.9. Observed water temperatures ($T_w(O)$) and predicted water temperatures ($T_w(P)$) at Catamaran Brook calculated from the predicted total heat flux using the deterministic model.

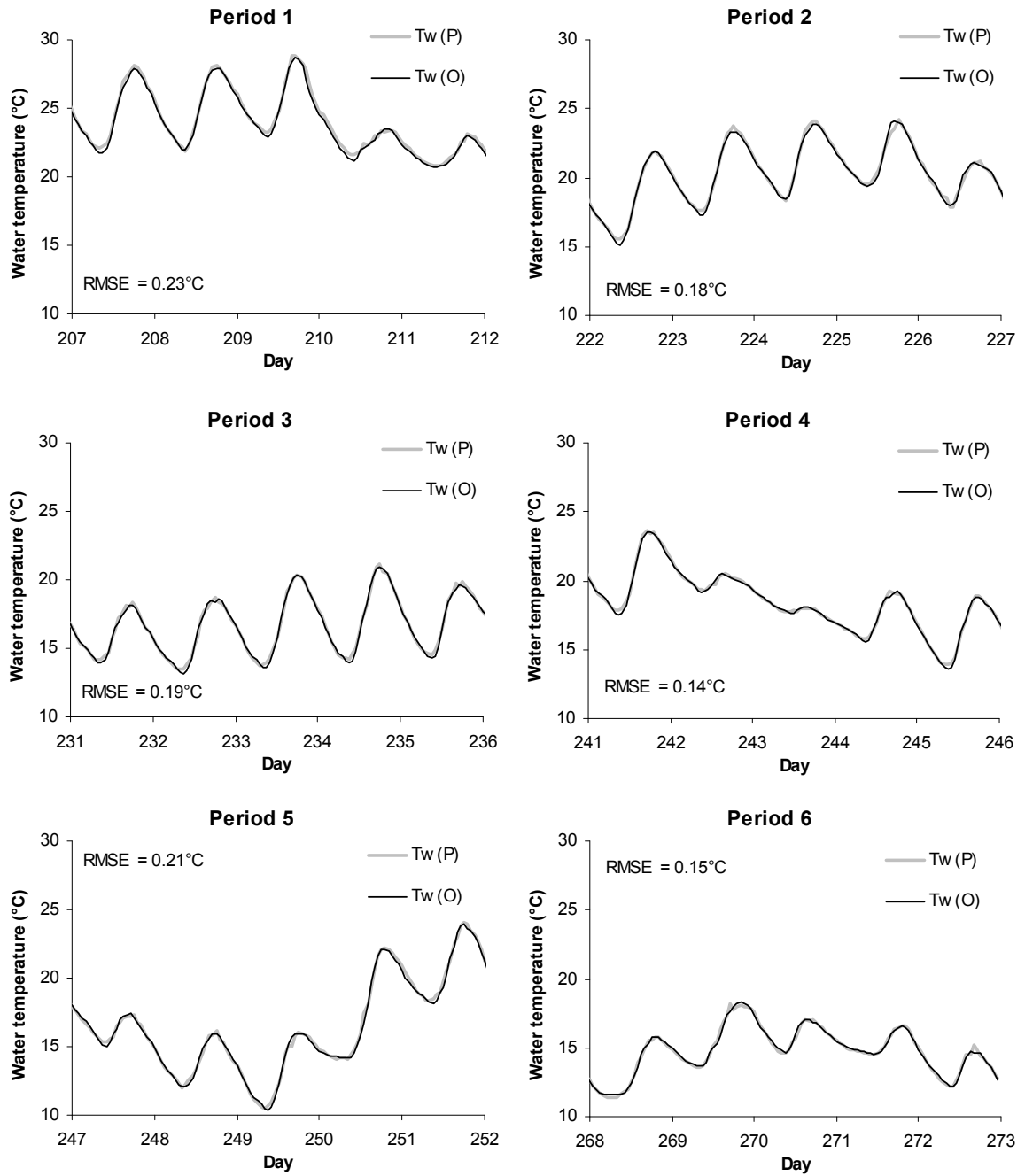


Figure 4.10. Observed water temperatures ($T_w(O)$) and predicted water temperatures ($T_w(P)$) at Little Southwest Miramichi calculated from the predicted total heat flux using the deterministic model.

4.2 EQUILIBRIUM TEMPERATURE MODEL

An equilibrium temperature model was developed to predict hourly water temperatures at both Cat Bk and LSWM. A linear relationship was used to calculate the equilibrium temperature for both studied watercourses, as presented in Equation (3.21). The coefficients α and β were optimized using the minimum square of errors between the predicted and observed water temperatures for the calibration years (1998-2002). The linear regression coefficient α was calculated at 0.87 at Cat Bk and slightly higher at LSWM with 1.08. The linear regression coefficient β was 0 °C at both study streams. A constant thermal exchange (K) was calculated with a value of 2.7 W m⁻² °C⁻¹ at Cat Bk and of 13.1 W m⁻² °C⁻¹ at LSWM. These parameters were then used to estimate hourly water temperatures using Equation (3.24). The above parameters developed during the calibration period (i.e., linear regression between air and equilibrium temperature and the thermal exchange coefficient (K)) were then used to validate the model (years 2003-2007).

A sensitivity analysis was performed to address the uncertainty of the model's coefficient α and the thermal exchange coefficient K of the equilibrium temperature model. For instance, based on literature, the coefficient (α) would most likely be between 0.9 to 1.1 and K would be between 2 W m⁻² °C⁻¹ and 30 W m⁻² °C⁻¹. The results of the sensitivity analysis showed that the current water temperature model was more sensitive to the air/equilibrium temperature linear coefficient (α) than the thermal exchange coefficient (K). At Cat Bk, if K was increased or decreased by 50%, the increase in *RMSE* was generally within 9%, which represented an increase of error less than 0.14°C for both the calibration and validation periods. At LSWM, the same modifications in K ($\pm 50\%$)

produced changes in RMSE of less than 9% (0.46 °C). The model's coefficient α was more sensitive than K. This coefficient only needs a slight change of 5% (0.04 at Cat Bk and 0.05 at LSWM) to increase the error by 0.2 °C. Modification of α by 25% (0.13 to 0.16) can increase the RMSE by 2 °C to 2.5 °C. This suggests that the estimation of α (i.e., representing the total heat flux at the water surface) is the most important parameter of the current equilibrium temperature model.

Figures 4.11 and 4.12 show predicted vs. observed water temperatures for each year at both Cat Bk and LSWM. Some years had days without measurements due to equipment malfunctions and were not included in the modeling. Figures 4.11a-e show the calibration years at Cat Bk. Results showed reasonable agreement between predicted and observed water temperatures. However, some periods were clearly overestimated, spring of 1998 and 2001, and some periods clearly showed underestimation, late autumn 1999 and 2002. Overall, the year 1998 showed significant overestimation of water temperatures during the high summer temperatures (days 165 to 225).

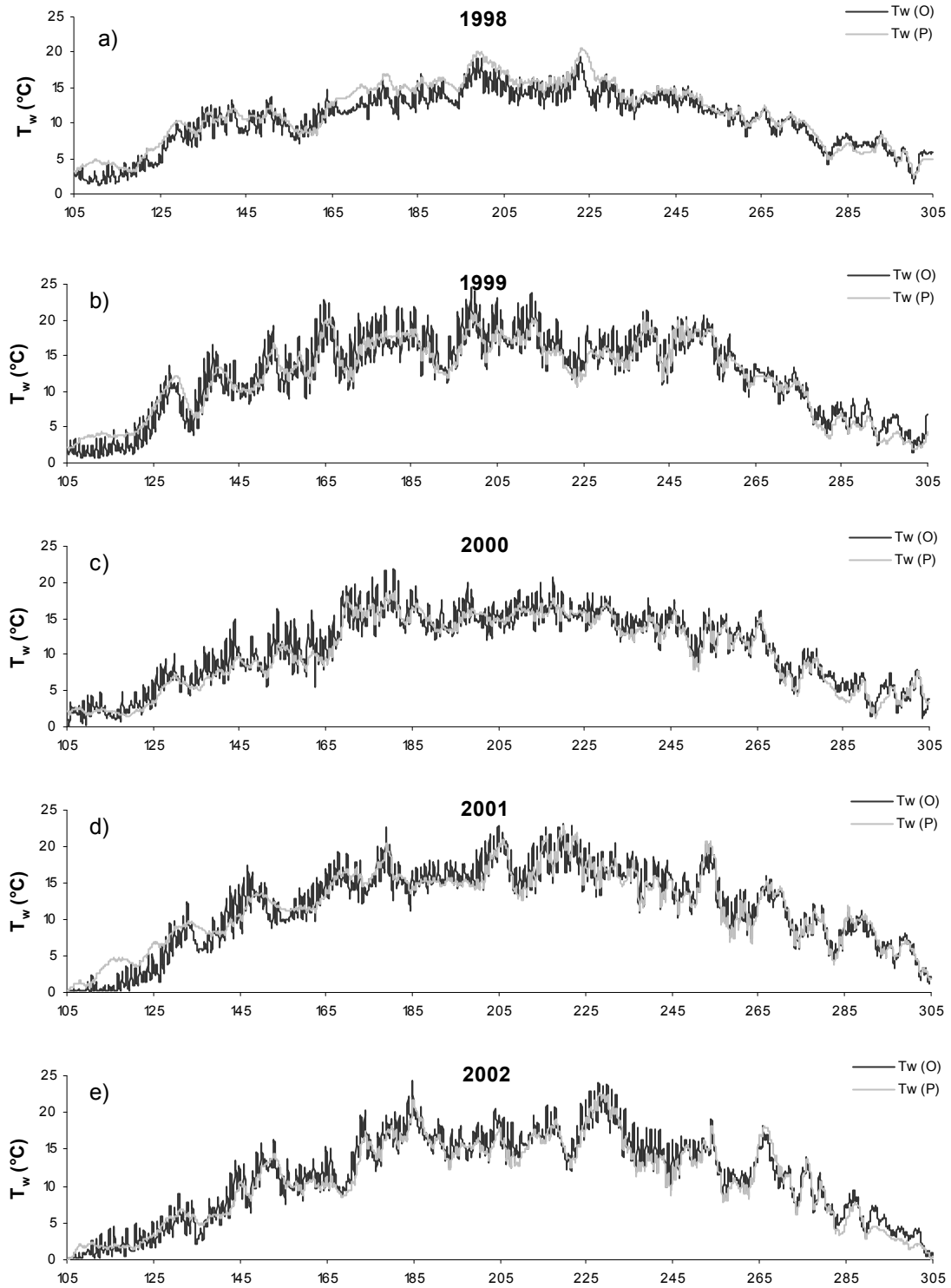


Figure 4.11. Observed water temperatures ($T_w(O)$) and predicted water temperatures ($T_w(P)$) obtained from the equilibrium temperature model at Catamaran Brook.

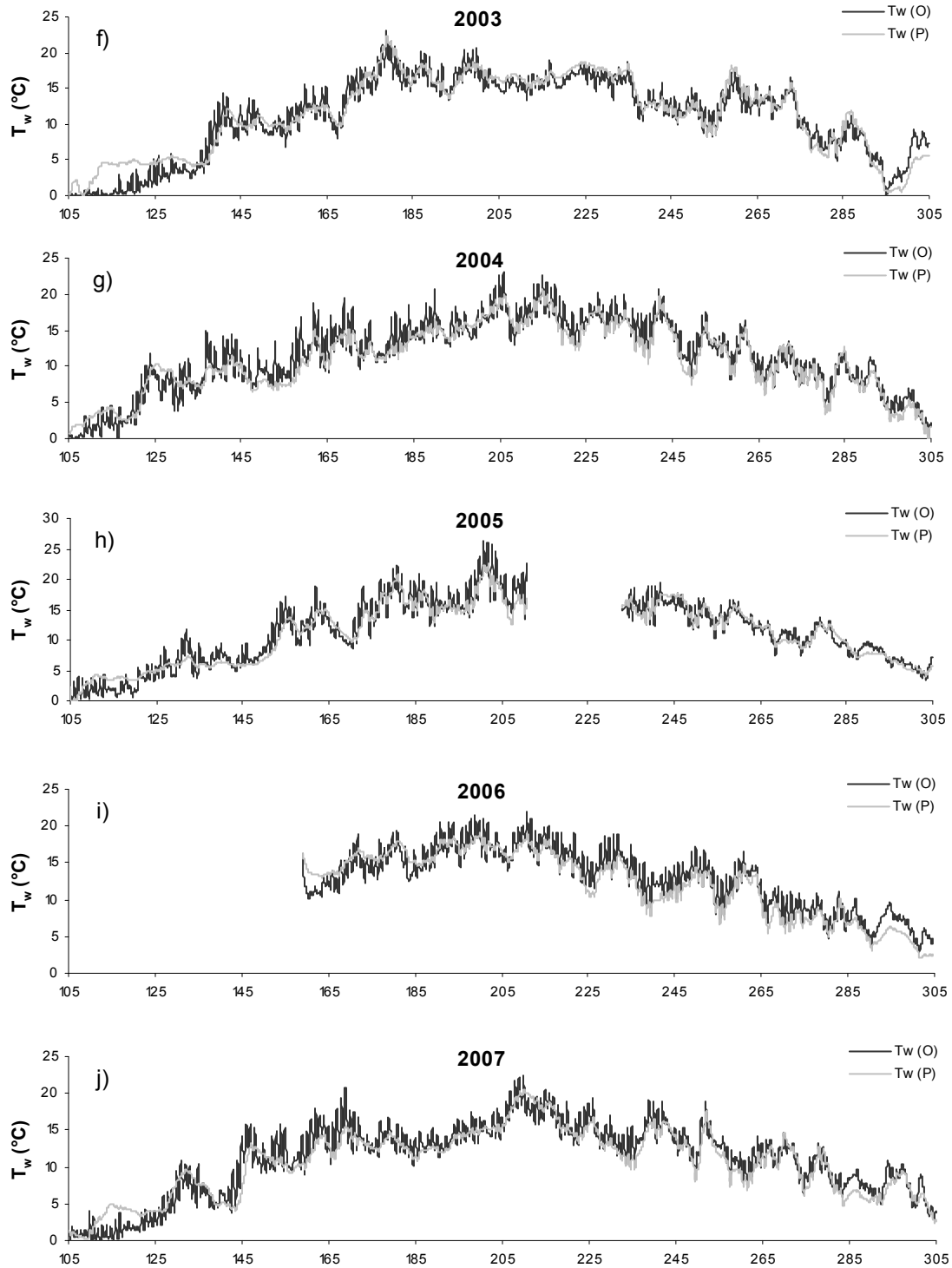


Figure 4.11. Observed water temperatures ($T_w(O)$) and predicted water temperatures ($T_w(P)$) obtained from the equilibrium temperature model at Catamaran Brook.

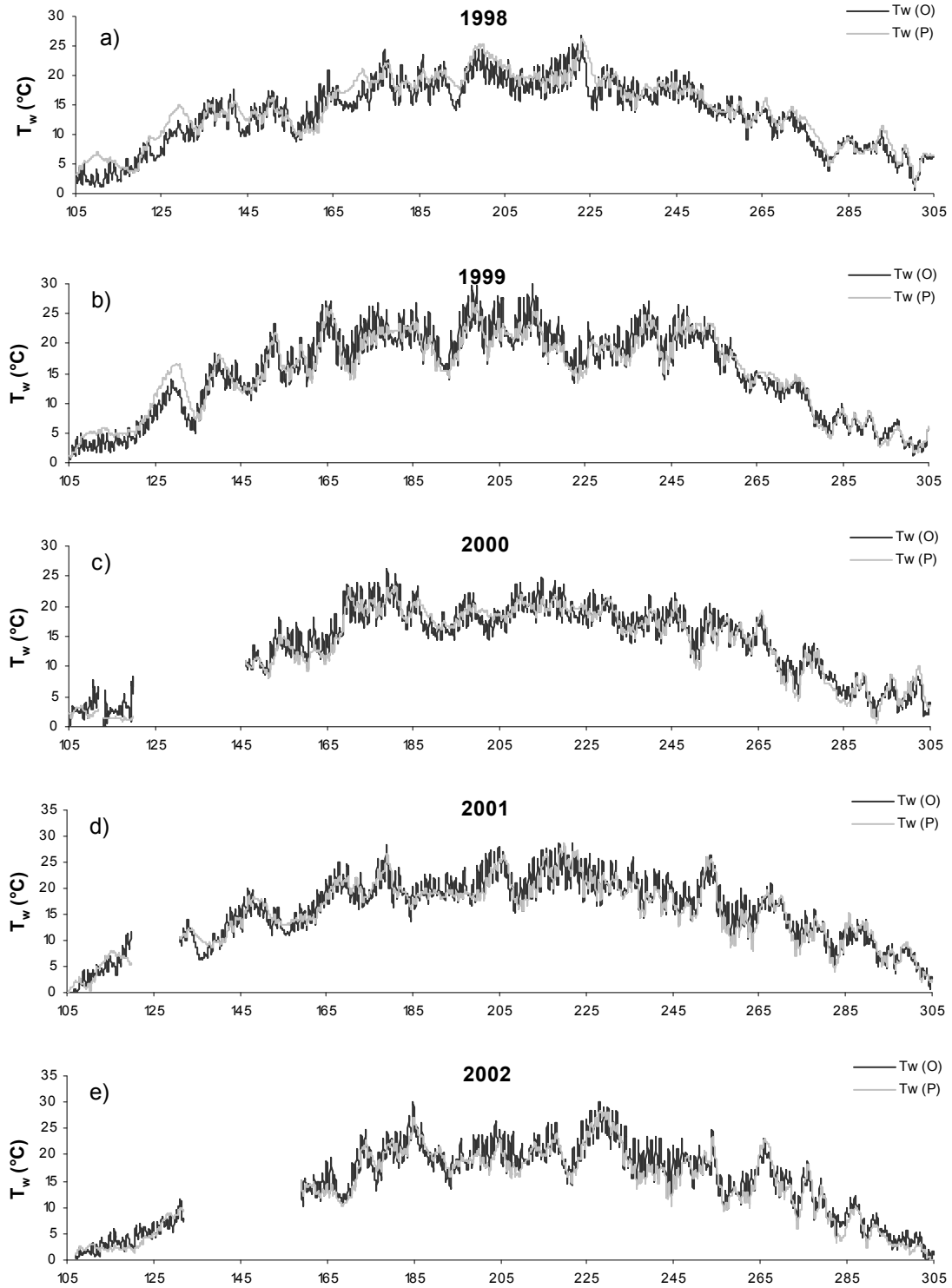


Figure 4.12. Observed water temperatures ($T_w(O)$) and predicted water temperatures ($T_w(P)$) obtained from the equilibrium temperature model at Little Southwest Miramichi.

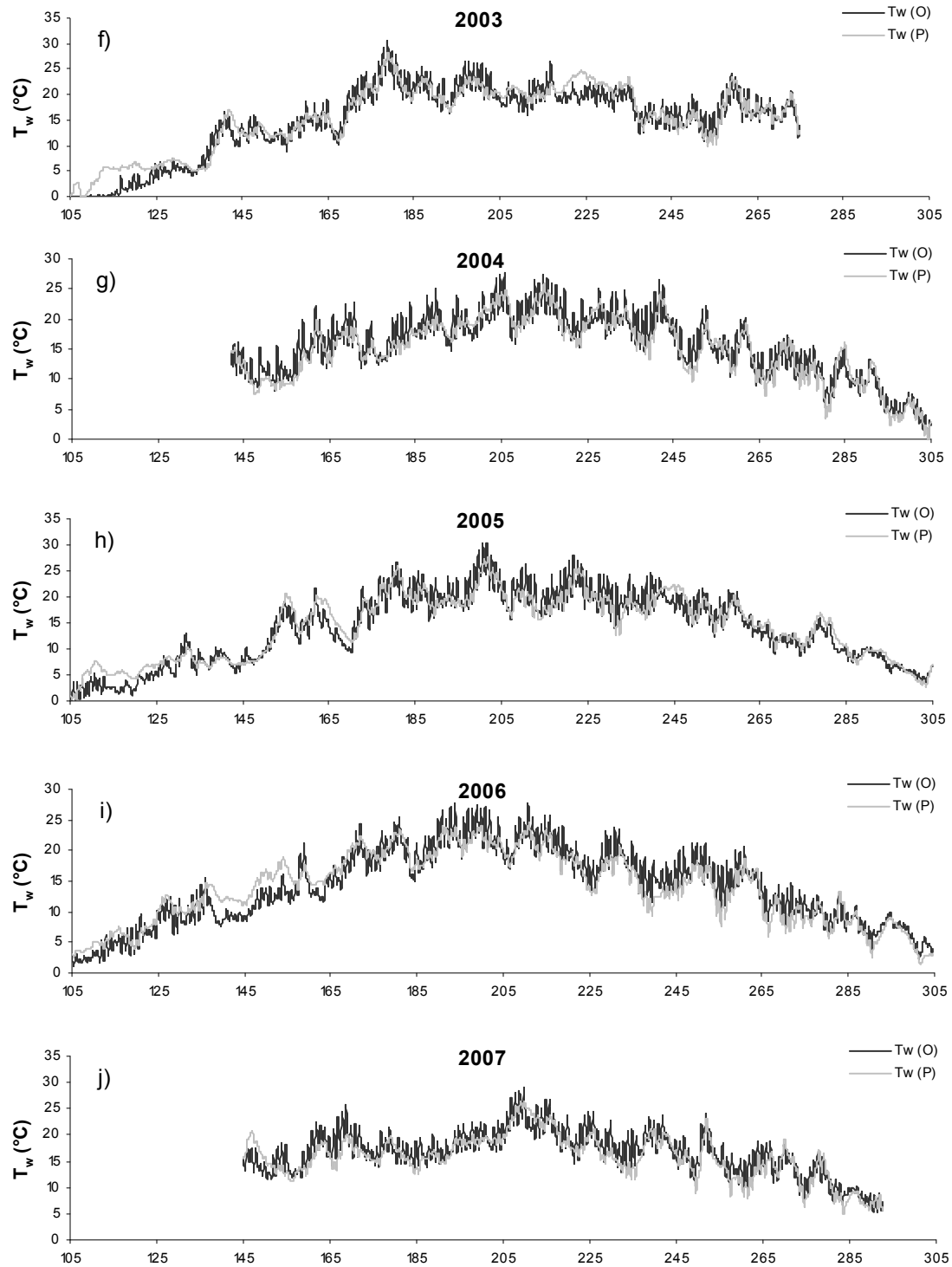


Figure 4.12. Observed water temperatures ($T_w(O)$) and predicted water temperatures ($T_w(P)$) obtained from the equilibrium temperature model at Little Southwest Miramichi.

The validation years (2003-2007) indicated in Figures 4.11f-j, showed results similar to those of the calibration years, with clear over-estimation in spring periods, especially years 2003 and 2007. An underestimation was also observed in the last few days of autumn (days 285-305). During most days, for all the years, predicted water temperature did not seem to effectively capture the diel variation.

Results were similar for the LSWM (Figures 4.12a-e). Spring water temperatures were also overestimated during the calibration years, especially in years 1998 and 1999, however, a clear underestimation was not observed in autumn similar to the calibration period at Cat Bk. The year 1998 showed less overestimation during the summer. For the validation years (Figures 4.12f-j), important overestimation was also observed in spring and early summer (2003, 2005 and 2006), but agreement was observed in late autumn, unlike in Cat Bk.

Table 4.6 shows the model performance of the developed equilibrium temperature model for the calibration years, the validation, for all years and for each year. The model performance was similar throughout the years at Cat Bk (all years: $RMSE = 1.52$ °C, $R^2 = 0.914$ and bias = -0.15 °C), although the calibration years were slightly better ($RMSE = 1.49$ °C, $R^2 = 0.920$ and bias = -0.01 °C). The validation period performance was similar with a $RMSE$ of 1.54 °C, a R^2 of 0.910 and a bias of -0.29 °C.

At LSWM, the calibration years showed the best performance ($RMSE = 1.81$ °C, $R^2 = 0.923$ and bias = -0.03 °C). Unlike Cat Bk, the validation years at LSWM showed a poorer performance, with a $RMSE$ of 2.15 °C, a R^2 of 0.877 and a bias of -0.15 °C, than

the calibration period. Overall, the LSWM showed a significant agreement between predicted and observed water temperatures with an overall (all years) *RMSE* of 1.98 °C a R^2 of 0.902 and a bias of -0.09 °C.

Table 4.6. Results of the equilibrium temperature model for prediction of hourly water temperatures at Catamaran Brook and Little Southwest Miramichi.

Period	Catamaran Brook			Little Southwest Miramichi		
	RMSE (°C)	R ²	Bias (°C)	RMSE (°C)	R ²	Bias (°C)
Calibration (1998-2002)	1.49	0.920	-0.01	1.81	0.923	-0.03
1998	1.53	0.924	0.93	1.92	0.907	0.87
1999	1.63	0.918	-0.21	1.86	0.933	0.05
2000	1.35	0.937	-0.53	1.60	0.936	-0.31
2001	1.55	0.928	0.21	1.84	0.919	-0.25
2002	1.37	0.950	-0.46	1.81	0.946	-0.66
Validation (2003-2007)	1.54	0.910	-0.29	2.15	0.877	-0.15
2003	1.55	0.925	0.36	2.02	0.924	0.51
2004	1.46	0.924	-0.51	2.18	0.851	-0.70
2005	1.50	0.924	-0.27	2.19	0.897	0.23
2006	1.62	0.892	-0.72	2.09	0.885	-0.16
2007	1.60	0.903	-0.43	2.28	0.758	-0.81
All years (1998-2007)	1.52	0.914	-0.15	1.98	0.902	-0.09
Seasonal Analysis						
Calibration (1998-2002)						
Spring	1.74	0.872	0.25	2.01	0.885	0.21
Summer	1.44	0.714	-0.07	1.87	0.709	-0.21
Autumn	1.10	0.913	-0.32	1.37	0.908	0.06
Validation (2003-2007)						
Spring	1.92	0.856	0.17	2.34	0.844	0.75
Summer	1.38	0.764	-0.42	2.21	0.651	-0.62
Autumn	1.28	0.881	-0.65	1.59	0.845	-0.24
All years (1998-2007)						
Spring	1.82	0.864	0.21	2.17	0.863	0.47
Summer	1.41	0.735	-0.24	2.05	0.676	-0.42
Autumn	1.19	0.896	-0.48	1.47	0.885	-0.07

A seasonal analysis was also performed to examine the performance of the model under different conditions. Three seasons were selected (spring, summer and autumn). Spring was between April 15 and June 20 (day 105-171), summer between June 21 and September 20 (day 172-263) and autumn between September 22 and October 31 (day 264-305). At both Cat Bk and LSWM, spring showed poorer performance of all periods although its performance was better during the calibration period. At Cat Bk, the performance in spring had a *RMSE* between 1.74 °C and 1.92 °C, R^2 between 0.856 and 0.872 and a bias between 0.17 °C and 0.25 °C. At LSWM, the performance in spring showed a *RMSE* between 2.01 °C and 2.34 °C, R^2 between 0.844 and 0.885 and a bias between 0.21 °C and 0.75 °C. Autumn showed the best performance for watercourses, and best performances were observed during the calibration years. In autumn, *RMSEs* were as low as 1.10 °C to 1.28 °C at Cat Bk and 1.37 °C to 1.59 °C at LSWM. The R^2 ranged between 0.845 and 0.913 the bias varied between -0.48 °C and 0.06 °C for both Cat Bk and LSWM. At LSWM, spring and summer had similar performances. At Cat Bk, the performance in summer was close to the autumn performances.

Four different time periods of 7 days were selected over the entire study period (1998-2007) to compare observed ($T_w(O)$) and predicted ($T_w(P)$) water temperatures as a function of air temperature (T_a). They were selected to examine in more detail the performance of the equilibrium temperature model under different meteorological and hydrological conditions. The selection of periods was made to include two training periods and two validation periods over the three seasons: spring, summer and autumn (Table 4.7). Results are presented in Figure 4.13. The two training periods consisted of 1) days in summer of 1998 (days 221-227) where a significant change in temperature was

observed and 2) in spring 1999 (days 132-138) where water temperatures increased rapidly. The two validation periods included a period of autumn 2006 (days 292-298) to reflect the autumn conditions and days of summer 2007, to look at the warmest temperature conditions (days 203-209).

Table 4.7. Description of the four selected study periods to examine the performance of the water temperature model under different hydrological conditions.

Sample	Season	Year	Day of year	Dates	Hydrological Conditions
Training	Summer	1998	221-227	August 9 – August 15	Sudden decrease of air and water temperatures
Training	Spring	1999	132-138	May 12 – May 18	Gradual increase of air and water temperatures
Validation	Autumn	2006	292-298	October 19 – October 25	Autumn conditions
Validation	Summer	2007	203-209	July 22 – July 29	Warmest temperature conditions

In the first detailed period, including days 221 to 227 (August 9 to 15, 1998), air temperatures decreased rapidly from 31.7 °C to 4.6 °C at both Cat Bk and LSWM over a period of 5 days (Figures 4.13a and 4.13b). Predicted water temperature did not effectively predict the observed water temperature, especially during the decrease of air and water temperatures. At Cat Bk, where observed water temperatures ($T_w(O)$) varied from 19.4 °C to 11.8 °C, predicted water temperatures ($T_w(P)$) never decreased to less than 15.7 °C. At LSWM, before the decreased of air and water temperatures, both predicted and observed water temperatures were around 26 °C before the decrease. However, observed water temperatures showed values as low as 14.2 °C, whereas the lowest predicted water temperatures was 17.8 °C. It was only towards the end of the period that predicted water temperature became close to observed values.

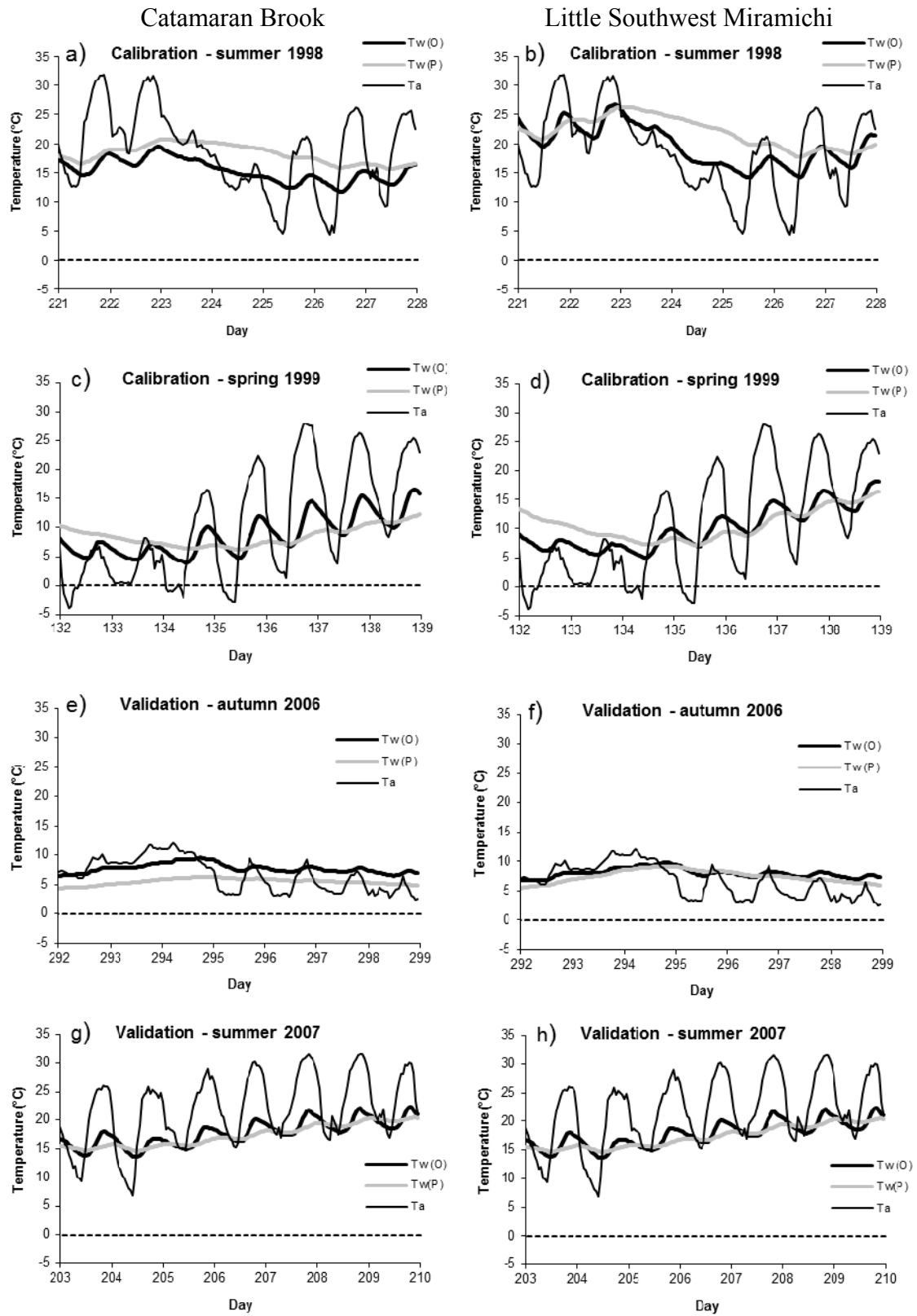


Figure 4.13. Observed water temperatures ($T_w(O)$), predicted water temperatures ($T_w(P)$) from the equilibrium temperature model and air temperatures (T_a) for four detailed time periods at Catamaran Brook and Little Southwest Miramichi.

For the period in spring of 1999 from May 12 to May 18 (days 132 to 138), air temperatures varied between $-3.5\text{ }^{\circ}\text{C}$ and $26.4\text{ }^{\circ}\text{C}$ (Figures 4.13c and 4.13d). Observed water temperatures varied similarly at both streams ($4.7\text{ }^{\circ}\text{C}$ to $18.2\text{ }^{\circ}\text{C}$). Predicted water temperatures showed a general increasing trend; however it was not possible to capture the diel variations observed in water temperatures. Predicted water temperatures varied from $6.2\text{ }^{\circ}\text{C}$ to $12.2\text{ }^{\circ}\text{C}$ at Cat Bk, and were higher at LSWM, varying between $7.2\text{ }^{\circ}\text{C}$ and $16.5\text{ }^{\circ}\text{C}$.

Air and water temperatures were low during the period of autumn 2006 (days 292 to 298: October 19 to 25). Air temperatures were higher in the first 3 days, and decreased slightly afterwards anywhere between $2.4\text{ }^{\circ}\text{C}$ and $12.0\text{ }^{\circ}\text{C}$ (Figures 4.13e and 4.13f). Water temperatures did not showed much diel variability during those days. In fact, water temperatures only slightly varied between $6.4\text{ }^{\circ}\text{C}$ and $9.8\text{ }^{\circ}\text{C}$ at both Cat Bk and LSWM. Predicted water temperatures at Cat Bk did not truly represent observed water temperatures, with values ranging between $4.4\text{ }^{\circ}\text{C}$ and $6.3\text{ }^{\circ}\text{C}$. At LSWM, predicted water temperatures showed a better agreement with the observed water temperatures, between $5.4\text{ }^{\circ}\text{C}$ and $9.1\text{ }^{\circ}\text{C}$.

The validation period during the summer of 2007 included the warmest air and water temperatures (days 203 to 209; July 22 to 29). Air temperatures increased from $6.9\text{ }^{\circ}\text{C}$ to reach temperatures as high as $31.6\text{ }^{\circ}\text{C}$ (Figures 4.13g and 4.13h). Observed water temperatures at Cat Bk ($13.6\text{ }^{\circ}\text{C}$ to $22.4\text{ }^{\circ}\text{C}$) varied similarly as in LSWM ($16.8\text{ }^{\circ}\text{C}$ to $28.9\text{ }^{\circ}\text{C}$). Predicted water temperatures generally showed an increasing trend, however, the

diel variations were not captured by the model. Water temperatures varied between 14.7 °C and 20.5 °C at Cat Bk, and between 18.0 °C and 26.4 °C at LSWM.

4.3 ARTIFICIAL NEURAL NETWORK MODEL

In the present study, an ANN model was developed to predict hourly water temperature for two Catamaran Brook (Cat Bk) and the Little Southwest Miramichi (LSWM). The results of the ANN models (*RMSE*, R^2 , and bias) are represented in Table 4.8. The ANN model generally provided the best results for Cat Bk with a root-mean-square error (*RMSE*) of 0.63 °C for the training period and 1.19 °C for the validation period. At Cat Bk, the coefficient of determination (R^2) was 0.986 (training) and 0.948 (validation). The bias was 0.00 °C for the training period and -0.28 °C for the validation period. For the LSWM, the ANN model performed comparably well, especially during training (*RMSE* = 0.69 °C and R^2 = 0.989). However, during the validation period, the *RMSE* was higher, at 1.62 °C, with a correspondingly lower R^2 at 0.930. The bias for LSWM was 0.00 °C (training) and 0.05 °C (validation). Overall (all years), the ANN model performed well for both watercourses, with a *RMSE* of 0.94 °C (Cat Bk) and 1.23 °C (LSWM) and a R^2 values of 0.967 (Cat Bk) and 0.962 (LSWM). Water temperatures were slightly underestimated at Cat Bk, with a bias of -0.13 °C. The overall bias for LSWM was very low, at 0.02 °C.

A comparison by year showed consistent results during the training period, with the *RMSE* being less than 0.91 °C and R^2 being over 0.980 (Table 4.8). The bias was consistent over the years and was generally low (less than ± 0.06 °C). The validation *RMSE*'s were 2 to 3 times higher than for those of the training years. Cat Bk showed

RMSE's between 1.02 °C and 1.40 °C. LSWM showed *RMSE*'s between 1.33 °C and 1.91 °C during the validation period. Coefficients of determination (R^2) were similar throughout the validation years at Cat Bk (0.948 to 0.959) but were variable at LSWM (between 0.868 and 0.971). The bias was highest at Cat Bk in 2005 (-0.66 °C) and 2006 (-0.69 °C) with correspondingly lower values for the LSWM (± 0.40 °C).

Table 4.8 also shows the performance of the model on a seasonal basis. Spring was between April 15 and June 21 (days 105-171), summer between June 22 and September 20 (days 172-263) and autumn between September 22 and October 31 (days 264-305). For the training period, autumn showed the best performance with a *RMSE* of 0.47 °C (Cat Bk) and 0.52 °C (LSWM). Spring (training period) showed a poorer performance with *RMSE* values of 0.70 °C (Cat Bk) and 0.85 °C (LSWM). *RMSE*'s during the summer were similar at Cat Bk and LSWM, with values of 0.64 °C and 0.67 °C, respectively. Coefficients of determination (R^2) were similar in autumn and spring with values over 0.979; however, lower values were observed in the summer (0.942-0.961). The biases were generally small for both watercourses for the training period, with seasonal values less than ± 0.02 °C.

Table 4.8 Results of artificial neural network (ANN) models for the prediction of hourly water temperatures at Catamaran Brook and Little Southwest Miramichi.

Period	Catamaran Brook			Little Southwest Miramichi		
	RMSE	R ²	Bias	RMSE	R ²	Bias
Training (1998-2002)	0.63	0.986	0.00	0.69	0.989	0.00
1998	0.53	0.984	0.06	0.55	0.990	0.01
1999	0.71	0.984	0.00	0.63	0.992	0.01
2000	0.63	0.984	-0.05	0.63	0.989	0.00
2001	0.63	0.987	0.03	0.91	0.980	-0.01
2002	0.63	0.988	-0.04	0.70	0.991	-0.01
Validation (2003-2007)	1.19	0.948	-0.28	1.62	0.930	0.05
2003	1.22	0.953	0.21	1.50	0.971	0.34
2004	1.02	0.959	-0.15	1.71	0.898	0.22
2005	1.40	0.948	-0.66	1.91	0.920	0.10
2006	1.17	0.948	-0.69	1.33	0.953	-0.03
2007	1.13	0.950	-0.25	1.58	0.868	-0.40
All years (1998-2007)	0.94	0.967	-0.13	1.23	0.962	0.02
	Seasonal Analysis					
Training (1998-2002)						
Spring	0.70	0.979	0.01	0.85	0.979	0.02
Summer	0.64	0.942	0.00	0.67	0.961	-0.02
Autumn	0.47	0.979	0.00	0.52	0.985	0.02
Validation (2003-2007)						
Spring	1.38	0.920	-0.02	1.76	0.922	0.78
Summer	1.02	0.865	-0.32	1.61	0.776	-0.20
Autumn	1.25	0.856	-0.53	1.39	0.890	-0.47
All years (1998-2007)						
Spring	1.06	0.951	-0.01	1.38	0.947	0.39
Summer	0.85	0.901	-0.16	1.23	0.868	-0.11
Autumn	0.94	0.915	-0.27	1.00	0.943	-0.19

Seasonal results were similar during the validation period, although *RMSE*'s and biases were generally higher, with lower R^2 . Highest *RMSE*'s were observed during the spring (1.38 °C Cat Bk and 1.76 °C LSWM) and best performances were in summer in Cat Bk (1.02 °C) and autumn in LSWM (1.39 °C). Summer had the lowest R^2 (0.776), whereas spring had the highest R^2 (0.922). Spring showed a general overestimation of predicted water temperature in LSWM, with a bias of 0.78 °C. In general (all years), the ANN model showed similar seasonal performances in Cat Bk and a better performance in summer and autumn for LSWM.

Figure 4.14 shows observed water temperatures ($T_w(O)$) and predicted water temperatures ($T_w(P)$) at Cat Bk. The training period (Figures 4.14a-e) showed good agreement between observed ($T_w(O)$) and predicted water temperatures ($T_w(P)$). However, the validation period (Figures 4.14f-j) showed more discrepancies between observed and predicted water temperatures, mainly in early spring (days 105-120) and late autumn (days 290-305). Figures 4.15a-e show substantial agreement between predicted water temperatures ($T_w(P)$) via the ANN model, compared to observed water temperatures ($T_w(O)$) for LSWM. As with Cat Bk, the validation years at LSWM (Figures 4.15f-j) show more differences between observed ($T_w(O)$) and predicted water temperatures ($T_w(P)$) in early spring and late autumn.

Four different time periods of 7 days were selected over the entire study period (1998-2007) to compare the observed ($T_w(O)$) and predicted ($T_w(P)$) water temperatures as a function of air temperature (T_a) (Figure 4.16). They were selected to examine, in more detail, the performance of the ANN model under different meteorological and

hydrological conditions. These periods were the same as those used for the equilibrium temperature model. The selection was made to include two training periods and two validation periods over the three seasons: spring, summer and autumn (Table 4.7). The two training periods comprised of i) days in summer of 1998 (days 221-227) where a significant change in temperature was observed and ii) spring of 1999 (days 132-138) where water temperatures increased rapidly. The two validation periods included a period of autumn 2006 (days 292-298) to reflect the autumn conditions, and part of the summer of 2007, to look at the warmest conditions (days 203-209).

Figure 4.16a and 4.16b shows days 221 to 227 of summer 1998 (August 9 to August 15). This period showed a sudden decrease in air temperature (T_a) and observed water temperature ($T_w(O)$) at both Cat Bk and LSWM, caused by rain and heavy fog on day 223. The predicted water temperature ($T_w(P)$) was slightly overestimated during the first two days, where air temperature was higher. There was also a slight overestimation during the decrease of air temperature (T_a), where water levels increased from 0.088 m to 0.313 m at Cat Bk and from 0.374 m to 0.970 m at LSWM. The following days, the predicted water temperature ($T_w(P)$) closely followed the observed water temperature ($T_w(O)$).

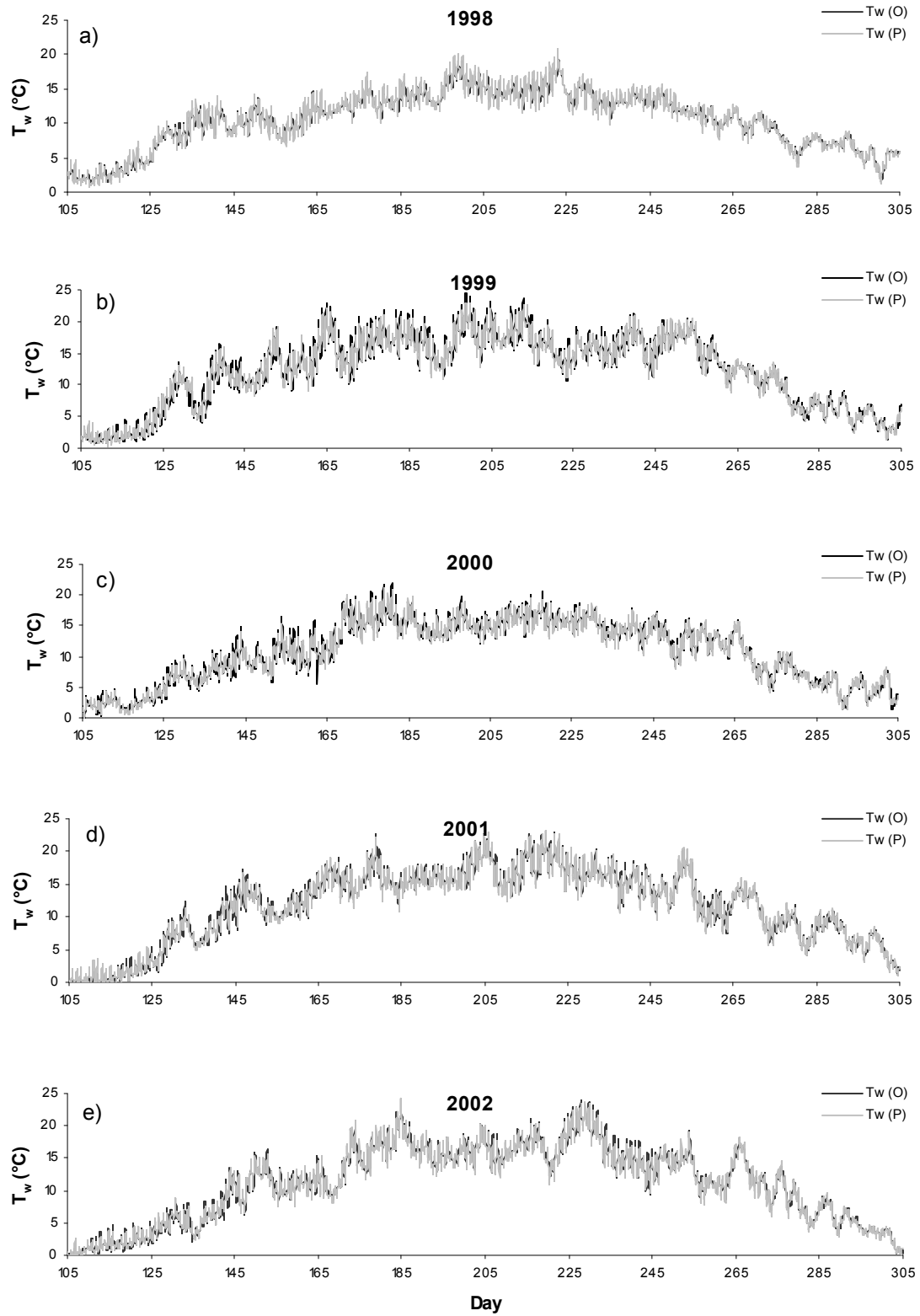


Figure 4.14. Observed water temperatures ($T_w(O)$) and predicted water temperatures ($T_w(P)$) obtained from the ANN model at Catamaran Brook.

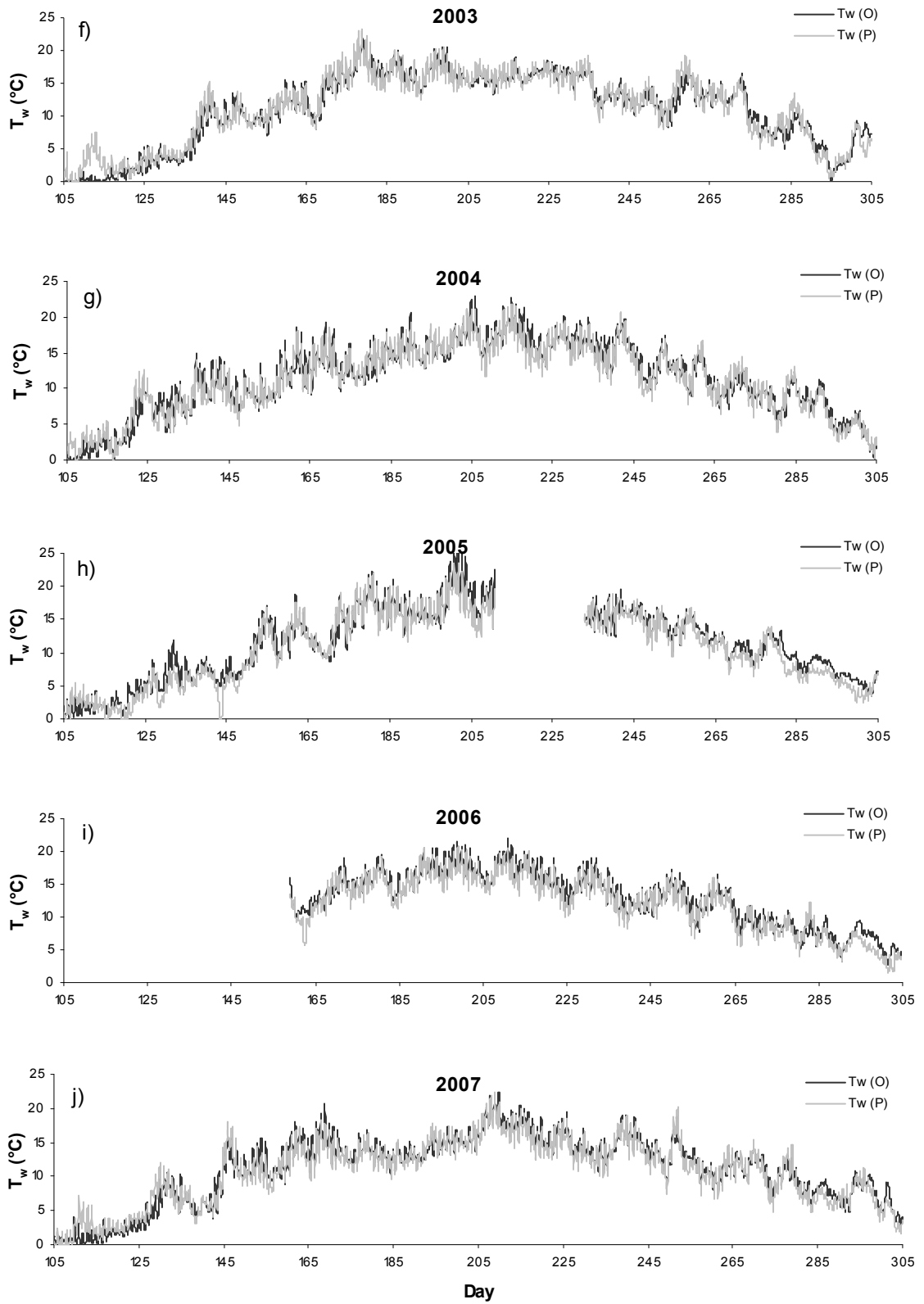


Figure 4.14. Observed water temperatures (Tw(O)) and predicted water temperatures (Tw(P)) obtained from the ANN model at Catamaran Brook.

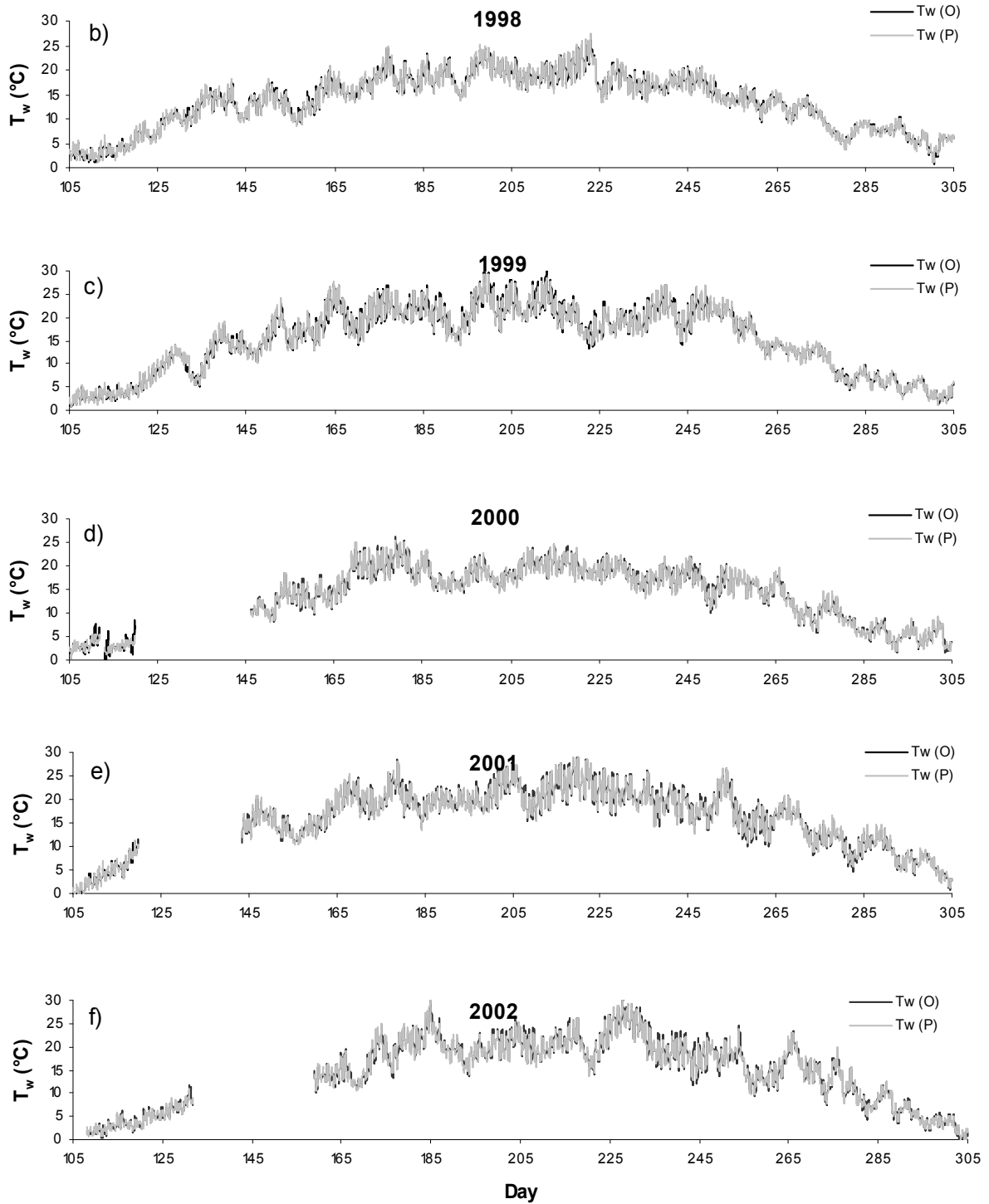


Figure 4.15. Observed water temperatures ($T_w(O)$) and predicted water temperatures ($T_w(P)$) obtained from the ANN model at Little Southwest Miramichi.

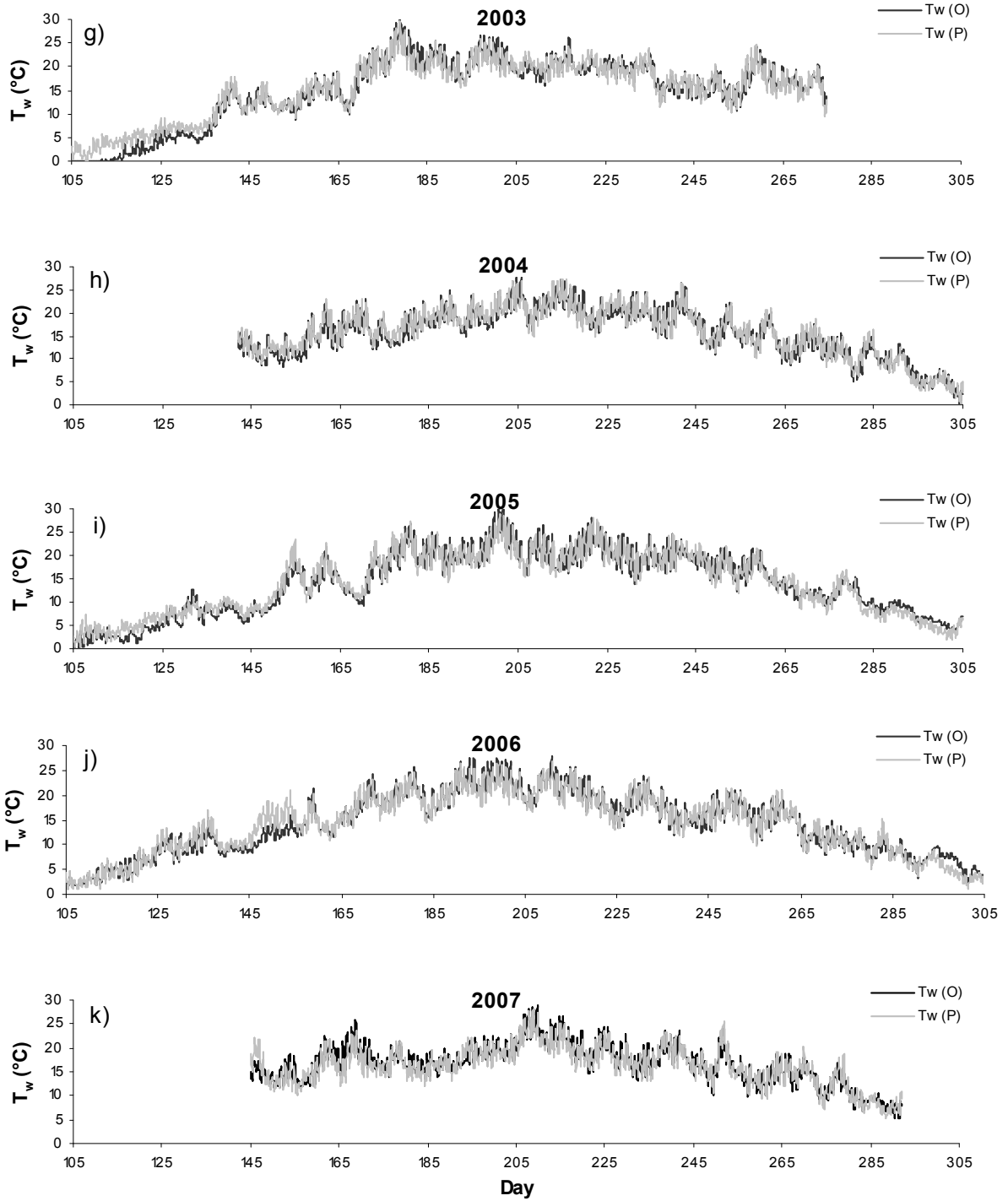


Figure 4.15. Observed water temperatures ($T_w(O)$) and predicted water temperatures ($T_w(P)$) obtained from the ANN model at Little Southwest Miramichi.

The second period included days 132-138 (May 12 to May 18) in the spring of 1999 (Figure 4.16c and 4.16d). The first days, 132-133 experienced a few showers, followed by days of mainly clear sky. Water levels decreased throughout the period at both Cat Bk and LSWM. At Cat Bk (Figure 4.16c), the ANN model showed some difficulty in estimating water temperatures, as compared to LSWM (Figure 4.16d). Water temperatures at night were generally underestimated, whereas day time temperatures were generally overestimated. At LSWM, predicted water temperatures closely followed observed water temperature throughout the period.

In 2006, during the validation period, days 292 to 298 (October 19 to October 25) were analyzed (Figure 4.16e and 4.16f). This period reflected autumn conditions, with low air temperature and an increase in water level due to precipitation on day 294. Predicted water temperatures were clearly underestimated compared to observed water temperatures at both watercourses. The differences between the observed and predicted water temperatures was up to 2.8 °C at Cat Bk and up to 3.4 °C at LSWM.

Figure 4.16g and 4.16h included a period of warm air temperatures (T_a) and water temperatures ($T_w(O)$) during the summer of 2007 from July 22 to July 29 (days 203 to 209). Predicted water temperatures ($T_w(P)$) closely followed the observed water temperatures ($T_w(O)$) during a gradual increase in air temperatures (T_a) at both Cat Bk and LSWM. During most of the days, water temperatures were slightly underestimated and delayed, except at LSWM wherein a slight overestimation occurred at night.

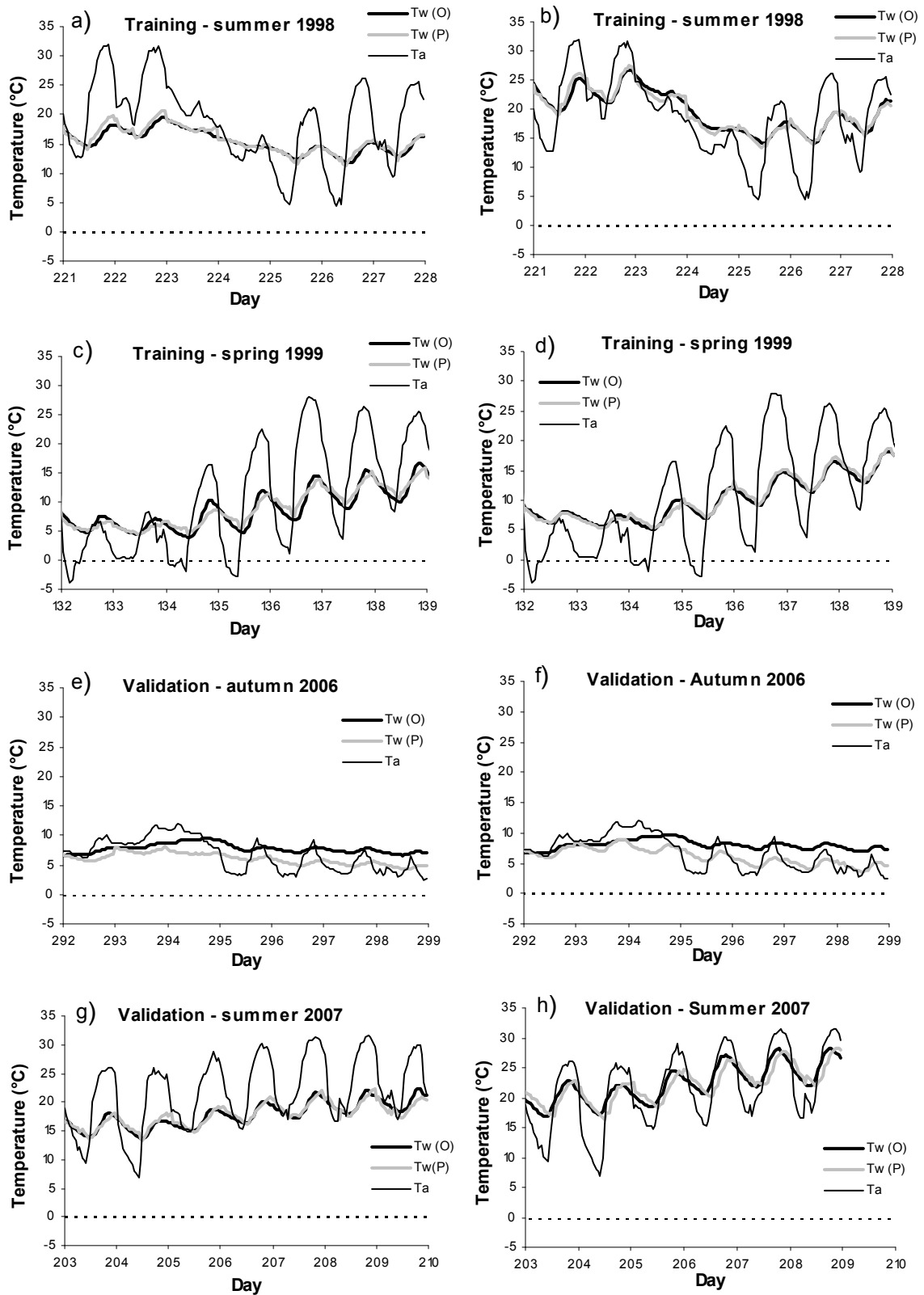


Figure 4.16. Observed water temperatures ($T_w(O)$), predicted water temperatures ($T_w(P)$) from the ANN model and air temperatures (T_a) for the four detailed time periods at Catamaran Brook and Little Southwest Miramichi.

CHAPTER 5: DISCUSSION AND ANALYSIS OF RESULTS

5.1 DETERMINISTIC MODEL

The present study implemented a deterministic water temperature model using near stream microclimate data to better reflect heat exchanges occurring at the river level. This study also considered streambed heat fluxes in the modeling. The application of deterministic models permits a comparison of different fluxes and their relative contributions (Raphael 1962; Morin and Couillard, 1990; Morin *et al.*, 1994). Results of this study are reflective of summer and autumn conditions from July 4 to October 2, and therefore different results would be expected during other times of year, such as in winter.

Results of the present study showed a clear difference between meteorological conditions at the remote site (MetSta) and those collected within the river environment as those near stream conditions/microclimate sites as shown in Table 4.2. Differences between remote vs. microclimate stations were especially significant for solar radiation and wind speed whereas other parameters, such as air temperature and relative humidity, showed similar values. The LSWM site experienced higher solar radiation and wind speed than Cat Bk. Conversely, the relative humidity was 3% to 16% higher at Cat Bk which was the more sheltered site, than at LSWM and the MetSta. Wind speed at Cat Bk was approximately 4%-7% of the values at the MetSta, whereas LSWM showed values of 23%-38%. Since wind speed plays such an important role in the evaporative and convective heat fluxes, only wind speed at the microclimate level will truly capture these fluxes. Similar observations can be made for solar radiation. At Cat Bk, incoming solar radiation was

27%-44% of the values observed at the MetSta and LSWM. The incoming solar radiation between the MetSta and LSWM was less than 4%. Benyahya *et al.* (2010) predicted daily stream temperatures using microclimate and regional meteorological data coming from three sites located within the Miramichi River system. As in this study, the two parameters showing the most variability between microclimate sites and the regional meteorological station were solar radiation and wind speed. With such differences between remote and microclimate sites, microclimate data are therefore important to capture near stream heat fluxes, especially in smaller watercourses (Brown, 1969; Johnson, 2003; Johnson, 2004; Benyahya *et al.*, 2010).

The analysis of different periods revealed varied heat flux conditions for both Cat Bk and LSWM (Figures 4.2 to 4.7). For example, results showed significant agreement between predicted and observed total flux (H_t) during most periods with the exception of Period 1 (Figure 4.2). It is expected that the precipitation event in which 40 mm of rain fell in over 10 hours played a role in Period 1. During this important rainfall event, the calculated precipitation fluxes (Equation (3.13)) experienced both a gain (2.9 W m^{-2}) and a loss (-0.17 W m^{-2}) which could not explain the observed difference of almost -150 W m^{-2} to -200 W m^{-2} between observed and predicted total heat flux. Therefore, a significant heat loss was missing from this event which can only be explained by other processes. Heat fluxes may not have been added by direct precipitation falling into the river, but rather by advected heat flux inputs, coming from surface and near-subsurface hillslope pathways and groundwater (Brown and Hannah, 2007). It was also found in other studies that the amount of heat added by a rainfall is highly dependent on atmospheric conditions such as dew point, air temperature, and solar radiation, before and after a storm event as well as

the intensity and duration of the rainfall event (Herb *et al.*, 2008). Due to this large difference in fluxes, Period 1 were excluded from the calculations when comparing mean fluxes of different periods and between surface and streambed contributions.

When comparing flux contributions as in Table 4.3, it was observed that the surface heat flux contributed 83% of the total energy gain and 77% of the energy loss at Cat Bk, excluding Period 1. The streambed flux at Cat Bk contributed 17% of the total energy gains and 23% of the losses. The surface heat flux was more important at LSWM (93% of the total energy gain and 88% of the total energy loss). The streambed flux at LSWM was lower, with gains of only 7% and losses of 12%. These results are consistent with those of Evans *et al.* (1998) who found that over 82% of the total heat exchange occurred at the air/water surface. Our study permits a comparison of different size rivers in a similar climatic region. A higher streambed contribution would also be expected for smaller streams than Cat Bk which would experience corresponding lower wind speed and solar radiation as well as higher groundwater contributions.

Solar radiation accounted for most of the daytime energy gain, as reported in previous studies (Webb and Zhang, 1997; Webb and Zhang, 1999; Younus *et al.*, 2000; Webb and Crisp, 2006; Cozzetto *et al.*, 2006; Caissie *et al.*, 2007). In fact, solar radiation contributed, on average, 63% of the total heat gain at Cat Bk and 89% at LSWM. Solar radiation is very much a function of site conditions and predominately related to the degree of shading (Johnson, 2004). For instance, solar radiation was much lower at Cat Bk (up to 254 W m^{-2}) than at LSWM (up to 674 W m^{-2}). In most heat budget models, solar radiation was either estimated with equations or measured on a meteorological

station near the stream. A shading factor was needed to be included to account for the shading of each specific river depending on forest cover and topography (Younus, 2000; Caissie *et al.*, 2007). In this study, measurements were made directly on the stream, better representing the contribution of solar radiation.

Both evaporative fluxes and longwave radiation were the predominant heat loss components. Evaporative flux losses were similar between Cat Bk (31%) and LSWM (25%) whereas the longwave radiation flux losses were higher in LSWM (56%) than in Cat Bk (40%). The convective heat flux played a smaller role, generally less than 10% for both gains and losses, within the heat budget for both watercourses.

Only a few studies were found within the literature to have taken into account the longwave radiation emitted from the forest canopy within the modeling study (Rutherford *et al.*, 1997; Benyahya *et al.*, 2010). As the forest cover becomes important, the incoming atmospheric longwave radiation is replaced by the forest cover longwave radiation. The longwave radiation was usually found to be the main component of energy loss in most stream water temperature heat budgets along with evaporative fluxes. In our study, losses were more important at LSWM (52% to 63% of the total energy) than at Cat Bk (35% to 48%). Others studies (Evans *et al.*, 1998; Webb and Zhang, 1997) showed longwave radiation losses of 54% and 49% of the total energy which were closer to values for LSWM.

The evaporative heat flux was also a major source of energy loss (Table 4.3). At Cat Bk, this heat loss accounted for 31% compared to 56% for LSWM. Notably, the major source

of heat loss in Cat Bk was the longwave radiation whereas in LSWM the major source of heat loss was the evaporative flux. Webb and Zhang (1997) showed that the evaporative heat flux can be an important source of energy loss with contributions reaching 30% of the total heat flux, values close to those observed in Cat Bk. Cozzetto *et al.* (2006) observed that the evaporation tended to increase not only with wind speed but with stream temperatures as well.

The convective heat flux was relatively small with gain and loss values less than 3.0 W m^{-2} at Cat Bk and less than 6.3 W m^{-2} at LSWM (Table 4.3). The convective heat flux at Cat Bk contributed similarly to the total heat flux gain (6%) and loss (7%), somewhat neutral overall. For LSWM, convective heat gains were relatively small (1%) compared to losses (7%). The convective heat fluxes were, in general, small compared to other heat fluxes (Caissie *et al.*, 2007).

Most studies have neglected the precipitation heat flux within the modeling (Evans *et al.*, 1998; Hannah *et al.*, 2008) mainly because it contributed to less than 1% of the daily heat budget (Webb and Zhang, 1997). In this study, precipitation heat fluxes were included; however, it contributed less than 1.2 % to the total heat flux for both watercourses during Periods 1, 4, and 6, which included rainfall events. Precipitation heat fluxes were less than 0.2 W m^{-2} at Cat Bk and less than 0.7 W m^{-2} at LSWM (Table 4.3). Although the precipitation fluxes were relatively low compared to other fluxes, it was clear that the rainfall event during Period 1 had a significant cooling effect on water temperatures at both Cat Bk and LSWM (Figures 4.2a and 4.2e). Results suggest that the precipitation and corresponding flow generation processes most likely played an important role on

water temperature dynamics that was not captured by the precipitation heat flux equations. For instance, concepts of streamflow generation, such as the variable area contribution (Freeze, 1974), most likely provided other sources of cold water to these watercourses than just direct channel precipitation during rainfall events. More research is needed to better understand water temperature dynamics in response to rainfall events.

Studies have shown the importance of streambed fluxes in water temperature dynamics (Jobson, 1977; Jobson and Keefer, 1979; Sinokrot and Stefan, 1993; Moore *et al.*, 2005a). The streambed acted as an energy sink during the middle of the day and as an energy source later in the day and at night (Figure 4.2 to 4.7). For Cat Bk and LSWM, the most important streambed flux contribution occurred in late afternoon (e.g., 1500-1700h) with losses reaching -50 W m^{-2} . The net streambed heat flux was predominantly an energy loss over the entire period at both Cat Bk (23%) and LSWM (12%), excluding Period 1 (Table 4.3) and may be attributed mainly to heat losses from the advective fluxes (H_g). In addition, the streambed contribution relative to the overall heat budget tended to be more important for smaller streams (20% at Cat Bk vs. 10% for LSWM). Among the streambed fluxes, the heat flux by conduction was more important than the heat flux by advection on a diel basis. The streambed advective heat flux was much smaller than the flux by conduction during summer conditions. In autumn, Period 6, for example, and during winter, conditions were reversed where the heat flux by advection was more important. Diel water temperature variability was significantly reduced and therefore the flux by conduction was correspondingly lower.

Predicted ($H_t(P)$) vs. observed total heat flux ($H_t(O)$) showed slightly better results at LSWM than at Cat Bk (Figure 4.2 to 4.7) and correspondingly higher R^2 at LSWM. This was most likely related to the dominant surface heat fluxes at LSWM. It is expected that the estimation of surface heat fluxes have less uncertainties than corresponding streambed fluxes. Such results can be observed from Figure 4.8 where the LSWM, a surface flux dominated river, shows a better agreement between predicted and observed heat gains than Cat Bk, again, excluding Period 1. Heat gains in Cat Bk were slightly underestimated, presumably due to a lower solar radiation contribution. In fact, the main component of the heat gain for both sites was solar radiation, which was obtained by direct measurements using a pyranometer. Figure 4.8 also suggests a better estimation of heat gains than losses (losses showed more variability). Important components of heat losses, such as the evaporation rates, which are difficult to estimate, may have played an important role in higher uncertainties in the estimation of losses.

Predicted water temperatures ($T_w(P)$) were calculated from Equation (3.2b), using the predicted total heat flux ($H_t(P)$). Predicted water temperatures were very well estimated at both study streams with $RMSEs$ less than 0.33 °C, R^2 higher than 0.969 and bias less than 0.20 °C for all six periods (Table 4.5). As with the total heat fluxes, predicted water temperatures for both study watercourses were better estimated in Period 6, and had a poorer, but still a good performance, in Period 1. In Period 1, the total heat flux was underestimated during the important rainfall event. Even if the prediction of total heat flux was poor in Period 1, the estimation of water temperatures was very effective with very low $RMSE$ at both study streams (Table 4.5). LSWM had a slightly better performance for water temperature predictions (Figure 4.10) than Cat Bk, as in the

prediction of total heat flux. At Cat Bk, as shown in Figure 4.9, many days of different periods showed slight overestimation of daily maximum water temperatures (<1 °C). Results showed that Cat Bk was more sensitive to the estimation of total heat flux since water levels were generally lower than at LSWM. The deterministic model was effective in the predictions of hourly water temperatures at both study streams and for all periods.

5.2 EQUILIBRIUM TEMPERATURE MODEL

Deterministic models have been shown to be effective modeling tools for predicting temperatures (Evans *et al.*, 1998; Younus *et al.*, 2000; Caissie *et al.*, 2007; Hannah *et al.*, 2008), but they require a lot of input data. A simplified model was developed, assuming that total heat flux was proportional to the difference between the water temperature and an equilibrium temperature (Edinger *et al.*, 1968). Most equilibrium temperature models were developed to study the thermal regime of rivers (Novotny and Krenek, 1973; Gu, 1998; Mohseni and Stefan, 1999), but few have used it to model long-term time series of water temperatures (Caissie *et al.*, 2005; Larnier *et al.*, 2010). No studies could be found within the literature where this modeling approach was applied at hourly time scales. However, for a daily time scale, studies have shown (Caissie *et al.*, 2005; Larnier *et al.*, 2010) that air temperature was highly related to equilibrium temperatures, permitting the expression of equilibrium temperature as a linear function of air temperature. This resulted in good modeling performance of daily water temperatures.

The coefficient of the relationship between air and equilibrium temperature was optimized by minimizing the minimum square of errors between observed and predicted water temperatures. The coefficient α of the equilibrium temperature model only reflects

the total heat flux represented by the air temperature. A coefficient α higher than 1 means that the bulk energy component is higher than the measures of air temperature (Caissie *et al.*, 2007; Larnier *et al.*, 2011). The coefficient α was 0.87 at Cat Bk and 1.08 at LSWM. This reflects that LSWM is more exposed to meteorological factors than at Cat Bk, suggesting the importance of solar radiation as well as other parameters, than air temperature. The values calculated within the present study for hourly temperatures were in the range found in many studies using the equilibrium temperature concept. Caissie *et al.* (2005) calibrated both the same study streams with coefficient α at 0.81 at Cat Bk and of 1.05 at LSWM. Marcé and Armengol (2008) found the coefficient α varying in the range of 0 to 2. Larnier *et al.* (2010) found the coefficient α (1.12) closer to the LSWM, since the Garonne River was wide and unsheltered by streamside vegetation similar to LSWM. The coefficient β was calibrated at 0 °C, like in Caissie *et al.* (2005). However, other studies have shown values of β at 0.44 °C (Larnier *et al.*, 2010) and -10 °C to 45 °C (Marcé and Armengol, 2008).

The thermal exchange coefficients K were calculated at 2.7 W m⁻² °C⁻¹ (Cat Bk) and at 13.1 W m⁻² °C⁻¹ (LSWM). Caissie *et al.* (2005), who also studied the same two rivers (Cat Bk and LSWM), but at a daily time scale, calibrated the model with similar coefficients α and β , however, the thermal exchange coefficients K were higher (6.3 W m⁻² °C⁻¹ (Cat Bk) and 29.1 W m⁻² °C⁻¹ (LSWM)). Again, Larnier *et al.* (2010) showed results close to the LSWM with a thermal exchange coefficient K of 34.4 W m⁻² °C⁻¹. Marcé and Armengol (2008) showed thermal exchange coefficients ranging from 0 to 23.3 W m⁻² °C⁻¹. Herb and Stefan (2011), who also predicted hourly water temperatures, calculated a thermal exchange coefficient close to those calculated in this study. The

South Branch (Minnesota, USA) had a thermal exchange coefficient K of $9.0 \text{ W m}^{-2} \text{ }^{\circ}\text{C}^{-1}$ and the main stem had a coefficient K at $13.1 \text{ W m}^{-2} \text{ }^{\circ}\text{C}^{-1}$. The hourly exchange coefficients K found in the present study were lower than studies of daily mean water temperatures, showing less exchange of energy at an hourly scale.

The thermal exchange coefficient K was assumed constant throughout the year in the equilibrium temperature model. In order to evaluate the relationship between K and the time of year, the thermal exchange coefficient K was calibrated for each individual month at both studied streams (Table 5.1). The months of May, September and October had a coefficient K closest to the coefficient K value calibrated annually (2.7 and $13.1 \text{ W m}^{-2} \text{ }^{\circ}\text{C}^{-1}$). From June to August, values of K were higher, reflecting a better heat exchange during the highest air and water temperatures usually observed in summer. The month of April had values significantly lower than other months at Cat Bk ($0.74 \text{ W m}^{-2} \text{ }^{\circ}\text{C}^{-1}$) and LSWM ($5.2 \text{ W m}^{-2} \text{ }^{\circ}\text{C}^{-1}$). The equilibrium temperature model had the poorest performance in spring at both study streams. These results showed poorer heat exchange (low value of K) and modeling performance this time of year, as a result of poorer relationship between air and water temperatures, due to snowmelt conditions leading to higher water levels.

A regression analysis was fitted between the thermal exchange coefficient K (annual) and meteorological parameters: Air temperature ($^{\circ}\text{C}$), water temperature ($^{\circ}\text{C}$), incoming solar radiation (W m^{-2}), water level (m), relative humidity (%), and wind speed (m s^{-1}). The coefficient of regression (R^2) for each relation is presented in Table 5.2. Relative humidity did not show any significant relationship ($p > 0.650$) with the thermal exchange

Table 5.1. The values of the thermal exchange coefficient (K) calibrated for each month (April to October) at both Catamaran Brook (Cat Bk) and Little Southwest Miramichi (LSWM).

Month	Catamaran Brook	Little Southwest Miramichi
	K ($W\ m^{-2}\ ^\circ C^{-1}$)	K ($W\ m^{-2}\ ^\circ C^{-1}$)
April	0.74	5.2
May	2.84	9.0
June	6.62	21.0
July	5.83	31.8
August	3.98	25.6
September	2.81	12.2
October	2.60	12.7

coefficient K ($R^2 < 0.0041$). Wind speed was not significantly ($p < 0.022$) related to the thermal exchange coefficient with values of R^2 lower than 0.09 at both streams. The R^2 between the incoming solar radiation and thermal exchange coefficient was not significant at LSWM ($R^2 = 0.07$; $p > 0.051$), however, was more significant at Cat Bk ($R^2 = 0.15$; $p < 0.002$), since it is a small sheltered stream. Water level had a significant relationship ($p < 0.005$) to K with R^2 of 0.12 and 0.19 at both Cat Bk and LSWM. The thermal exchange coefficient K was significantly ($p < 0.001$) related to two parameters: Air and water temperatures. The R^2 values ranged from 0.32 to 0.35 between these parameters.

The $RMSE$ obtained with the equilibrium temperature model were similar or slightly higher than those observed in other studies, with $RMSE$ values of 1.52 °C (Cat Bk) and 1.98 °C (LSWM). Most equilibrium temperature models were developed to estimate daily temperatures. The modified equilibrium temperature model developed in Herb and Stefan (2011) estimated daily average stream temperatures with a $RMSE$ of 1.2 °C for a small tributary and of 1.4 °C for a larger stream.

Table 5.2. Coefficient of determination (R^2) of the regression analysis between the thermal exchange coefficient (K) and selected meteorological parameters (air temperature ($^{\circ}\text{C}$), water temperature ($^{\circ}\text{C}$), incoming solar radiation (W m^{-2}), water level (m), relative humidity (%), and wind speed (m s^{-1})) at Catamaran Brook (Cat Bk) and Little Southwest Miramichi (LSWM).

	Cat Bk R^2	LSWM R^2
Air temperature ($^{\circ}\text{C}$)	0.33	0.32
Water temperature ($^{\circ}\text{C}$)	0.35	0.33
Water level (m)	0.12	0.19
Incoming solar radiation (W m^{-2})	0.15	0.07
Wind speed (m s^{-1})	0.07	0.09
Relative humidity (%)	0.00	0.00

Marcé and Armengol (2008) found a similar *RMSE* for Cat Bk, around 1.40°C . Larnier *et al.* (2010) calculated *RMSEs* of 1.22°C (calibration) and 1.31°C (validation) between daily observed and predicted water. Caissie *et al.* (2005) applied the same equilibrium temperature model as in the present study on both Cat Bk and LSWM, but at the daily scale, and showed lower *RMSEs* (1.21°C = Cat Bk; 1.52°C = LSWM).

A seasonal analysis was performed at both Cat Bk and LSWM over the entire study period for three seasons: Spring (April 15 to June 20), summer (June 21 to September 20) and autumn (September 21 to October 31). This analysis showed that the best performance of the equilibrium temperature model was during autumn and the poorest performance was in spring, results found in most temperature modeling studies (Caissie *et al.*, 1998, 2005; Chenard and Caissie, 2008). Spring showed less efficient energy exchange probably caused by the snowmelt. Other studies have shown that snowmelt in spring can influence the relationship between air and water temperatures (Webb and Nobilis 1997). Autumn showed better predictions of water temperatures, presumably due

to lower water levels usually observed during that time of year and a better heat exchange (relation) between air and water temperatures.

Predicted hourly water temperatures were used to estimate daily mean water temperatures (T_{mean}) (Table 5.3). The performance of the daily mean water temperatures (T_{mean}) was better than the hourly water temperatures. The *RMSE* for all years was 1.20 °C for Cat Bk and 1.54 °C for LSWM. The coefficient of determination R^2 was varied between 0.937 and 0.949 at both study streams. The biases for daily mean temperatures were also lower than at an hourly scale, with values less than -0.29 °C. These results were also comparable to other equilibrium temperature results estimating daily water temperatures. In fact, estimating daily water temperatures using predicted hourly water temperatures gave similar results than the model directly estimating daily water temperatures (Caissie *et al.*, 2005).

Daily maximum water temperatures have been shown to have an important influences on biological conditions (Beschta *et al.*, 1987; Breau *et al.*, 2007). The predicted hourly water temperatures were also used to calculate the daily maximum water temperatures (T_{max}) (Table 5.3). The equilibrium temperature model gave a *RMSE* (all years) of 1.98 °C for Cat Bk and 2.26 °C for LSWM. The coefficient of determination was between 0.909 and 0.935 and biases were between -1.16 °C and -1.34 °C at both Cat Bk and LSWM. The equilibrium temperature model did not effectively estimate the daily maximum water temperatures. Evaporative cooling has been shown to affect the relationship between air and stream temperatures at high temperatures. For example, Erickson and Stefan (2000) stated that the relationship between air and stream

temperature differed from linearity at air temperatures over 25 °C, where water temperature does not increase at the same rate as air temperature. Mohseni and Stefan (1999) set that limit at 20 °C.

Table 5.3. Results of the estimation of the daily mean (T_{mean}) and the daily maximum stream temperature (T_{max}) calculated from the predicted hourly water temperatures (equilibrium temperature model) at Catamaran Brook and Little Southwest Miramichi.

Tw	Period	Catamaran Brook			Little Southwest Miramichi		
		RMSE	R ²	Bias	RMSE	R ²	Bias
Daily mean T _{mean} (°C)	Calibration (1998-2002)	1.16	0.949	-0.01	1.44	0.949	-0.03
	Validation (2003-2007)	1.25	0.940	-0.29	1.64	0.924	-0.15
	All years (1998-2007)	1.20	0.943	-0.15	1.54	0.937	-0.09
Daily maximum T _{max} (°C)	Calibration (1998-2002)	1.91	0.926	-1.16	2.17	0.935	-1.21
	Validation (2003-2007)	2.05	0.920	-1.34	2.35	0.909	-1.17
	All years (1998-2007)	1.98	0.921	-1.25	2.26	0.923	-1.19

A comparison of observed versus predicted daily mean (T_{mean}) and maximum (T_{max}) water temperatures was carried out for both Cat Bk and LSWM (Figure 5.1). Significant agreement was observed between predicted and observed daily maximums with R^2 of 0.921 (Cat Bk) and 0.923 (LSWM). Higher agreement between predicted and observed daily mean water temperatures with R^2 of 0.943 (Cat Bk) and 0.937 (LSWM) was observed.

The equilibrium temperature models have shown poorer performance at an hourly time scale compared to studies of daily mean stream temperatures. The relationship between

air and stream temperature can be affected by many factors, such as wind sheltering, stream shading, ground-water inputs or artificial heat inputs (Erickson and Stefan, 2000). Significant deviation of the relationship between air and water temperatures is evident for hourly temperatures; however, other studies have shown that as the time scale increases (e.g., daily, weekly) the relationship is better (Webb *et al.*, 2003). Time lag is also known to affect the air/stream relationship, especially at an hourly scale, and for shallow streams (Erickson and Stefan, 2000). Time lag is the time delay of the impact of air temperature on stream temperatures and can be from a few hours to a few days, and is reported to be directly proportional to the average stream depth (Stefan and Preud'homme, 1993).

5.3 ARTIFICIAL NEURAL NETWORK MODEL

The present study developed an artificial neural network (ANN) model to estimate hourly river water temperatures from the available hydrological and meteorological data. Hourly water temperature models are not as common as mean daily temperature models, but they have the advantage of predicting the diel variability in water temperature. This variability can, in many cases, be more important for aquatic resources than average temperature. For instance, during periods of high water temperatures, it is important to predict both maximum and minimum temperatures in order to assess the stress and subsequent recovery periods of aquatic resources, such as salmonids (Breau *et al.*, 2007). The ANN model was applied to two thermally different streams: Catamaran Brook (Cat Bk) and Little Southwest Miramichi (LSWM). Previous studies have shown that ANN models were good models for the prediction of mean daily river water temperatures (Bélanger *et al.*, 2005; Karaçor *et al.*, 2007; Chenard and Caissie, 2008). However, few studies have

used ANN models for predicting hourly river water temperatures, one being Risley *et al.* (2003).

The developed ANN model used the hourly air temperature of the present (°C) and previous days (°C), daily water level (m), mean daily water temperature (°C) (predicted from a previous ANN model), time of year (day) and time of day (hour). This study showed that ANN models were good for the prediction of hourly river water temperatures, with overall *RMSE* of 0.94 °C (Cat Bk) and 1.23 °C (LSWM) and R^2 of 0.967 (Cat Bk) and 0.962 (LSWM), as referred to in Table 4.8. The ANN model generally underestimated the water temperatures at Cat Bk with a bias of -0.13 °C and a very small bias at LSWM (0.02 °C). No data are available from the literature to compare ANN models to stochastic models. However, these models may be expected to show similar results (performances).

The ANN modeling results were compared with those of previous studies that predicted daily mean water temperatures. The modeling of hourly stream water temperatures was found to be as good as the modeling of daily mean stream water temperatures. For example, Chenard and Caissie (2008) modeled daily mean stream temperatures in Catamaran Brook using an ANN and they achieved similar results with overall *RMSE* of 0.96 °C and R^2 of 0.971. Bélanger *et al.* (2005) calculated an overall *RMSE* of 1.06 °C when applying an ANN model at Catamaran Brook for daily mean temperatures. The study by Bélanger *et al.* (2005) used only air temperatures and water levels as input parameters. Karacol *et al.* (2007) used only past stream temperature data to predict maximum stream temperatures of the five days ahead. They achieved results with

average prediction error of less than 1 °C. Risley *et al.* (2003) developed an ANN model for 148 sites in western Oregon to predict hourly water temperatures from June 21 to September 20, 1999. Three different ANN models were developed to estimate hourly water temperatures along 1st, 2nd, and 3rd order streams using meteorological data, including air temperature, dew-point temperature, short-wave solar radiation, air pressure, and precipitation, as well as riparian habitat characteristics which included stream bearing, gradients, depth, substrate, wetted widths, and canopy cover, and basin topographical and vegetative landscape characteristics, acquired from a geographic information system (GIS). Their results showed *RMSE* ranging between 0.05 °C and 0.59 °C and with R^2 ranging from 0.88 to 0.99.

The results of the present ANN model were comparable to and/or better than those of deterministic and stochastic models. Marceau *et al.* (1986) developed both deterministic and stochastic models of daily water temperature with higher *RMSEs*. For instance, their models showed an overall *RMSE* of 1.86 °C for the stochastic model and an overall *RMSE* of 2.30 °C for the deterministic model. The present study results compared well with studies applied at both Cat Bk and LSWM, using stochastic and temperature equilibrium models. At Cat Bk, a stochastic model estimating daily mean stream temperatures (Caissie *et al.*, 1998) showed a higher *RMSE* of 1.26 °C. The equilibrium temperature model (Caissie *et al.*, 2005) developed for both Cat Bk and LSWM also showed slightly poorer performance than the ANN model developed in this study. They showed *RMSEs* of 1.21 °C and 1.52 °C for Cat Bk and LSWM, respectively.

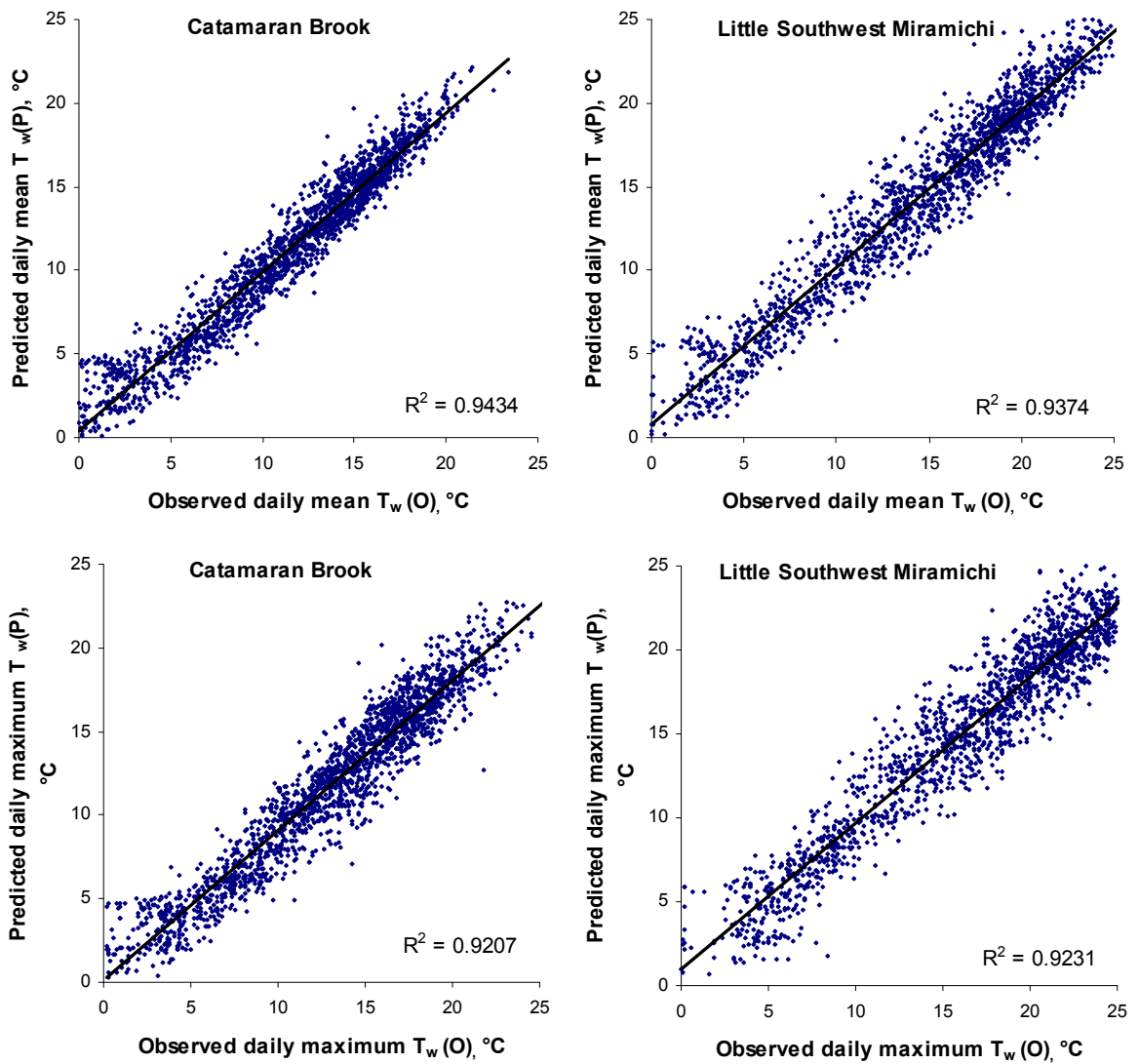


Figure 5.1. Predicted ($T_{\text{mean}}(P)$) versus observed daily mean water temperatures ($T_{\text{mean}}(O)$) and predicted ($T_{\text{max}}(P)$) versus observed daily maximum water temperatures ($T_{\text{max}}(O)$) at Catamaran Brook and Little Southwest Miramichi, using the equilibrium temperature model.

The predicted hourly water temperatures from the ANN model were used to estimate the daily mean and maximum water temperatures and are shown in Table 5.4. The daily mean water temperatures estimated from the training period showed very low *RMSE* for both Cat Bk (0.24 °C) and LSWM (0.39 °C). The *RMSEs* for the daily mean water temperatures were slightly better than the ones calculated with hourly water temperatures using ANN model for the validation period. The *RMSEs* were of 1.04 °C at Cat Bk and 1.10 °C at LSWM. The *RMSEs* estimated for daily mean water temperatures over all years were lower than those of similar studies discussed previously (Bélanger *et al.*, 2005; Chenard *et al.*, 2008) with values of 0.74 °C at Cat Bk and 0.82 °C at LSWM. The predicted hourly water temperatures from the ANN model were also used to estimate the daily maximum water temperatures in Table 5.4, as maximum water temperatures have been shown by Lund *et al.* (2002) to be important for aquatic resources. The *RMSEs* were of 1.04 °C and 1.09 °C for the predicted daily maximum water temperatures, at Cat Bk and LSWM, respectively. A comparison of observed versus predicted daily mean (T_{mean}) and maximum (T_{max}) water temperatures was carried out for both Cat Bk and LSWM and is shown in Figure 5.2. Results showed notable agreement for the daily maximum with R^2 of 0.979 (Cat Bk) and 0.982 (LSWM) and a slightly better agreement for the daily mean water temperatures with R^2 of 0.964 (Cat Bk) and 0.975 (LSWM). These results showed that hourly water temperatures developed with the ANN model could be used to improve the prediction of daily mean and maximum water temperatures.

A comparison of seasonal performance showed that the ANN model performed best in summer and autumn, which is consistent with other temperature models (Caissie *et al.*, 1998, 2005; Chenard and Caissie, 2008). High water levels seemed to have had an

important influence on the modeling of water temperatures using the ANN model, mostly when water levels experienced important increase following storm events or during the spring high flows. The poorer performance in spring could be explained by the higher discharge from snowmelt, resulting in a poorer air to water temperature relationship (Caissie *et al.*, 1998). As high water levels seemed to have resulted in a poorer performance, low water levels (usually observed in autumn and mid-summer) have resulted in more effective thermal exchange and therefore better performances.

Table 5.4. Results of the estimation of the daily mean (T_{mean}) and the daily maximum stream temperature (T_{max}) calculated from the predicted hourly water temperatures (artificial neural network model) at Catamaran Brook and Little Southwest Miramichi.

		Catamaran Brook			Little Southwest Miramichi		
	Period	RMSE	R ²	Bias	RMSE	R ²	Bias
Daily mean T_{mean} (°C)	Calibration (1998-2002)	0.24	0.998	0.00	0.39	0.998	0.00
	Validation (2003-2007)	1.04	0.959	-0.28	1.10	0.983	0.05
	All years (1998-2007)	0.74	0.979	-0.13	0.82	0.991	0.03
Daily maximum T_{max} (°C)	Calibration (1998-2002)	0.69	0.985	-0.16	0.75	0.995	-0.24
	Validation (2003-2007)	1.31	0.943	-0.37	1.36	0.979	0.02
	All years (1998-2007)	1.04	0.966	-0.26	1.09	0.979	-0.12

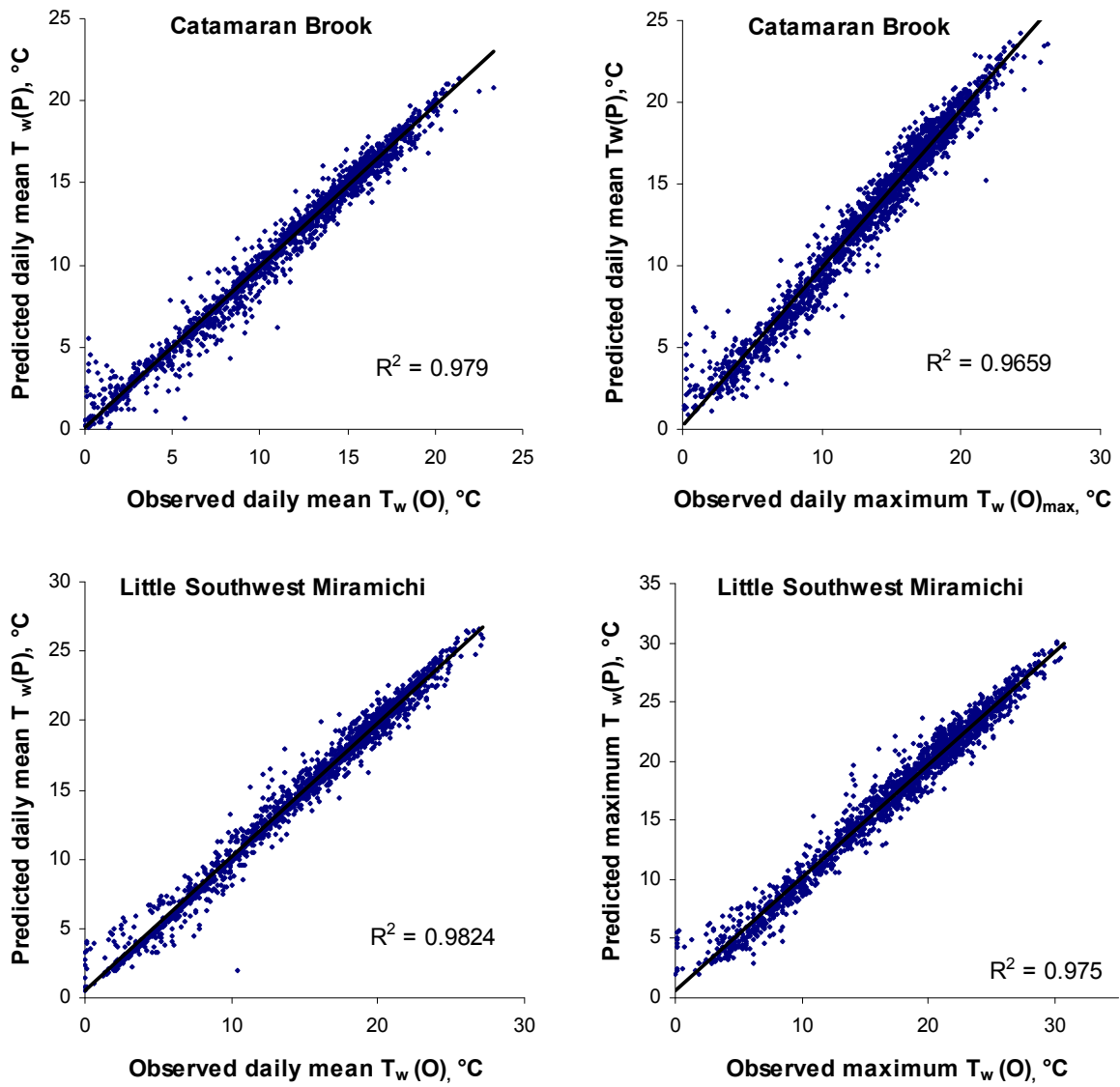


Figure 5.2. Predicted ($T_{mean}(P)$) versus observed daily mean water temperatures ($T_{mean}(O)$) and predicted ($T_{max}(P)$) versus observed daily maximum water temperatures ($T_{max}(O)$) at Catamaran Brook and Little Southwest Miramichi, using the artificial neural network model.

At LSWM, the ANN model performed best in autumn for all years, whereas at Cat Bk, some years had their best performance during summer. These results suggest that the thermal exchange is more efficient for less sheltered rivers under low flows as in autumn at LSWM. Cat Bk is more sheltered and could potentially be influenced by other factors, such as groundwater, reducing the efficiency of the thermal exchange. For example, results of the deterministic model in Section 4.1, showed that the impact of groundwater on hourly water temperatures was more significant on smaller streams, such as Cat Bk.

The training period showed better results than the validation period, which is consistent in modeling. Daily water levels were used in the modeling rather than hourly temperatures and were estimated using power functions (Caissie, 2004). Using hourly water levels instead of daily water levels could have potentially improved the modeling, especially during days that discharge varied significantly. However, hourly water levels were not available for the present study.

Good modeling results were obtained using ANN models with few input parameters. As such, the advantage of ANNs lies in their capability as a universal approximation tool, as well as in their simplicity in model development and model update capability. ANN models have an advantage over more commonly used water temperature models, as they do not need a lot of input data. In the present study, only air temperature and water level were used to achieve accurate predictions. For instance, deterministic models need many hydrological and meteorological parameters that are not always readily available, such as solar radiation. Another major advantage of ANNs is that they are easy to use and very simple in their application. However, ANN models cannot give a physical explanation of

the relationship between the input and output data. These models should be used with caution, especially when using input data that are outside the range of the calibration period, because the model may not be trained for such conditions (Risley *et al.*, 2003).

5.4 COMPARISON OF WATER TEMPERATURE MODELS

Three water temperature models were developed and applied on two thermally different watercourses (Cat Bk and LSWM) to estimate hourly water temperatures: A deterministic model, an equilibrium temperature model, and an artificial neural network model. The results showed that all models were effective in predicting hourly water temperatures at both Cat Bk and LSWM. In the present study, the deterministic models outperformed the other two models; however, it was only developed for the year 2007, due to the availability of microclimate and streambed temperature data. The *RMSEs* for the 6 study periods (year 2007) was between 0.18 °C and 0.33 °C at Cat Bk and between 0.14 °C and 0.23 °C at LSWM. The two other models, equilibrium temperature and ANN, were developed for the years 1998-2007. The *RMSEs* for the ANN model were also low with values between 0.53 °C and 1.40 °C at Cat Bk and between 0.55 °C and 1.91 °C at LSWM, when comparing among years (1998-2007). The equilibrium temperature model had the poorest performance of all 3 models with *RMSEs* values of between 1.35 °C and 1.63 °C at Cat Bk and between 1.60 °C and 2.28 °C at LSWM (1998-2007).

The selection of a particular water temperature model by engineers and scientists will ultimately depend on the type of problems under investigation and most likely data availability. For instance, Table 5.5 outlines major differences between models considered within the present study and other common models. ANN and equilibrium

temperature models are generally low in data requirement while deterministic models require a whole suite of input parameters that may not always be readily available including solar radiation and streambed fluxes. As such, ANN and equilibrium temperature models are better adapted for extending water temperature time series under natural conditions and they can be applied in areas where data are limited. However, when dealing with impact studies where the energy components are important, such as the increase in solar radiation input due to streamside vegetation removal as in forestry impact studies, then deterministic models are better adapted for these analyses. The equilibrium temperature model does not require a lot of input data (only air temperature and water level in this study) and provides an advantage over other models. For example, by using only air temperatures, stochastic models are based on statistical relationships rather than modeling underlying physical processes.. Deterministic models performed best in this study, however this modeling approach requires an extensive list of inputs data, some not readily available, such as solar radiation and streambed temperatures, resulting in a high cost in development and application. Their main advantage is their possibility to extract pertinent information about the different physical processes that influences the thermal regime of rivers as with environmental impact studies.

Table 5.5. Comparison of advantages, disadvantages and data requirement of the three different types of water temperature models.

Water temperature models	Advantages	Disadvantages
Deterministic model	<ul style="list-style-type: none"> - Adapted to impact studies - Quantification of energy Components - Conceptual model 	<ul style="list-style-type: none"> - Numerous input parameters - Costly in development and application - High data requirements
Equilibrium temperature model	<ul style="list-style-type: none"> - Simple model - Few input parameters - Conceptual model - Low data requirements 	<ul style="list-style-type: none"> - Semi-empirical - Not well adapted to impact studies
Artificial neural network model	<ul style="list-style-type: none"> - Simple in application - Few input parameters - No need to know the relationship between the input and output - Low data requirements 	<ul style="list-style-type: none"> - No physical explanation of the underlying process - Applied with caution outside the calibration range
Stochastic model	<ul style="list-style-type: none"> - Simple in application - Low input requirement (usually only air temperature) 	<ul style="list-style-type: none"> - Not well adapted to environmental impact studies - Based on statistics relations rather than the physical processes

CHAPTER 6: CONCLUSION

6.1 CONCLUSION

Water temperature is an important component for water quality and biotic condition in rivers. Among other things, water temperature controls the rate of decomposition of organic matter, the dissolved oxygen content, and chemical reactions in general. The thermal regime of a river influences many aspects of fish habitat, life condition, and the distribution of aquatic species. It is therefore important to develop adequate stream temperature models to effectively manage water and fisheries resources.

This study dealt with the modeling of river water temperatures using a deterministic model, an equilibrium temperature model, and an artificial neural network model. The water temperature models were applied on two watercourses of different sizes and thermal characteristics, but within a similar meteorological region, namely, the Little Southwest Miramichi River and Catamaran Brook (New Brunswick, Canada).

The deterministic model showed the importance and the role of microclimate data to better estimate surface heat fluxes as well as the importance of the streambed flux contribution in the overall heat budget model. Results showed that for larger river systems surface heat fluxes are a dominant component of the heat budget with a correspondingly smaller contribution from the streambed. However, as watercourses become smaller and as groundwater contribution becomes more significant, the streambed contribution becomes an important component in the overall heat budget.

With the exception of Period 1, predicted fluxes from the deterministic model showed significant agreement with observed values. As such, deterministic models remain an effective tool in predicting the different heat flux components, which will ultimately contribute toward a better understanding of river thermal regimes.

Deterministic models have been shown to be very effective in estimating stream temperatures, but require a lot of data that are not available in most rivers. The equilibrium temperature model uses less input data, as the net surface heat flux can be expressed as a simpler equation. They also have an advantage over stochastic levels, since they use water level as an input, not relying on modelling for air temperature only. The equilibrium temperature model showed good performance, although slightly higher than other models with *RMSE* of 1.52°C and 1.98°C for both streams. These results suggest that the air and equilibrium temperature did not totally reflect the net surface heat flux at hourly time scales. Another component that may not have been captured by this model is the streambed contribution. Values higher than 1 for the coefficient α reflects rivers more exposed to other meteorological conditions, like solar radiation. At Cat Bk the coefficient α was of 0.87, reflecting a more sheltered stream, whereas at LSWM the coefficient was of 1.08, since it is more exposed to other meteorological parameters. The model's best performance was in autumn, during low water levels which presumably permitted a more efficient thermal exchange. In contrast, the spring resulted in poorer performance where the presence of snowmelt may have contributed to a lack of association between water and air temperature.

This study showed that an artificial neural network (ANN) could be an effective tool for the prediction of hourly stream temperatures. ANN models achieved comparable or better performances to other water temperature models reported in the literature, with *RMSE* of 0.94 °C at Cat Bk and 1.23 °C at LSWM. ANN models showed a good generalization capability by modeling well water temperature time-series. ANN was effectively applied on two thermally different streams and provides similar results and performances. As such, ANN models can be considered as an effective modeling tool in water resources and fisheries management.

6.2 RECOMMENDATIONS

In most water temperature studies, meteorological data are taken at the nearest meteorological station (usually the nearest airport) sometimes a few kilometres away. The deterministic model in this study examined different meteorological data (air temperature, relative humidity, wind speed, and incoming solar radiation) measured directly on both Cat Bk and LSWM (microclimate), as well as data coming from the nearest meteorological station (remote), which is usually used to describe both study sites. This comparison between microclimate and remote meteorological data was only available for the year 2007 (deterministic model), since microclimate data were not available for other years (1998-2007) used in the equilibrium temperature and ANN models. The most significant differences between remote and microclimate data were the solar radiation and the wind speed, which are primarily drivers of radiation, evaporative and convective heat fluxes. Using remote station data would not truly reflect the total heat flux at a stream, especially for smaller streams (Brown, 1969; Johnson, 2003; Johnson, 2004). Microclimate data provides a better fit to predict water temperatures due

to a better estimation of heat fluxes and a better reflection of site conditions (Benyahya *et al.*, 2010). This spatial variability needs to be taken into account in future studies dealing with the modeling of water temperatures. In order to truly estimate the energy exchange of streams, microclimate data should be used when available.

Most studies have only considered the longwave radiation emitted by the atmosphere and the water (Morin and Couillard, 1990; Sinokrot and Stefan, 1993; Caissie *et al.*, 2007). Few studies have considered the longwave radiation emitted by the forest canopy (Rutherford *et al.*, 1997; Sing and Singh, 2001; Benyahya *et al.*, 2010) in water temperature modeling. The contribution of the forest radiation can be significant especially for small streams (Benyahya *et al.*, 2010). It also plays an important role on cloudless nights by increasing stream temperatures (Rutherford *et al.*, 1997). This study considered the forest radiation by using a forest cover factor and assuming forest air temperature as the ambient air temperature. However, more studies should include the longwave radiation emitted by the forest in streams to effectively predict the heat budget, since the longwave radiation is a major source of energy loss in most streams.

Most water temperature models have neglected the contribution of the streambed, but this study and others have shown it can be an important part of the heat budget, especially for small streams (Jobson, 1977; Jobson and Keefer, 1979; Sinokrot and Stefan, 1993; Moore *et al.*, 2005). Better prediction of the overall heat budget will improve the modeling of water temperatures. The contribution of the streambed should be included in the estimation of energy budget, since it can contribute up to 20% of the total heat budget. Further work is needed to accurately quantify the impact of streambed in water

temperature modeling. To address this lack of knowledge of the streambed contribution to stream thermal regime, good databases need to be developed on streambed and groundwater temperatures, since these data are often not available but are required in the modeling.

Most water temperature studies have neglected the role of the precipitation heat flux. The deterministic model included the precipitation heat flux, according to the amount of rain (mm) and its temperature assumed to be equal to the air temperature. The precipitation heat flux only represented up to 1.2 % of the overall energy budget. Clearly, it did not represent the cooling effect during important rainfall events. The estimation of the precipitation heat fluxes should not only include precipitation directly falling on the river, but also include the contribution of other advective heat flux coming from surface and near-subsurface hillslope pathways and groundwater (Brown and Hannah, 2007). The amount of heat added by precipitation is also dependent on the intensity and the duration of the storm event (Herb *et al.*, 2008). Further work is needed on the impact of precipitation events on the stream temperature dynamics.

The water temperature models developed in this study generally experienced their poorest performance in spring, due to high water level caused by the snowmelt conditions. The ANN model, even with good overall prediction of water temperatures, was somewhat sensitive to high water levels. The equilibrium temperature model has also shown less effective thermal exchange during spring high water levels. The thermal regimes of rivers under snowmelt conditions are poorly understood and further investigations are required. Further research should address water temperatures and the thermal regime

during spring snowmelt conditions, to improve the modelling of stream temperatures. Research should address the importance of the different energy components during that time of year.

REFERENCES

- Acronley RM. (1999). Water temperatures within spawning beds in two chalk streams and implications for salmonid egg development. *Hydrological Processes* 13: 439-446.
- Ahmadi-Nedushan B, St-Hilaire A, Ouarda TBML, Bilodeau L, Robichaud E, Thiémonge N, Bobée B. (2007). Predicting river water temperature using stochastic models: case study of the Moisie River (Québec, Canada). *Hydrological Processes* 21(1): 21-34.
- Alderdice DF, Velsen FPJ. (1978). Relation between temperature and incubation time for eggs of Chinook salmon (*Oncorhynchus tshawytscha*). *Journal of the Fisheries Research Board of Canada* 35: 69-75.
- Allen RG. (1997). Self-calibrating method for estimating solar radiation from air temperature. *Journal of Hydrologic Engineering* 2(2): 56-67.
- Andersen ME, Jobson HE. (1982). Comparison of techniques for estimating annual lake evaporation using climatological data. *Water Resources Research* 18(3): 630-636.
- Arscott DB, Tockner K, Ward JV. (2001). Thermal heterogeneity along a braided floodplain river (Tagliamento River, northeastern Italy). *Canadian Journal of Fisheries and Aquatic Sciences* 58: 2359-2373.
- Baltz DM, Vondracek B, Brown LR, Moyle PB. (1987). Influence of temperature on microhabitat choice by fishes in a California stream. *Transactions of the American Fisheries Society* 116: 12-20.

- Bartholow JM. (1991). A modeling assessment of the thermal regime for an urban sport Fishery. *Environmental Management* 15(6): 833-845.
- Beer WN, Anderson JJ. (2001). Effect of spawning day and temperature on salmon emergence: interpretations of a growth model for Methow River chinook. *Canadian Journal of Fisheries and Aquatic Sciences* 58:943-949.
- Beitinger TL, Bennett WA. (2000). Quantification of the role of acclimation temperature in temperature tolerance of fishes. *Environmental Biology of Fishes* 58: 277-288.
- Bélangier M, El-Jabi N, Caissie D, Ashkar F, and Ribí JM. (2005). Estimation de la température de l'eau en rivière en utilisant les réseaux de neurones et la régression multiple. *Revue des Sciences de l'Eau* 18(3): 403-421.
- Benyaya L, St-Hilaire A, Ouarda TBMJ, Bobée B, Ahmadi-Nedushan. (2007). Modeling of water temperatures based on stochastic approaches: case study of the Deschutes River. *Journal of Environmental Engineering Sciences* 6: 437-448.
- Benyahya L, St-Hilaire A, Ouarda TBMJ, Bobée B, Dumas Jacques. (2008). Comparison of non-parametric and parametric water temperature models on the Nivelle River, France. *Hydrological Sciences* 53(3): 640-655.
- Benyahya L, Caissie B, El-Jabi N, Satish MG. (2010). Comparison of microclimate vs. remote meteorological data and results applied to a water temperature model (Miramichi River, Canada). *Journal of Hydrology* 380: 247-259.
- Beschta RL, Bilby RE, Brown GW, Holtby LB, Hofstra TD. (1987). Stream Salo and T.W. Cundy [ed.], Streamside management: Forestry and fishery interactions. University of Washington, Institute of Forest Resources, Contribution No. 57, pp.191-232.

- Beschta RL, Taylor RL. (1988). Stream temperature increases and land use in a forested Oregon watershed. *Water Resources Bulletin* 24 (1): 19-25.
- Beschta RL. (1997). Riparian shade and stream temperature: an alternative perspective. *Rangelands* 19: 25-28.
- Bhattacharya B, Lobbrecht AH, Solomatine DP. (2003). Neural networks and reinforcement learning in control of water systems. *Journal of Water Resources Planning and Management* 129(6): 458-465.
- Bogan T, Mohseni O, Stefan HG. (2003). Stream temperature-equilibrium temperature relationship. *Water Resources Research* 39(9): 1-12.
- Bogan T, Stefan HG, Mohseni O. (2004). Imprints of secondary heat sources on the stream temperature/equilibrium temperature relationship. *Water Resources Research* 40: W12510.
- Bogan T, Othmer J, Mohseni O, Stefan H. (2006). Estimating extreme stream temperatures by the standard deviate method. *Journal of Hydrology* 317: 173-189.
- Bolsenga SJ. (1975). Estimating energy budget components to determine Lake Huron evaporation. *Water Resources Research* 11(5): 661-666.
- Bourque CPA, Pomeroy JH. (2001). Effects of forest harvesting on summer stream temperatures in New Brunswick, Canada: an inter-catchment, multiple-year comparison. *Hydrology and Earth System Sciences* 5(4): 599-613.
- Bowden GJ, Dandy GC, Maier HR. (2005a). Input determination for neural network models in water resources applications. Part1 – background and methodology. *Journal of Hydrology* 301: 75-92.

- Bowden GJ, Maier HR, Dandy GC. (2005b). Input determination for neural network models in water resources applications. Part2. Case study: forecasting salinity in a river. *Journal of Hydrology* 301: 93-107.
- Bowen IS. (1926). The ratio of heat losses by conduction and by evaporation for any water surface. *Phys. Rev.* 27: 316-355.
- Bradley AA, Holly FM, Walker WK, Wright SA. (1998). *Journal of the American Water Association* 34(3): 467-480.
- Breau C, Cunjak RA, Bremset G. (2007). Age-specific aggregation of wild juvenile Atlantic salmon *Salmo salar* at cool water sources during high temperature events. *Journal of Fish Biology*: 71: 1179-1191.
- Brosofske KD, Chen J, Naiman RJ, Franklin JF. (1997). Harvesting effects on microclimatic gradients from small streams to uplands in Western Washington. *Ecological Applications* 7(14): 1188-1200.
- Brown GW, Krygier JT. (1967). Changing water temperatures in small mountain streams. *Journal of Soil and Water Conservation* 22: 242-244.
- Brown GW. (1969). Predicting temperatures of small streams. *Water Resources Research* 5(1): 68-75.
- Brown GW. (1970). Predicting the effect of clear-cutclear-cutting on stream temperature. *Journal of Soil and Water Conservation*, Jan-Feb: 11-13.
- Brown GW, Krygier JT. (1970). Effects of clear-cutting on stream temperature. *Water Resources Research* 6 (4):1133-1139.
- Brown LE, Hannah DM. (2007). Alpine stream temperature response to storm events. *Journal of Hydrometeorology* 8:952-967.

- Brown Le, Hannah DM. (2008). Spatial heterogeneity of water temperature across an alpine river basin. *Hydrological Processes* 22: 954-967.
- Brown LE, Hannah DM, Milner AM. (2005). Spatial and temporal water column and streambed temperature dynamics within an alpine catchment: implications for benthic communities. *Hydrological Processes* 19: 1585-1610.
- Brown LE, Hannah DM, Milner AM. (2006). Hydroclimatological influences on water column and streambed thermal dynamics in an alpine river system. *Journal of Hydrology* 325: 1-20.
- Burton TM, Likens GE. (1973). The effects of stripe cutting on stream temperatures in the Hubbard Brook Experimental Forest, New Hampshire. *BioScience* 23: 433-435.
- Cadbury SL, Hannah DM, Milner AM, Pearson CP, Brown LE. (2008). Stream temperature dynamics within a New Zealand glacierized river basin. *River Research and Applications* 24: 68-89.
- Caissie D, El-Jabi N. (1995). Hydrology of the Miramichi River drainage basin. In: Water, Science, and the Public: the Miramichi ecosystem, Chadwick EMP (ed.). *Canadian Special Publication of Fisheries and Aquatic Sciences* No. 123. NRC Research Press: Ottawa; 83-93.
- Caissie D, Satish MG. (2001). Modelling water temperatures at depths within the stream substrate of Catamaran Brook (NB): potential implication of climate change. *Canadian Technical Report of Fisheries and Aquatic Sciences* 2365: 27p.
- Caissie D, Pollock TL, Cunjak RA. (1996). Variation I stream water chemistry and hydrograph separation I a small drainage basin. *Journal of hydrology* 178: 137-157.

- Caissie D, El-Jabi N, St-Hilaire A. (1998). Stochastic modelling of water temperatures in a small stream using air to water relations. *Canadian Journal of Civil Engineering* 25: 250-260.
- Caissie D, Satish MG, El-Jabi N. (2005). Predicting river water temperatures using the equilibrium temperature concept method with applications on Miramichi River Catchments (New Brunswick, Canada). *Hydrological Processes* 19: 2137-2159.
- Caissie D. (2004). Stream temperature modeling in forest catchments. PhD Thesis, Dalhousie University, Halifax NS, 207p.
- Caissie D. (2006). The thermal regime of rivers: a review. *Freshwater Biology* 51: 1389-1406.
- Caissie D, El-Jabi N, Satish MG. (2001). Modelling of maximum daily water temperatures in a small stream using air temperatures. *Journal of Hydrology* 251: 14-28.
- Caissie D, Satish MG, El-Jabi N. (2007). Predicting water temperatures using a deterministic model: Application on Miramichi River catchments (New Brunswick, Canada). *Journal of Hydrology* 336(3-4): 303-315.
- Castellano-Méndez M, Gonzalez-Manteiga W, Febrero-Bande, Prada-Sanchez JM, Lozano-Calderon R. (2004). Modelling of the monthly and daily behaviour of the runoff of the Xallas river using Box-Jenkins and neural networks methods. *Journal of Hydrology* 296: 38-58.
- Chaudhry MH, Cass DE, Edinger JE. (1983). Modeling of unsteady-flow water temperatures. *Journal of Hydraulic Engineering* 109(5): 657-669.

- Chen J, Frankin JF, Spies TA. (1995). Growing-season microclimatic gradients from clear-cut edges into old-growth Douglas-fir forests. *Ecological Applications* 5 (1): 74-86.
- Chen YD, Carsel RF, McCutcheon SC, Nutter WL. (1998a). Stream temperature simulation of forested riparian areas: I. Watershed-scale model development. *Journal of Environmental Engineering* 124(4): 304-315.
- Chen YD, McCutcheon SC, Norton DJ, Nutter WL. (1998b). Stream temperature simulation of forested riparian areas: II. Model application. *Journal of Environmental Engineering* 124(4): 316-328.
- Chenard J, Caissie D. (2008). Stream temperature modelling using artificial neural networks: application on Catamaran Brook, New Brunswick, Canada. *Hydrological Processes* 22(17): 3361-3372.
- Clark E, Webb BW, Ladle M. (1999). Microthermal gradients and ecological implications in Dorset rivers. *Hydrological Processes* 13: 423-438.
- Cluis DA. (1972). Relationship between stream water temperature and ambient air temperature - a simple autoregressive model for mean daily stream temperature fluctuations. *Nordic Hydrology* 3: 1025-1031.
- Combs BD. (1965). Effect of temperature on the development of salmon eggs. *Prog. Fish-Cult.* 27: 134-137.
- Combs BD, Burrows RE. (1957). Threshold temperatures for the normal development of Chinook salmon eggs. *Prog. Fish-Cult.* 19: 3-6
- Comer LE, Grenney WJ. (1977). Heat transfer processes in the bed of a small stream. *Water Resources* 11: 743-744.

- Cooter EJ, Cooter WS. (1990). Impacts of greenhouse warming on water temperature and water quality in the southern United States. *Climate Research* 1: 1-12.
- Coutant CC. (1977). Compilation of temperature preference data. *Journal of the Fisheries Research Board of Canada* 34: 739-745.
- Coutant CC. (1999). Perspective on temperature in the Pacific Northwest's fresh water. Environmental Sciences Division, Publication No. 4849, Oak Ridge National Laboratory, ORNL-TM-1999-44, 109p.
- Cox TJ, Rutherford JC. (2000a). Thermal tolerances of two stream invertebrates exposed to diurnally varying temperature. *New Zealand Journal of Marine and Freshwater Research* 34: 203-208.
- Cox TJ, Rutherford JC. (2000b). Predicting the effects of time-varying temperatures on stream invertebrates mortality. *New Zealand Journal of Marine and Freshwater Research* 34: 209-215.
- Cox MM, Bolte JP. (2007). A spatially explicit network-based model for estimating stream temperature distribution. *Environmental Modelling and Software* 22: 502-514.
- Cozzetto K, McKnight D, Nylén T, Fountain A. (2006). Experimental investigations into processes controlling stream and hyporheic temperatures, Fryxell Basin, Antarctica. *Advances in Water Resources* 29: 130-153.
- Crisp DT. (1990). Water temperature in a stream gravel bed and implications for salmonid incubation. *Freshwater Biology* 23: 601-612.
- Crisp DT, Howson G. (1982). Effect of air temperature upon mean water temperature in streams in the north Pennines and English Lake District. *Freshwater Biology* 12: 359-367.

- Cunjak RA, Caissie D, El-Jabi N. (1990). The Catamaran Brook Habitat Research Project: description and general design of study. *Canadian Technical Report of Fisheries and Aquatic Sciences* 1751: 14p.
- Curry RA, Scruton DA, Clarke KD. (2002). The thermal regimes of brook trout incubation habitats and evidence of changes during forestry operations. *Canadian Journal of Forested Resources* 32: 1200-1207.
- Dake JMK. (1972). Evaporative cooling of a body of water. *Water Resources Research* 8 (4): 1087-1091.
- Daliakopoulos IN, Coulibaly P, Tsanis IK. (2005). Groundwater level forecasting using artificial neural networks. *Journal of Hydrology* 309: 229-240.
- Danehy RJ, Christopher GC, Parrett KB, Duke SD. (2005). Patterns and sources of thermal heterogeneity in small mountain streams within a forested setting. *Forest Ecology and Management* 208: 287-302.
- Davies-Colley RJ, Payne GW, Elswijk MV. (2000). Microclimate gradients across a forest edge. *New Zealand Journal of Ecology* 24(2): 111-121.
- Dawson CW, Wilby RL. (2001). Hydrological modelling using artificial neural networks. *Progress in Physical Geography* 25(1): 80-108.
- Dent L, Vick D, Abraham K, Schoenholtz S, Johnson S. (2008). Summer temperature patterns in headwater streams of the Oregon coast range. *Journal of the American Water Resources Association*: 44(4): 803-813.
- Dingman SL. (2002). Physical Hydrology. Prentice-Hall Inc. Upper Saddle, New Jersey, 646p.

- Dogliani A, Giustolisi O, Savic DA, Webb BW. (2008). An investigation on stream temperature analysis based on evolutionary computing. *Hydrological Processes* 22: 315-326.
- Dong J, Chen J, Brosofske KD, Naiman RJ. (1998). Modelling air temperature gradients across managed small streams in western Washington. *Journal of Environmental Management* 53: 309-321.
- Dorvlo ASS, Jervase JA, Al-Lawati A. (2002). Solar radiation estimation using artificial neural networks. *Applied Energy* 71: 307-319.
- Dreyfus G, Martinez JM, Samulides M, Gordon MB, Badran F, Thiria S, Hérault L. (2002). Réseaux de neurones: Méthodologie et applications. Éditions Eyrolles: Paris, France.
- Dymond J. (1984). Water temperature change caused by abstraction. **ASCE, Journal of Hydraulic Engineering** 110 (7): 987-991.
- Eater JG, Scheller RM. (1996). Effects of climate warming on fish thermal habitat in streams of the United States. *Limnology and Oceanography* 41(5): 1109-1115.
- Ebersole JL, Liss WJ, Frissell CA. (2001). Relationship between stream temperature, thermal refugia and rainbow trout *Oncorhynchus mykiss* abundance in arid-land streams in the northwestern United States. *Ecology of Freshwater Fish* 10(1): 1-10.
- Ebersole JL, William JL, Frissell CA. (2003). Cold water patches in warm streams: physicochemical characteristics and the influence of shading. *Journal of the American Water Resources Association* 39(2): 355-368.
- Edinger JE, Duttweiler DW, Geyer JC. (1968). The response of water temperatures to meteorological conditions. *Water Resources Research* 4(5): 1137-1143.

- Edwards RW, Densem JW, Russell PA. (1979). An assessment of the importance of temperatures as a factor controlling the growth rate of brown trout in streams. *The Journal of Animal Ecology* 48(2): 501-507.
- Elliott JM, Hurley MA. (1997). A functional model for maxima growth of Atlantic Salmon parr, *Salmo salar*, from two populations in Northwest England. *Functional Ecology* 11(5): 592-603.
- Erickson TR, Stefan HG. (2000). Linear air/water temperature correlations for streams during open water periods. *Journal of Hydrologic Engineering* 5(3): 317-321.
- Evans EC, Greenwood MT, Petts GT. (1995). Short communication thermal profiles within river beds. *Hydrological Processes* 9: 19-25.
- Evans EC, Mcgregor GR, Petts GE. (1998). River energy budgets with special reference to river bed processes. *Hydrological Processes* 12: 575-595.
- Feller MC. (1981). Effects of clear-cutclear-cutting and slash burning on stream chemistry in southwestern British Columbia. *Water Resources Bulletin* 17: 863-867.
- Finch JW, Gash JHC. (2002). Application of a simple finite difference model for estimating evaporation from open water. *Journal of Hydrology* 255: 253-259.
- Foreman MGG, Lee DK, Morrison J, MacDonald D, Barnes D, Williams DV. (2001). Simulation and retrospective analyses of Fraser watershed flows and temperatures. *Atmosphere-Oceans* 39(2): 89-105.
- Freeze RA. (1974). Stream flow generation. *Rev. Geophys. Space Sci.* 12, pp. 627-647.
- Gaffield SJ, Potter KW, Wang L. (2005). Predicting the summer temperature of small streams in southwestern Wisconsin. *Journal of the American Water Resources Association* 41(1): 25-36.

- Garside ET. (1969). The upper lethal temperature and thermal resistance of parr of Atlantic salmon (*Salmo salar* L) in Terra Nova National Park, Newfoundland. Canadian Wildlife Service, Ottawa, Canada, 10p.
- Garside ET. (1973). Ultimate upper lethal temperature of Atlantic salmon (*Salmo salar* L.). *Canadian Journal of Zoology* 51: 898-900.
- Gomi T, Moore DR, Dhakal AS. (2006). Stream temperature response to clear-cut harvesting with different riparian treatments, coastal British Columbia, Canada. *Water Resources Research* 42: 11p.
- Gooseff MN, Strzepek K, Chapra SC. (2005). Modeling the potential effects of climate change on water temperature downstream of a shallow reservoir, Lower Madison River, MT. *Climatic Change* 68: 331-353.
- Govindaraju RS. (2000a). Artificial neural networks in hydrology. I: Preliminary concepts. *Journal of Hydrologic Engineering* 5(2): 115-123.
- Govindaraju RS. (2000b). Artificial neural networks in hydrology. II: Hydrologic Applications. *Journal of Hydrologic Engineering* 5(2): 124-137.
- Granger RJ, Hestrom N. (2011). Modelling hourly rates of evaporation from small lakes. *Hydrology and Earth System Sciences* 15: 267-277.
- Gravelle JA, Link TE. (2007). Influence of timber harvesting on headwater peak stream temperatures in a Northern Idaho watershed. *Forest Science* 53(2): 189-205.
- Gray JRA, Edington JM. (1969). Effect of woodland clearance on stream temperature. *Journal of the Fisheries Research Board of Canada* 26: 399-403.
- Gu R. (1998). A simplified river temperature model and its application to stream flow management. *Journal of Hydrology* 37(1): 35-54.

- Gu R, Montgomery S, Austin TA. (1998). Quantifying the effects of stream discharge on summer river temperature. *Hydrological Sciences Journal* 43(6): 885-904.
- Gu RR, Li Y. (2002). River temperature sensitivity to hydraulic and meteorological parameters. *Journal of Environmental Management* 66: 43-56.
- Guillemette N, St-Hilaire A, Ouarda TBMJ, Bergeron N, Robichaud E, Bilodeau L. (2009). Feasibility study of a geostatistical modelling of monthly maximum stream temperatures in a multivariate space. *Journal of Hydrology* 364: 1-12.
- Hammar L, Shen HT. (1995). Frazil evolution in channels. *Journal of Hydraulic Research* 33 (3): 291-306.
- Hannah DM, Malcolm IA, Soulsby C, Youngson AF. (2004). Heat exchanges and temperatures within a salmon spawning stream in the Cairngorms, Scotland: seasonal and sub-seasonal dynamics. *River Research and Applications* 20: 635-652.
- Hannah DM, Malcolm IA, Soulsby C, Youngson AF. (2008). A comparison of forest and moorland stream microclimate, heat exchanges and thermal dynamics. *Hydrological Processes* 22(7): 919-940.
- Haykin S. (1999). Neural networks: a comprehensive foundation, second edition. Prentice Hall, New Jersey, 842p.
- Hébert, C., Caissie, D., Satish, M.G., El-Jabi N. (2011). Study of stream temperature dynamics and corresponding heat fluxes within Miramichi River catchments (New Brunswick, Canada). *Hydrological Processes* 25: 2439-2455.
- Hembre B, Arnekleiv JV, L'abée-Lund JH. (2001). Effects of water discharge and temperature on the seaward migration of anadromous brown trout, *Salmo trutta*, smolts. *Ecology of Freshwater Fish* 10: 61-64.

- Herb WR, Stefan HG. (2011). Modified equilibrium temperature models for cold-water streams. *Water Resources Research* 47(W06519): 13p.
- Herb WR, Janke B, Mohseni O, Stefan HG. (2008). Thermal pollution of streams by runoff from paved surfaces. *Hydrological Processes* 22: 987-999.
- Hester ET, Doyle MW. (2011). Human impacts to river temperature and their effects on biological processes: a quantitative synthesis. *Journal of the American Water Resources Association* 47(3): 571-587.
- Hetrick NJ, Brusven MA. (1998). Changes in solar input, water temperature, periphyton accumulation, and allochthonous input and storage after canopy removal along two small salmon streams in Southeast Alaska. *Transactions of the American Fisheries Society* 127: 859-857.
- Hewlett JD, Fortson JC. (1982). Stream temperature under an inadequate buffer strip in the southeast piedmont. *Water Resources Bulletin* 18(6): 983-988.
- Hills RG, Viskanta R. (1976). Modeling of unsteady temperature distribution in rivers with thermal discharges. *Water Resources Research* 12(4): 712-722.
- Hills DK, Magnuson JJ. (1990). Potential effects of global climate warming on the growth and prey consumption of Great Lakes fish. *Transactions of the American Fisheries Society* 119: 265-275.
- Hockey JB, Owens IF, Tapper NJ. (1982). Empirical and theoretical models to isolate the effect of discharge on summer water temperatures in the Hurunui River. *Journal of Hydrology (New Zealand)* 21: 1-12.
- Holtby LB. (1988). Effects of logging on stream temperature in Carnation Creek, British Columbia, and associated impacts on the coho salmon (*Oncorhynchus kisutch*). *Canadian Journal of Fisheries and Aquatic Sciences* 45: 502-515.

- Holtby B, Newcombe CP. (1982). A preliminary analysis of logging-related temperature changes in Carnation Creek, British Columbia. In: Proceedings of the Carnation Creek Workshop, A 10.
- Hondzo M, Stefan HG. (1994). Riverbed heat conduction prediction. *Water Resources Research* 30(5): 1503-1513.
- Hopkins CL. (1971). The annual temperature regime of a small stream in New Zealand. *Hydrobiologia* 37(3-4): 397-408.
- Hostetler SW. (1991). Analysis and modeling of long-term stream temperatures on the steamboat creek basin, Oregon: implications for land use and fish habitat. *Water Resources Bulletin* 27(4): 637-647.
- Huntsman AG. (1942). Death of salmon and trout with high temperature. *Journal of the Fisheries Research Board of Canada* 5(5): 485-501.
- Hrachowitz M, Soulsby C, Imholt C, Malcolm IA, Tetzlaff D. (2010). Thermal regimes in a large upland salmon river: a simple model to identify the influence of landscape controls and climate change on maximum temperatures. *Hydrological Processes* 24: 3374-3391.
- Islam S, Kothari R. (2000). Artificial neural networks in remote sensing of hydrologic processes. *Journal of Hydrologic Engineering* 5: 128-144
- Jackson CR, Batzer DP, Cross SS, Haggerty SM, Sturm CA. (2001). Headwater streams and timber harvest: Channel, macroinvertebrate, and amphibian response and recovery. *Forest Science* 53(2): 356-370.
- Jain AK, Mao J, Mohiuddin KM. (1996). Artificial neural network: A tutorial. *Computer* 31-44.

- Jain A, Varshney AK, Joshi UC. (2001). Short-term water demand forecast modeling at IIT Kanpur using artificial neural networks. *Water Resources Management* 15: 299-321.
- Jensen AJ, Hvidsten NA, Johnsen BO. (1998). Effects of temperature and flow on the upstream migration of adult salmon in two Norwegian Rivers. Pages 45- 54 in: M. Jungwirth S, Schmutz S, Weiss S. [ed]. Fish migration and fish bypasses. Fishing News Books, Oxford.
- Jeppesen E, Iversen TM. (1987). Two simple models for estimating daily mean water temperatures and diel variations in a Danish low gradient stream. *Oikos* 49(2): 149-155.
- Jobson HE. (1977). Bed conduction computation for thermal models. *Journal of the Hydraulics Division* 103(HY10): 1213-1217.
- Jobson HE, Keefer TN. (1979). Modelling highly transient flow, mass and heat transfer in the Chattahoochee River near Atlanta, Georgia. Geological Survey Professional Paper 11136. US Gov. Printing Office, Washington D.C.
- Johnson FA. (1971). Stream temperatures in an alpine area. *Journal of Hydrology* 14:322-336.
- Johnson SL, Jones JA. (2000). Stream temperature responses to forest harvest and debris flows in western Cascades, Oregon. *Canadian Journal of Fisheries and Aquatic Sciences* 57: 30-39.
- Johnson SL. (2003). Stream temperature: scaling of observations and issues for modeling. *Hydrological Processes* 17: 497-499.

- Johnson SL. (2004). Factors influencing stream temperatures in small streams: substrate effects and a shading experiment. *Canadian Journal of Fisheries and Aquatic Sciences* 61: 913-923.
- Johnston TA. (1997). Downstream movement of young-of-the-year fishes in Catamaran Brook and the Little Southwest Miramichi River, New Brunswick. *Journal of Fish Biology* 51: 1047-1062.
- Jonsson B, Jonsson N. (2010). A review of the likely effects of climate change on anadromous Atlantic salmon *Salmo salar* and brown trout *Salmo trutta*, with particular reference to water temperature and flow. *Journal of Fish Biology* 75: 2381-2447.
- Karaçol AG, Sivri N, Uçan ON. (2007). Maximum stream temperature estimation of Degirmendere River using artificial neural network. *Journal of Scientific & Industrial Research* 66: 363-366.
- Keskin ME, Terzi O. (2006). Evaporation estimation models for Lake Egirdir, Turkey. *Hydrological Processes* 20: 2381-2391.
- Kim KS, Chapra SC. (1997). Temperature model for highly transient shallow streams. *Journal of Hydraulic Engineering* 123(1): 30-40.
- Kinouchi T, Yagi H, Miyamoto M. (2007). Increase in stream temperature related to anthropogenic heat input from urban wastewater. *Journal of Hydrology* 335: 78-88.
- Kjellström E, Bärring L, Jacob D, Jones R, Lenderink G, Schär C. (2007). Modelling daily temperature extremes: recent climate and future changes over Europe. *Climatic Change* 81: 249-265.

- Kobayashi D, Ishii Y, Kodama Y. (1999). Stream temperature, specific conductance and runoff process in mountain watersheds. *Hydrological Processes* 13: 865-876.
- Kothandaraman V. (1971). Analysis of water temperature variations in large rivers. *Journal of the Sanitary Engineering Division* 97: 19-31.
- Krajewski WF, Kraszewski AK, Grenney WJ. (1982). A graphical technique for river water temperature predictions. *Ecological Modelling* 17: 209-2224.
- Krause CW, Lockard B, Newcomb TJ, Lohani V, Orth DJ. (2004). Predicting influences or urban development on thermal habitat in a warm water stream. *Journal of the American Water Resources Association* 40(6): 1645-1658.
- Langan SJ, Johnston L, Donaghy MJ, Youngson AF, Hay DW, Soulsby C. (2001). Variation in river water temperatures in an upland stream over a 30-year period. *The Science of the Total Environment* 265: 195-207.
- Larnier K, Roux H, Dartus D, Croze O. (2010). Water temperature modeling in the Garonne River (France). *Knowledge and Management of Aquatic Ecosystems* 398(04): 20p.
- Larson LL, Larson SL. (1996). Riparian shade and stream temperature: a perspective. *Rangelands* 18(4): 149-152.
- Leach JA, Moore RD. (2011). Stream temperature dynamics in two hydrogeomorphically distinct reaches. *Hydrological Processes* 25: 679-690.
- Leblanc RT, Brown RD. (2000). The use of riparian vegetation in stream temperature modification. *Journal of the Chartered Institution of Water and Environmental Management* 14: 297-303.

- Leblanc RT, Brown RD, FitzGibbon JE. (1997). Modeling the effects of land use change on the water temperature in unregulated urban streams. *Journal of Environmental Management* 49: 445-469.
- LeBosquet M. (1946). Cooling water benefits increased river flow. *Journal of the New England Water Works Association* 60: 11-116.
- Lee RM, Rinne JN. (1980). Critical thermal maximum of five trout species in the Southwestern United States. *Transaction of the American Fisheries Society* 109(6): 632-635.
- Liu B, Yang D, Ye B, Berezovskaya S. (2005). Long-term open-water season stream temperature variations and changes over Lena River Basin in Siberia. *Global and Planetary Change* 48: 96-111.
- Lund SG, Caissie D, Cunjak RA, Vijayan MM, Tufts BL. (2002). The effects of environmental heat stress on heat-shock mRNA and protein expression in Miramichi Atlantic Salmon (*Salmo salar*) parr. *Canadian Journal of Fisheries and Aquatic Sciences* 59: 1553-1562.
- Lynch JA, Rishel GA, Corbett ES. (1984). Thermal alteration of streams draining clear-cut watersheds: quantification and biological implications. *Hydrobiologia* 111: 161-169.
- Macan TT. (1958). The temperature of a small stony stream. *Hydrobiologia* 12: 89-106.
- Maddonald JS, MacIsaac EA, Herunter HE. (2003). The effect of variable-retention riparian buffer zones on water temperatures in small headwater streams in sub-boreal forest ecosystems of British Columbia. *Canadian Journal of Fisheries and Aquatic Sciences* 33: 1371-1382.

- Mackey AP, Berrie AD. (1991). The prediction of water temperatures in chalk streams from air temperatures. *Hydrobiologia* 210: 183-189.
- Mackey PC, Barlow PM, Ries KG. (1998). Relations between discharge and wetted perimeter and other hydraulic-geometry characteristics at selected stream flow-gaging stations in Massachusetts. U.S. Geological Survey. Water-Resources Investigations Report 98-4094.
- Maier HR, Dandy GC. (1996). The use of artificial neural networks for the prediction of water quality parameters. *Water Resources Research* 32(4): 1013-1022.
- Malcolm IA, Soulsby C, Hannah DM, Bacon PJ, Youngson AF, Tezloff. (2008). The influence of riparian woodland on stream temperatures: implications for the performance of juvenile salmonids. *Hydrological Processes* 22: 968-979.
- Marcé R, Armengol J. (2008). Modelling river water temperature using deterministic, empirical, and hybrid formulations in a Mediterranean stream. *Hydrological Processes* 22: 3418-3430.
- Marceau P, Cluis D, Morin G. (1986). Comparaison des performances relatives à un modèle déterministe et à un modèle stochastique de température de l'eau en rivière. *Canadian Journal of Civil Engineering* 13: 352-364.
- Marsh P. (1990). Modelling water temperature beneath river ice covers. *Canadian Journal of Civil Engineering* 17(1): 36-44.
- Marcotte N, Duong VL. (1973). Le calcul de la température de l'eau des rivières. *Journal of Hydrology* 18: 273-287.
- Markarian RK. (1980). A study of the relationship between aquatic insect growth and water temperature in a small stream. *Hydrobiologia* 75: 81-95.

- Martinez JMM, Alvarez VM, Conzalez-Real, Baille A. 2006. A simulation model for predicting hourly pan evaporation from meteorological data. *Journal of Hydrology* 318: 250-261.
- Meier W, Bonjour C, Wüest A, Reichert P. (2003). Modeling the effect of water diversion on the temperature of mountain streams. *Journal of Environmental Engineering* 129: 755-765.
- Meisner JD, Rosenfeld JS, Regier HA. (1988). The role of groundwater in the impact of climate warming on stream Salmonines. *Fisheries* 13(3): 2-8.
- Meisner JD. (1990). Potential loss of thermal habitat for Brook Trout, due to climatic warming, in two Southern Ontario streams. *Transactions of the American Fisheries Society* 119: 282-291.
- Mellina E, Moore RD, Hinch SG, Macdonald JS, Pearson G. (2002). Stream temperature responses to clear-cut logging in British Columbia : the moderating influences of groundwater and headwater lakes. *Canadian Journal of Fisheries and Aquatic Sciences* 59: 1886-1900.
- Minns CK, Randall RG, Chadwick EMP, Moore JE, Green R. (1995). Potential impact of climate change on the habitat and population dynamics of juvenile Atlantic salmon (*Salmo salar*) in eastern Canada. *Climate change and northern fish population. Canadian Special Publications of Fisheries and Aquatic Sciences* 121: 699-708.
- Minns AW, Hall MJ. (1996). Artificial neural networks as rainfall-runoff models. *Hydrological Sciences Journal* 41(3): 399-417.
- Mitchell AC, James CB, Edinger JE. (1995). Analyses of flow modifications on water quality in Nechako River. *Journal of Energy Engineering* 121(2): 73-80.

- Mitchell S. (1999). A simple model for estimating mean monthly stream temperatures after riparian canopy removal. *Environmental Management* 24(1): 77-83.
- Mohseni O, Stefan HG. (1999). Stream temperature-air temperature relationships: a physical interpretation. *Journal of Hydrology* 218: 128-141.
- Mohseni OM, Erickson TR, Stefan HG. (2002). Upper bounds for stream temperatures in the contiguous United States. *Journal of Environmental Engineering* 128(1) : 4-11.
- Mohseni O, Stefan HG, Eaton JG. (2003). Global warming and potential changes in fish habitat in U.S. streams. *Climatic Change* 59: 389-409.
- Moore MV, Pace ML, Mather JR, Murdoch PS, Howarth RW, Folt CL, Chen CY, Hemond HF, Flebbe PA, Driscoll CT. (1997). Potential effects of climate change on freshwater ecosystems of the New England/Mid-Atlantic region. *Hydrological Processes* 11: 925-947.
- Moore RD, Sutherland P, Gomil T, Dhakal A. (2005a). Thermal regime of a headwater stream within a clear-cut, coastal British Columbia, Canada. *Hydrological Processes* 19: 2591-2608.
- Moore RD, Spittlehouse DL, Story A. (2005b). Riparian microclimate and stream temperature response to forest harvesting: a review. *Journal of the American Water Resources Association* 41(4): 813-834.
- Moradkhani H, Hsu KL, Gupta HV, Sorooshian S. (2004). Improved stream flow forecasting using self-organizing radial basis function artificial neural networks. *Journal of Hydrology* 295: 246-262.

- Morin G, Couillard D. (1990). Predicting river temperatures with a hydrological model. In Encyclopedia of Fluid Mechanics, Surface and Groundwater Flow Phenomena, Vol 10, Cheremisinoff NP (ed.). Gulf Publishing Company, Houston, Texas, pp.171-209.
- Morin C, Nzakimuena TJ, Sochanski W. (1994). Préviation des températures de l'eau en rivières a l'aide d'un modèle conceptuel: le cas de la rivière Moisie. *Canadian Journal of Civil Engineering* 21(1): 63-75.
- Morrill JC, Bales RG, Conklin MH. (2005). Estimating stream temperature from air temperature: Implication for future water quality. *Journal of Environmental Engineering* 131(1): 139-146.
- Morrison J, Quick MC, Foreman MGG. (2002). Climate change in the Fraser River watershed: flow and temperature projections. *Journal of Hydrology* 263: 230-244.
- Morse WL. (1972). Stream temperature prediction under reduced flow. *ASCE, Journal of the Hydraulics Division* 98 (HY6): 1031-1047.
- Mosley MP. (1983). Variability of water temperatures in the braided Ashley and Rakaia rivers. *New Zealand Journal of Marine and Freshwater Research* 17: 331-342.
- Murray GLD, Edmonds RL, Marra JL. (2000). Influence of partial harvesting on stream temperatures, chemistry, and turbidity in forests on the western Olympic Peninsula. *Washington. Northwest Science* 74 (2): 151-164.
- Myrick CA, Cech JJ. (2000). Swimming performances of four California stream fishes: temperature effects. *Environmental Biology of Fishes* 58: 289-295.

- Nagasaka A, Nakamura F. (1999). The influence of land-use changes on hydrology and riparian environment in a northern Japanese landscape. *Landscape Ecology* 14: 543-556.
- Nayebi M, Khalili, Amin S, Zand-Parsa S. (2006). Daily stream flow prediction capability of artificial neural networks as influenced by minimum air temperature data. *Biosystems Engineering* 95(4): 557-567.
- Nelson KC, Palmer MA. (2007). Stream temperature surges under urbanization and climate change: data, models, and responses. *Journal of the American Water Resources Association* 34(2): 440-452.
- Nemerow NL. (1985). Stream Lake, Estuary and Ocean Pollution. Van Nostrand Reinhold: New York.
- Neumann DW, Rajagopalan B, Zagona EA. (2003). Regression model for daily maximum stream temperature. *Journal of Environmental Engineering* 129(7): 667-674.
- Neumann DW, Zagona EA, Rajagopalan B. (2006). A decision support system to manage summer stream temperatures. *Journal of the American Water Resources Association* 42(5): 1275-1284.
- Nimikou MA, Baltas E, Varanou E, Pantazis K. (2000). Regional impacts of climate change on water resources quantity and quality indicators. *Journal of Hydrology* 234: 95-109.
- Novotny V, Krenkel PA. (1973). Simplified mathematical model of temperature changes in rivers. *Journal of the Water Pollution Control Federation* 45(2): 240-248.

- Parks Canada. (1999). Climate change scenario, summer and winter temperatures, 2090. Air Issues Bulletin No. 100, Air Quality, Climate Change and Canada's National Parks. Ottawa, Natural Resources Branch, Parks Canada.
- Penman HL. (1948). Natural evaporation for open water, bare soil and grass. *Proceedings of the Royal Society of London. Series A, Mathematical and Physical* 193(1032) : 120-145.
- Peterson RH, Spinney HC, Sreedharan A. (1977). Development of Atlantic salmon (*Salmo salar*) eggs and alevins under varied temperature regimes. *Journal of the Fisheries Research Board of Canada* 34: 31-43.
- Pilgrim JM, Fang X, Stefan HG. (1998). Stream temperature correlations with air temperature in Minnesota: implications for climatic warming. *Journal of the American Water Resources Association* 34(5): 1109-1121.
- Poole GC, Berman CH. (2001). An ecological perspective on in-stream temperature: natural heat dynamics and mechanisms of human-caused thermal degradation. *Environmental Management* 27(6): 787-802.
- Preud'homme EB, Stefan HG. (1992). Errors Related to Random Stream Temperature Data Collection in the Upper Mississippi River Watershed. *Water Resources Bulletin* 28(6): 1077- 1082.
- Priestley CHB, Taylor RJ. (1972). On the assessment of surface heat flux and evaporation using large-scale parameters. *Monthly Weather Review* 100(2): 81-92.
- Raphael JM. (1962). Prediction of temperature in rivers and reservoirs. *Journal of the Power Division* 88: 157-181.

- Rasmussen AH, Hondzo M, Stefan HG. (1995). A test of several evaporation equations for water temperature simulations in lakes. *Water Resources Bulletin* 31(6): 1023-1028.
- Rayne S, Henderson G, Gill P, Forest K. (2008). Riparian forest harvesting effects on maximum water temperatures in wetland-sourced headwater streams from the Nicola River watershed, British Columbia, Canada. *Water Resources Management* 22: 565-578.
- Rehman S, Mohandes M. (2008). Artificial neural network estimation of global solar radiation using air temperature and relative humidity. *Energy Policy* 36: 571-576.
- Ringler NH, Hall JD. (1975). Effects of logging on water temperature and dissolved oxygen in spawning beds. *Transactions of American Fisheries Society* 1: 111-121.
- Ringold PL, Sickie JV, Rasar K, Schacher J. (2003). Use of hemispheric imagery for estimation stream solar exposure. *Journal of the American Water Association* 39(6): 1373-1384.
- Rishel GB, Lynch JA, Corbett ES. (1982). Seasonal stream temperature changes following forest harvesting. *Journal of Environmental Quality* 11: 112-116.
- Risley JC, Roehl EA Jr., Conrads PA. (2003). Estimating water temperatures in small stream in Western Oregon using neural network models. U.S. Geological Survey (USGS) Water-Resources Investigations Report 02-4218, 59p.
- Robinson AT, Childs MR. (2001). Juvenile growth of native fishes in the Little Colorado River and in a thermally modified portion of the Colorado River. *North American Journal of Fisheries Management* 21: 809-815.

- Rosenberry DO, Winter TC, Buso DC, Likens GE. (2007). Comparison of 15 evaporation methods applied to a small mountain lake in the northeastern USA. *Journal of Hydrology* 340: 149-166.
- Rutherford JC, Blackett S, Blackett C, Saito L, Davies-Colley RJ. (1997). Predicting the effects of shade on water temperature in small streams. *New Zealand Journal of Marine and Freshwater Research* 31(5): 707-721.
- Rykken JJ, Chan SS, Moldenke AR. (2007). Headwater riparian microclimate patterns under alternative forest management treatments. *Forest Science* 53(2): 270-280.
- Salvatore SR. (1987). Effect of water temperature on food evacuation rate and feeding activity of age-0 Gizzard Shad. *Transactions of the American Fisheries Society* 116: 67-70.
- Samani Z. (2000). Estimating solar radiation and evapotranspiration using minimum climatological data. *Journal of Irrigation and Drainage Engineering* 124(4): 265-267.
- Schamseldin AY, Nasr AE, O'Connat KM. (2002). Comparison of different forms of the Multi-layer Feed-Forward Neural Network method used for river flow forecasting. *Hydrology and Earth System Sciences* 6(4): 671-684.
- Schindler DW. (2001). The cumulative effects of climate warming and other human stresses on Canadian freshwaters in the new millennium. *Canadian Journal of Fisheries and Aquatic Sciences* 58(1): 18-29.
- Scrivener JC, Andersen BC. (1984). Logging impacts and some mechanisms that determine the size of spring and summer population of coho salmon fry (*Oncorhynchus kisutch*) in Carnation Creek, British Columbia. *Canadian Journal of Fisheries and Aquatic Sciences* 41: 1097-1105.

- Shanley JB, Peters NE. (1988). Preliminary observations of stream flow generation during storms in a forested piedmont watershed using temperature as a tracer. *Journal of Contaminant Hydrology* 3: 349-365.
- Shamseldin AY, Nasr AE, O'Connor KM. 2002. Comparison of different forms of the Multi-layer Feed-Forward Neural Network method used for river flow forecasting. *Hydrology and Earth System Sciences* 6 (4): 671-684.
- Shen HT, Wang DS, Wasantha A. (1995). Numerical simulation of river ice processes. *ASCE, Journal of Cold Regions Engineering* 9 (3): 107-118.
- Shigidi A, Garcia LA. (2003). Parameter estimation in groundwater hydrology using artificial neural networks. *Journal of Computing in Civil Engineering* 17(4): 281-289.
- Singh P, Singh VP. (2001). Snow and Glacier Hydrology. Kluwer Academic Publishers, Dordrecht, The Netherlands p. 221.
- Singh VP, Xu CY. (1997a). Evaluation and generalization of 13 mass-transfer equations for determining free water evaporation. *Hydrological Processes* 11: 311-323.
- Singh VP, Xu CY. (1997b). Sensitivity of mass transfer-based evaporation equations to errors in daily and monthly input data. *Hydrological Processes* 11: 1465-1473.
- Sinokrot BA, Stefan HG. (1993). Stream temperature dynamics: Measurements and modeling. *Water Resources Research* 29(7): 2299-2312.
- Sinokrot BA, Stefan HG. (1994). Stream water temperature sensitivity to weather and bed parameters. *Journal of Hydraulic Engineering* 120(6): 722-736.
- Sinokrot BA, Stefan HG, McCormick JH, Eaton JG. (1995). Modeling of climate change effects on stream temperatures and fish habitats below dams and near groundwater inputs. *Climatic Change* 30: 181-200.

- Sinokrot BA, Gulliver JS. (2000). In-stream flow impact on river water temperatures. *Journal of Hydraulic Research* 38(5): 339-349.
- Sivri N, Kilic N, Ucan O. (2007). Estimation of stream temperature in Firtinia Creek (Rize-Turkiye) using artificial neural network model. *Journal of Environmental Biology* 28(1): 67-72.
- Smith K. (1972). River water temperatures: an environmental review. *Scottish Geographical Magazine* 88: 211-220.
- Smith K. (1975). Water temperature variations within a major river system. *Nordic Hydrology* 6: 155-169.
- Smith K, Lavis ME. (1975). Environmental influences on the temperature of a small upland stream. *Oikos* 26(2): 228-236.
- Smith M. (1993). Neural networks for statistical analysis. Van Nostrand Reinhold, New York, 235p.
- Song CCS, Chen CY. (1977). Stochastic properties of daily temperature in rivers. *Journal of the Environmental Engineering Division* 103: 217-231.
- Sridhar V, Sansone AL, LaMarche J, Dubin T, Lettenmaier DP. (2004). Prediction of stream temperature in forested watersheds. *Journal of the American Water Resources Association* 40(1): 197-213.
- Stefan HG, Preud'homme EB. (1993). Stream temperature estimation from air temperature. *Water Resources Bulletin* 29: 27-45.
- St-Hilaire A, Morin G, El-Jabi N, Caissie D. (2000). Water temperature modelling in a small forested stream: implication of forest canopy and soil temperature. *Canadian Journal of Civil Engineering* 27: 1095-1108.

- Story A, Moore RD, Macdonald JS. (2003). Stream temperatures in two shaded reaches below cutblock and logging roads: downstream cooling linked to subsurface hydrology. *Canadian Journal of Forest Resources* 33: 1383-1396.
- Sudheer KP, Gosain AK, Rangan DM, Saheb SM. (2002). Modelling evaporation using an artificial neural network algorithm. *Hydrological Processes* 16: 3189-3202.
- Suen JP, Eheart WJ. (2003). Modeling nitrate concentration in natural streams by using artificial neural networks. *Worlds Water and Environmental Resources Congress*: 1311-1318.
- Swansburg EO, Chaput G, Moore D, Caissie D, El-Jabi N. (2002). Size variability of juvenile Atlantic salmon: links to environmental conditions. *Journal of Fish Biology* 61: 661-683.
- Swift LW, Messer JB. (1971). Forest cuttings raise temperatures of small streams in the southern Appalachians. *Journal of Soil and Water Conservation* 26: 111-116.
- Tague C, Farrell M, Grant G, Lewis S, Rey S. (2007). Hydrogeologic controls on summer stream temperatures in the McKenzie River basin, Oregon. *Hydrological Processes* 21: 3288-3300.
- Tan SBK, Shuy EB, Chua LHC. (2007). Modelling hourly and daily open-water evaporation rates in areas with an equatorial climate. *Hydrological Processes* 21: 486-499.
- Theurer FD, Lines I, Nelson T. (1985). Interaction between riparian vegetation, water temperature and salmonids habitat in the Tucannon River. *Water Resources Bulletin* 21: 53-64.
- Thirumalaiah K, Deo MC. (2000). Hydrological forecasting using neural networks. *Journal of Hydrologic Engineering* 5(2): 1061-1084.

- Thomas RE, Gharrett JA, Carls MG, Rice SD, Moles A, Korn S. (1986). Effects of fluctuating temperature on mortality, stress, and energy reserves of juvenile Coho Salmon. *Transactions of the American Fisheries Society* 115: 52-59.
- Thornwaite CW. (1948). An approach toward a rational classification of climate. *Geographical Review* 38(1): 55-94.
- Tokar AS, Johnson PA. (1999). Rainfall-runoff modeling using artificial neural networks. *Journal of the Hydrological Engineering* 4(3): 232-239.
- Tokar AS, Markus M. (2000). Precipitation-runoff modeling using artificial neural networks and conceptual models. *Journal of Hydrologic Engineering* 5(2): 156-161.
- Torgersen CE, Price DM, Li HW, McIntosh BA. (1999). Multiscale thermal refugia and stream habitat associations of Chinook salmon in Northeastern Oregon. *Ecological Applications* 9(1): 301-319.
- Torgersen CE, Faux RN, McIntosh Ba, Poage NJ, Norton DJ. (2001). Airborne thermal sensing for water temperature assessment in rivers and streams. *Remote Sensing of Environment* 76: 386-398.
- Troxler RW, Thackston EL. (1977). Predicting the rate of warming of rivers below hydro-electric installations. *Journal of the Water Pollution Control Federation*, August: 1902-1912.
- Tung CP, Lee TY, Yang YC. (2006). Modeling climate-change impacts on stream temperature of Formosan landlocked salmon habitat. *Hydrological Processes* 20: 1629-1649.

- Tung CP, Yand YCE, Lee TY, Li MH. (2007). Modification of a stream temperature model with Beer's law and application to GaoShan Creek in Taiwan. *Ecological Modelling* 200: 217-224.
- Valantzas JD. (2006). Simplified versions for the Penman evaporation equation using routine weather data. *Journal of Hydrology* 331: 690-702.
- Vannote RL, Minshall GW, Cummins KW, Sedell JR, Cushing CE. (1980). The river continuum concept. *Canadian Journal of Fisheries and Aquatic Sciences* 37: 130-137.
- Vannote R, Sweeney BW. (1980). Geographic analysis of thermal equilibria: A conceptual model for evaluating the effects of natural and modified thermal regimes on aquatic insect communities. *American Naturalist* 115(5): 667-695.
- Vugts H.F. (1974). Calculation of temperature variations of small mountain streams. *Journal of Hydrology* 23: 267-278.
- Ward JV. (1985). Thermal characteristics of running waters. *Hydrobiologia* 125: 31-46.
- Webb BW. (1996). Trends in stream and water temperatures. *Hydrological Processes* 10: 205-226.
- Webb BW, Crisp DT. (2006). Afforestation and stream temperature in a temperate maritime environment. *Hydrological Processes* 20: 51-66.
- Webb BW, Walling DE. (1986). Spatial variation of water temperature characteristics and behaviour in Devon river systems. *Freshwater Biology* 16: 585-608.
- Webb BW, Walling DE. (1993). Temporal variability in the impact of river regulation on thermal regime and some biological implications. *Freshwater Biology* 29: 167-182.

- Webb BW, Walling DE. (1996). Long-term variability in the thermal impact of river impoundment and regulation. *Applied Geography* 16(3): 211-223.
- Webb BW, Walling DE. (1997). Complex summer water temperature behaviour below a UK regulating reservoir. *Regulated Rivers: Research and Management* 13: 463-477.
- Webb BW, Nobilis F. (1995). Long-term water temperature trends in Austrian rivers. *Hydrological Sciences* 40: 83–96.
- Webb BW, Nobilis F. (1997). Long-term perspective on the nature of the air-water temperature relationship: a case study. *Hydrological Processes* 11: 137-147.
- Webb BW, Zhang Y. (1997). Spatial and seasonal variability in the components of the river heat budget. *Hydrological Processes* 11: 79-101.
- Webb BW, Zhang Y. (1999). Water temperatures and heat budgets in Dorset chalk water courses. *Hydrological Processes* 13: 309-321.
- Webb BW, Zhang Y. (2004). Intra-annual variability in the non-advective heat energy budget of Devon streams and rivers. *Hydrological Processes* 18: 2117-2146.
- Webb BW, Crisp DT. (2006). Afforestation and stream temperature in a temperate maritime environment. *Hydrological Processes* 20: 51-66.
- Webb BW, Clack PD, Walling DE. (2003). Water-air temperature relationships in a Devon river system and the role of flow. *Hydrological Processes* 17: 3069-3084.
- Webb BW, Hannah DM, Moore RD, Brown LE, Nobilis F. (2008). Recent advances in stream and river temperature research. *Hydrological Processes* 22(7): 902-918.
- Wichert GA, Lin P. (1996). A species tolerance index of maximum water temperature. *Water Quality Resources Journal of Canada* 31(4): 875-893.

- Wilkerson E, Hagan JM, Siegel D, Whitman AA. (2006). The effectiveness of different buffer widths for protecting headwater stream temperature in Maine. *Forest Science* 52(3): 221-231.
- Wright SA, Holly FM Jr, Bradley AA, Krajewski W. (1999). Long-term simulation of thermal regime of Missouri River. *ASCE, Journal of Hydraulic Engineering* 125(3): 242-252.
- Xu CY, Singh VP. (1998). Dependence of evaporation on meteorological variables at different time-scales and intercomparison of estimation methods. *Hydrological Processes* 12: 429-442.
- Xu CY, Singh VP. (2000). Evaluation and generalization of radiation-based methods for calculating evaporation. *Hydrological Processes* 14: 339-349.
- Xu CY, Singh VP. (2001). Evaluation and generalization of temperature-based methods for calculating evaporation. *Hydrological Processes* 15: 305-319.
- Yang K, Koike T. (2002). Estimating surface solar radiation from upper-air humidity. *Solar Energy* 72(2): 177-186.
- Yang K, Koike T. (2005). A general model to estimate hourly and daily solar radiation for hydrological studies. *Water Resources Research* 41: W10403.
- Yonaba H, Anctil F, Fortin V. (2010). Comparing sigmoid transfer functions for neural network multistep ahead stream flow forecasting. *Journal of Hydrologic Engineering* 15(4): 275-283.
- Younus M, Hondzo M, Engel BA. (2000). Stream temperature dynamics in upland agricultural watershed. *Journal of Environmental Engineering* 126(6): 518-526.
- Zealand CM, Burn DH, Simonovic SP. (1999). Short term stream flow forecasting using artificial neural networks. *Journal of Hydrology* 214: 32-48.

Zwieniecki MA, Newton M. (1999). Influence of streamside cover and stream features on temperature trends in forested streams of Western Oregon. *Western Journal of Applied Forestry* 14: 106-113.

APPENDIX A. Free Body Diagram

